University of Zagreb
Faculty of Mechanical Engineering and Naval Architecture

Tamara Petranović

RISK-BASED METHOD FOR PREDICTION OF EXTREME WAVE LOADS OF SHIP STRUCTURES

DOCTORAL THESIS

Zagreb, 2026

Sveučilište u Zagrebu
Fakultet strojarstva i brodogradnje

Tamara Petranović

RISK-BASED METHOD FOR PREDICTION OF EXTREME WAVE LOADS OF SHIP STRUCTURES

DOCTORAL THESIS

Supervisor:
Prof. Joško Parunov, PhD

Zagreb, 2026

Sveučilište u Zagrebu
Fakultet strojarstva i brodogradnje

Tamara Petranović

METODA ZASNOVANA NA RIZIKU ZA ODREĐIVANJE EKSTREMNOGA VALNOGA OPTEREĆENJA BRODSKIH KONSTRUKCIJA

DOKTORSKI RAD

Mentor:
Prof. dr. sc. Joško Parunov

Zagreb, 2026.

BIBLIOGRAPHY DATA

UDK:

Key words: Closed-form expressions (CFE), Extreme wave load prediction, Model uncertainty analysis, Probabilistic operability diagrams, Risk-based decision support.

Scientific area: Technical sciences

Scientific field: Naval Architecture

Institution: Faculty of Mechanical Engineering and Naval Architecture

Thesis supervisor: Prof. Joško Parunov, PhD

Number of pages: 43

Number of pages (in total): 111

Number of figures: 12

Number of tables: 10

Number of references: 42

Date of examination:

Thesis defence committee:

PhD Ivan Ćatipović, full professor - Chairman of the defence committee

PhD Jasna Prpić-Oršić, full professor - Member

PhD Marko Katalinić, associate professor - Member

Archive: Faculty of Mechanical Engineering and Naval Architecture

ZAHVALE

Zahvaljujem svom mentoru, prof. dr. sc. Jošku Parunovu, na stručnom vodstvu, strpljenju i kontinuiranoj podršci tijekom izrade ovoga rada. Vaše znanje i konstruktivne kritike bili su od iznimne važnosti za uspješan završetak ove disertacije.

Svim kolegama s kojima sam radila na projektu želim zahvaliti na suradnji, razmjeni ideja te na zajedničkom suočavanju s raznim izazovima.

Posebnu zahvalu upućujem prijateljima koji su doktorski studij učinili lakšim i ljepšim. Ivona, Ivana, Ružica, Mateja i Ivan, hvala.

Od srca zahvaljujem svojim roditeljima Ani i Marku na ljubavi, razumijevanju i bezuvjetnoj podršci kroz cijelo moje školovanje. Vaša vjera u mene temelj je na kojem je ovaj uspjeh izgrađen.

Ovaj rad posvećujem svom suprugu Eduardu te mojim kćerima Mariji Josipi i Juliji, kao i bebici koja uskoro stiže. Vi dajete smisao svakom koraku koji činim.

Na kraju, zahvaljujem dragom Bogu na daru života, snazi, ustrajnosti i svim blagoslovima kojima me obasipa.

Tamara Petranović

SPECIAL ACKNOWLEDGEMENT

I would like to express my deepest gratitude to the Croatian Science Foundation for financially supporting the research presented in this thesis through the project "Modelling Uncertainty of Ship Response Prediction in the Adriatic Sea" (MODUS, IP-2019-04-2085), led by Prof. Joško Parunov, PhD.

CONTENTS

LIST OF FIGURES

LIST OF TABLES

NOMENCLATURE

Abbreviations

2D	Two-dimensional
3D	Three-dimensional
AIS	Automatic Identification System
C	Cruise ship
CF	Canadian Frigate
CFD	Computational Fluid Dynamics
CFE	Closed-Form Expressions
CoV	Coefficient of Variation
CS	Container Ship
CT	Chemical Tanker
ECMWF	European Centre for Medium-Range Weather Forecasts
ERA	ECMWF Reanalysis
FC	Fully Correlated
FIME	Frequency Independent Model Error
FM	Fast Monohull
FORM	First-Order Reliability Method
IACS	International Association of Classification Societies
IOWAGA	Integrated Ocean Waves for Geophysical and other Applications
JONSWAP	Joint North Sea Wave Project
LC	Large Containership
LNG	Liquefied Natural Gas
LNGC	LNG carrier
MC	Monte Carlo
MODUS	Modelling Uncertainty of Ship Response Prediction in the Adriatic Sea
MPEV	Most Probable Extreme Value
MSI	Motion Sickness Incidence
NATO	North Atlantic Treaty Organization

NOAA	National Oceanic and Atmospheric Administration
NORA	Norwegian Reanalysis
NORDFORSK	Nordic Research (Nordic + Forskning/Forsk, Swedish/Norwegian for research)
OI	Operability Index
OT	Oil product Tanker
POI	Probabilistic Operability Index
RMS	Root Mean Square
RNLI	Royal National Lifeboat Institution
SI	Statistically Independent
SORM	Second-Order Reliability Method
ST	Strip Theory
SWAN	Simulating Waves Nearshore
TEU	Twenty-foot Equivalent Unit
U.S.	United States
VWBM	Vertical Wave Bending Moment
WAM	Wave Modelling
WAMSI	Weighted Average Motion Sickness Incidence
WWA	World Wave Atlas

Variables

C	Consequence
F	Probability of non-exceedance of the long-term extreme VWBM
M	Risk control ratio
$MPEV(VWBM)$	Most probable extreme value of vertical wave bending moment (Nm)
OI	Operability Index (%)
P	Probability of an event
POI	Probabilistic Operability Index (%)
Q	Probability of exceedance of the long-term extreme VWBM
R	Risk
RP	Return period (years)

ABSTRACT

The objective of the thesis is the development of a method for the computation of long-term extreme wave loads using hindcast wave databases and risk-based ship operability analysis, considering epistemic uncertainties of seakeeping responses and the operability limiting values. The thesis is based on three connected sub-topics, i.e., model uncertainty analysis of the seakeeping method used, development of the risk-based operability diagrams, and development of the method for the extreme wave loads calculation, where each sub-topic is published in a journal article. The first article quantifies the uncertainty of closed-form expressions (CFE) for ship seakeeping by comparing it with model-scale measurements. The second article introduces epistemic uncertainties into ship operability assessment and develops probabilistic operability diagrams as a basis for risk-based decision support. The third article develops a route-based procedure for predicting extreme vertical wave bending moments using a hindcast wave database and explicit operational restrictions. As a result of the thesis, three scientific contributions are achieved for each of the three main research phases. Firstly, the thesis proposes modelling uncertainty of CFE for heave, pitch, and vertical wave bending moment predictions. Secondly, the model uncertainty of CFE and the uncertainty of limiting seakeeping operability criteria are explicitly included in limit state functions, resulting in the probabilistic operability diagrams, which offer a more informative description of operational risk compared to the deterministic approach. Finally, the thesis shows how heavy weather avoidance and speed reduction influence the long-term extreme vertical wave bending moment for the example of the passenger ship in the Adriatic Sea. The overall scientific contribution of the dissertation lies in linking uncertainty-qualified seakeeping calculations, probabilistic operability assessment, and extreme wave load prediction into one coherent methodological chain.

Key words: Closed-form expressions (CFE), Extreme wave load prediction, Model uncertainty analysis, Probabilistic operability diagrams, Risk-based decision support.

PROŠIRENI SAŽETAK

Ovaj se doktorski rad bavi određivanjem ekstremnih valnih opterećenja brodske konstrukcije uz eksplicitno uvažavanje nesigurnosti numeričkih metoda te graničnih kriterija operabilnosti na plovidbenoj ruti. Rad je izrađen prema skandinavskom modelu i temelji se na tri objavljena znanstvena članka. Zajednička istraživačka nit članaka jest povezivanje proračuna odziva broda na valovima, procjene operabilnosti i dugoročnog proračuna ekstremnih valnih opterećenja u jedinstveni, probabilistički okvir. Razlika u odnosu na prethodna istraživanja se ogleda u proračunu vjerojatnosti nepovoljnih događaja koristeći metode pouzdanosti konstrukcija, što omogućava određivanje i upravljanje rizikom u različitim fazama projektiranja i eksploatacije broda.

Ekstremna se valna opterećenja brodova tradicionalno određuju pomoću dugoročnih statističkih postupaka, pri čemu se kratkoročni odzivi broda ponderiraju vjerojatnostima pojavljivanja stanja mora. Takvi postupci često koriste globalne ili regionalne valne statistike, ali ne opisuju dovoljno dobro izbjegavanje teškog vremena, promjenu brzine i kursa u nevremenu, kao ni nesigurnosti numeričkih modela proračuna pomorstvenosti. Zbog toga je bilo potrebno razviti odgovarajuću metodologiju koja će spojiti analizu pomorstvenosti, procjenu operabilnosti i proračun ekstremnih valnih opterećenja, uz uvažavanje nesigurnosti proračunskih modela.

U prvom dijelu rada razmatra se nesigurnost polu-analitičkih izraza (Closed-Form Expressions, CFE) za vertikalna gibanja broda na valovima (poniranje i posrtanje) i vertikalni valni moment savijanja. CFE metoda je korisna u konceptualnim istraživanjima i sustavima odlučivanja kad su važni brzina proračuna i numerička efikasnost, jer zahtijeva samo glavne dimenzije broda, koeficijent istisnine, brzinu i smjer nailaska valova. U radu je korištena frekvencijski-neovisna pogreška modeliranja (Frequency Independent Model Error, FIME), kojom se kvantificira sustavna pogreška između izračunatih prijenosnih funkcija i rezultata modelskih ispitivanja dostupnih u literaturi. Usporedbom CFE metode s vrpčastom metodom i 3D panel metodom pokazano je da CFE ima veću nesigurnost rezultata, osobito za valni moment savijanja, ali i da se regresijskom analizom može smanjiti ta nesigurnost.

U drugom dijelu rada razvijen je vjerojatnosni pristup operabilnosti broda na valovima. Umjesto uobičajenog determinističkog pristupa, kod kojeg je kriterij operabilnosti ili zadovoljen ili nije, u disertaciji su numerički odzivi broda i granične vrijednosti kriterija

operabilnosti definirani kao slučajne varijable. Predložene su pripadne funkcije graničnih stanja kuteva posrtanja i ljuljana broda, vertikalnog ubrzanja pramca, te učestalosti izranjanja propelera i udara pramca o valove. Vjerojatnosti prekoračenja kriterija operabilnosti određene su metodama pouzdanosti, a rezultati su predočeni u obliku polarnih vjerojatnosnih dijagrama operabilnosti. Takvi dijagrami opisuju ovisnost operabilnosti ne samo o stanju mora, smjeru valova i brzini broda, već i odabranoj razini vjerojatnosti premašivanja kriterija, pružajući više informacija od uobičajenih polarnih "determinističkih" dijagrama operabilnosti. Metoda ujedno otvara i praktične mogućnosti primjene odlučivanja zasnovanih na riziku, kao npr. u sustavima za taktičko odlučivanje na brodu o manevrima u teškim vremenskim prilikama.

Treći dio rada povezuje analizu operabilnosti i ekstremna valna opterećenja. Na primjeru putničkog broda koji plovi relacijom Split–Ancona analizirana su stanja mora iz tzv. "hindcast" valografske baze. Za svako kratkoročno stanje mora određuje se najvjerojatnija ekstremna vrijednost valnog opterećenja, a zatim se iz godišnjih maksimuma određuje dugoročna raspodjela ekstrema pomoću Gumbelove funkcije vjerojatnosti. U metodu je uključeno i statističko povezivanje ekstremnih vrijednosti duž rute, pri čemu se razmatraju donja i gornja granica vjerojatnosti sustava potpuno koreliranih i statistički neovisnih stanja mora. Rezultati pokazuju da operativna ograničenja imaju snažan utjecaj na projektna opterećenja: potpuno izbjegavanje nepovoljnih morskih stanja približno prepolovljuje ekstremni valni moment savijanja, dok smanjenje brzine u takvim stanjima smanjuje opterećenje za približno petinu. Predloženi pristup omogućava učinkovitiju primjenu suvremenih "hindcast" valografskih baza u odnosu na uobičajenu metodu dugoročne analize valnog opterećenja .

Znanstveni doprinos rada sastoji se u tri međusobno povezana elementa: (1) kvantifikaciji nesigurnosti CFE metode usporedbom s dostupnim rezultatima modelskih ispitivanja, (2) razvoju koncepta probabilističkih dijagrama operabilnosti broda koji uključuju nesigurnosti odziva broda na valovima i nesigurnosti graničnih vrijednosti kriterija operabilnosti, te (3) razvoju metode za proračun dugoročnih ekstremnih valnih opterećenja na osnovi "hindcast" baza podataka i operativnih ograničenja broda. Time je postavljen novi metodološki okvir zasnovan na riziku, koji je primjenjiv za projektiranje brodskih konstrukcija , planiranje plovidbe te potporu odlučivanju u teškim vremenskim prilikama.

1. Introduction

The aim of the dissertation is the development of a rational framework for the computation of long-term extreme wave loads using hindcast wave databases and risk-based ship operability analysis, considering uncertainties of seakeeping responses and limiting values of ship operability criteria. The dissertation is based on three published journal papers, in which different sub-topics of the problem are considered independently, but together make a coherent contribution toward the aim of the thesis.

The first article quantifies the model uncertainty of closed-form expressions (CFE) by comparison with model-scale measurements [1]. The second article develops probabilistic ship operability diagrams and discusses risk-based methods in different decision-making applications [2]. The third article develops a novel procedure for extreme vertical wave bending moments using a hindcast wave database and ship operability analysis [3].

The present synopsis explains the scientific context, clarifies the methodological links among the papers, and highlights their common contribution.

1.1. State of the Art

Seagoing ships are predominantly loaded by still water and wave-induced loads. While still water loads are relatively easily determined by ship hydrostatic analysis, wave-induced loads are difficult to predict for several reasons. Firstly, physics behind ship motion and loads in a seaway is complex, secondly, ships are operating in a stochastic and unpredictable wave environment, and finally, the influence of voluntary actions of shipmasters on extreme wave loads is huge but difficult to predict [4]. Because of their complexity and key role in ship structural design and analysis, wave environment and wave-induced loads on ships have been the subject of research for several decades. Progress is being regularly reported by two relevant committees of the International Ships and Offshore Structure Congress [5, 6]. Despite significant efforts being made in the last decades in that field, uncertainties in the prediction of wave-induced loads are still not satisfactorily quantified, and research on that subject is emphasized as one of the priorities of the international community concerned by ship's structural safety [7].

Wave-induced loads on ships used in ship structural design are commonly determined by the long-term procedure consisting of weighting responses in short-term sea states by their probabilities of occurrence [8]. The transfer functions of ship responses in regular waves are combined with the wave spectra to define responses in short-term sea states, assumed to be stationary in a period spanning from several minutes to several hours. Rough seas are usually described by two integral wave parameters, significant wave height and mean zero-crossing period. The statistics of sea states, i.e., joint probabilities of occurrence of these two parameters are contained in the wave scatter diagram and used to compute the long-term distribution of wave loads, from which extreme values with large return periods are derived. Wave scatter diagrams have been extracted from wave databases obtained by numerical wave hindcasting [9]. These databases use wind field as input and then integral sea state characteristics are obtained using wave energy transport equations implemented in the third-generation numerical wave models as WAM, WAVEWATCH-III, MIKE 21, and SWAN [10]. Databases assimilate measurements from satellite missions and available wave buoys with numerical results. Hindcasted wave databases are available for the period of several decades, with integral sea state parameters obtained in regular time intervals of 1,3 or 6 hours and with a different geographical space resolution of 0.5° x 0.5° on average. Examples of databases in use today are ERA-Interim, ERA 5, NORA 10, NOAA, WAVERYS, IOWAGA, WWA. Although hindcasted wave databases nowadays represent a state-of-the-art source for the analysis of marine structures, they do not include the effect of the avoidance of heavy weather and therefore are not directly applicable for ships. It has become challenging how to use these big wave data sets in the calculation of wave loads for ship structural design. Namely, all sea states are included in these databases, which becomes too conservative for the analysis of ships, as shipmasters often avoid the most severe sea states. Recently, de Hauteclocque et al. [9] used data from the Automatic Identification System (AIS) to exclude the most severe weather conditions where ships have not been sailing. Another issue is that different wave databases, even if referring to the same geographical location, show discrepancies in wave data, mainly because of differences in the wind forcing model, different spatial and temporal resolutions employed, and the source of assimilated wave data and those used for calibration, affecting the predictions of the ship responses [10]. During the development of this thesis, IACS came out with the new procedure for the long-term prediction of the extreme wave loads, based on the hindcast wave database [11]. The consequence assessment showed that the extreme wave load, according to Rev. 2, was reduced by 10% to 30% compared to Rev. 1 [12], which was based on the visual wave observations [13].

As explained in the preceding paragraph, if hindcast databases are used in the analysis of ships, effects of the avoidance of heavy seas and heavy weather manoeuvring are to be explicitly accounted for. A convenient way to do this is by performing ship operability analysis [14]. Ship operability analysis represents the comparison of ship seakeeping responses to a set of predefined operability limiting criteria. If these limiting operability values are exceeded, either ship's speed is to be reduced or the wave heading angle is to be changed. These manoeuvres often lead to the reduction of wave responses below operability limits, although in some very severe sea states, ships cannot satisfy operability limiting values irrespective of speed and course changes. Ship operability analysis is commonly performed when acquiring a new ship to predict the operability index, i.e., the percentage of time when the ship would be able to operate normally in certain water area (e.g., [15]). There are two significant sources of uncertainty in ship operability analysis, i.e., modelling uncertainty of wave-induced responses and accuracy of the limiting operability values [16].

Ship wave-induced response is predicted by seakeeping methods of different complexity that have, in general, different modelling uncertainties [14]. Seakeeping methods in use today are, ordered according to their complexity, 2D strip theory, 3D panel methods formulated in frequency or time domain, and Computational Fluid Dynamics (CFD) methods [17]. Comparisons with experiments have shown that employing the method of higher complexity does not guarantee better agreement to the measurements [18]. Having that in mind, it is interesting to mention semi-analytical closed-form expressions (CFE) for ships motions and global wave loads formulated by Jensen et al, 2004 [19], which are the simplest among the seakeeping methods. CFE has been employed in conceptual studies of ship hydro-elastic responses [20], decision support systems [21], and for tuning transfer function for prediction of ship responses [22].

Several operability criteria are considered in ship operability analysis, namely, the root mean square (RMS) of roll, the RMS of pitch, the RMS of the vertical acceleration at the forward perpendicular (FP), the probability of slamming, the probability of green water, the probability of propeller emergence, and human comfort criterion [14]. Limiting values of these criteria are uncertain, as different values may be found in the literature [14]. Some of the limiting values are general for all ships, while some of them are applicable to specific ship types only [23]. Therefore, the outcome of the operability analysis will depend on the seakeeping method used and seakeeping limiting criteria values, that are rather uncertain [16].

1.2. Objectives and hypotheses of the research

The main objective of the research is developing a method for the computation of long-term extreme wave loads using hindcast wave databases and risk-based ship operability analysis while explicitly considering model uncertainty of seakeeping responses and uncertainties in the definition of operability limiting values.

Hypotheses of the research are:

1. Model uncertainty of closed-form expressions for vertical ship motions and loads can be quantified, and it is comparable to commonly used seakeeping methods,
2. Risk-based operability assessment procedure can be defined using closed-form expressions for seakeeping responses with corresponding model uncertainties and operability criteria limiting values presented as random variables.
3. A method for the long-term distribution of extreme wave loads can be developed based on the risk-based operability diagrams and model uncertainty of the seakeeping method.

1.3. Scientific contribution

Scientific contributions of the research are:

1. Modelling uncertainty of closed-form expression for linear vertical ship motions and wave bending moments and comparison with modelling uncertainty of commonly used seakeeping tools.
2. Concept of risk-based operability analysis and presentation of results as novel risk-based operability polar plots.
3. A method for calculation of long-term extreme wave loads based on wave hindcast databases and risk-based operability analysis.

1.4. Thesis outline

The structure of this thesis has been developed to systematically address the defined research objectives, test the proposed hypotheses, and demonstrate the intended scientific contributions. The dissertation follows the Scandinavian model and is based on three published scientific articles [1-3], referred to in this thesis as Article 1, Article 2, and Article 3 respectively. Each article addresses a specific sub-topic of the overall research framework, while together they form an integrated methodological sequence leading from uncertainty quantification of seakeeping predictions, through probabilistic operability assessment, to the prediction of long-term extreme wave loads.

Article 1 provides the methodological foundation for the first part of the thesis and is directly related to the first research hypothesis, namely that the model uncertainty of closed-form expressions for vertical ship motions and loads can be quantified and used in probability-based applications. This article investigates the Frequency Independent Model Error (FIME) of closed-form expressions for heave, pitch, and vertical wave bending moment amidships by comparing their transfer functions with model-scale experimental results and with predictions obtained by strip theory and 3D panel methods. In addition, multiple linear regression analysis is employed to express FIME as a function of the most relevant parameters, such as block coefficient, Froude number, and heading angle. In this way, Article 1 establishes the uncertainty model of the seakeeping method used throughout the thesis and demonstrates that the bias of simplified predictions can be reduced, while the dispersion can be explicitly described and used in probabilistic formulations.

Article 2 is directly aligned with the second research hypothesis, which states that a risk-based operability assessment procedure can be developed by combining seakeeping predictions, model uncertainty, and uncertain operability limiting values. Building on the uncertainty framework introduced in the previous research phase, this article incorporates epistemic uncertainties in both seakeeping responses and limiting criteria and formulates ship operability as a probabilistic problem rather than a deterministic one. The resulting probabilistic operability diagrams show the probability of exceedance of selected criteria for different headings, speeds, and sea states, thus providing a more informative alternative to conventional operability plots. In this article, the Second-Order Reliability Method (SORM) is used to evaluate the exceedance probabilities, and the concept of a Probabilistic Operability Index is introduced as a rational extension of the conventional Operability Index. Therefore, Article 2 represents the central contribution of the thesis in the domain of uncertainty-aware operability assessment and risk-based decision support in ship operation.

Article 3 is directly related to the third research hypothesis, namely that a method for the long-term prediction of extreme wave loads can be developed using hindcast wave databases and ship operability analysis. In this article, a route-based procedure is proposed for the prediction of extreme vertical wave bending moments on a passenger ship sailing across the Adriatic Sea. The method combines hindcast wave data, short-term extreme response estimation, fitted Gumbel distributions of annual maxima, and a system reliability approach for combining extreme values along the route. The important progress achieved in this article is the explicit inclusion of operational restrictions derived from operability analysis. In this way, the article shows that long-term extreme wave loads are not only a function of environmental exposure, but also of the operational behaviour of the ship, including the avoidance of sea states in which operability criteria are not satisfied and the reduction of speed in severe conditions. The results confirm that such restrictions have a pronounced influence on the predicted extremes and therefore represent an essential component of realistic structural load assessment.

The interconnection of the three articles is described as follows. Article 1 provides the uncertainty description of the simplified seakeeping model; Article 2 uses this uncertainty framework to formulate probabilistic operability diagrams; and Article 3 applies operability-based restrictions on the long-term prediction of extreme wave loads.

The scientific contributions of the thesis are therefore achieved through the combined results of all three articles. First, the thesis quantifies and reduces the bias of simplified closed-form seakeeping predictions and formulates their uncertainty in a form suitable for probabilistic use. Second, it develops a probabilistic framework for ship operability assessment that includes both modelling uncertainty and arbitrariness in the limiting criteria. Third, it integrates operability diagrams into a practical route-based method for predicting long-term extreme wave loads using hindcast wave databases and explicit operational restrictions. In that sense, the thesis advances from deterministic seakeeping and operability analysis toward a unified risk-based methodology applicable to ship design, structural assessment, and operational decision support.

2. Materials and methods

The research is divided into three phases, model uncertainty analysis of the seakeeping method used, i.e., CFE, development of the risk-based uncertainty diagrams, and development of the method for the extreme wave loads calculation.

2.1. Seakeeping Analysis

2.1.1. CFE for transfer functions

The closed-form expressions developed by Jensen et al. [19] are used for the estimation of the transfer functions of wave-induced ship motions and vertical wave bending moment (VWBM) at midship. These expressions are semi-analytical transfer functions derived from the assumptions embedded in the linear strip-theory and require only the main ship particulars: length, width, draft, block coefficient, speed, and heading angle. Their advantage is computational efficiency, which makes them suitable for conceptual studies, sensitivity analyses, route studies, and operational decision support. At the same time, the underlying assumption, besides those of the linear strip theory must be clarified: coupling terms between heave and pitch are neglected, the sectional added mass is assumed as constant and equal to the displaced water and hydrodynamic damping is simplified.

The transfer functions of heave Φ_w and pitch Φ_θ are given as:

$$\Phi_w = \eta F, \tag{1}$$

$$\Phi_\theta = \eta G, \tag{2}$$

where F and G are the heave and pitch forcing functions, and η is a function of the wave number, Froude number, heading angle, sectional hydrodynamic damping and wave amplitude [19]. The transfer functions for the relative vertical motion and the vertical acceleration are derived from equations (1) and (2).

The transfer function of VWBM at midship is given by the following expression:

$$\begin{gathered}\Phi_M = \kappa \frac{1-kT}{\left(k_e L_p\right)^2}\left[1-\cos\left(\frac{k_e L_p}{2}\right)-\frac{k_e L_p}{4}\sin\left(\frac{k_e L_p}{2}\right)\right]\cdot \\ \cdot F_V(F_n)\cdot F_C(C_B)\cdot\sqrt[3]{|\cos\beta|}\cdot\rho g B_0 L_p^2\end{gathered} \tag{3}$$

where k_e represents the effective wave number, β is the heading angle, κ is the Smith correction factor, $F_V(F_n)$ is the speed correction factor, $F_C(C_B)$ is the correction factor for the block coefficient, $\rho = 1025\ kg/m^3$ is the sea density, and B_0 is the measured maximum ship breadth at the waterline.

The transfer function of roll can be written as:

$$\Phi_\varphi = \frac{|M|}{\sqrt{[-\overline{\omega}^2(T_N/2\pi)^2+1]^2 C_{44}^2 + \overline{\omega}^2 B_{44}^2}}, \tag{4}$$

where $|M|$ is the amplitude of the roll excitation moment, B_{44} is the hydrodynamic roll damping, C_{44} is the restoring moment coefficient, T_N is the natural roll period, and $\overline{\omega}$ is the encounter frequency. Full expressions and explanations of various terms appearing in Equation (4) may be found in ref. [19].

2.1.2. Wave spectrum

For engineering purposes, short-term stationary irregular sea states are described using wave energy spectra. The choice of wave energy spectra depends on the geographical area, local bathymetry, and the severity of the sea state. The Pierson-Moskowitz spectrum is commonly used for fully developed seas of the open ocean, while the JONSWAP spectrum is more suitable for fetch-limited, developing conditions.

The one-parameter Tabain wave energy spectrum, originally developed for the Adriatic Sea, was used in earlier practice and can be expressed as [24]:

$$S(\omega) = 0.862\frac{0.0135g^2}{\omega^5} exp\left[-\frac{5.186}{\omega^4 H_S^5}\right] 1.63^p$$

$$p = exp\left[-\frac{(\omega-\omega_m)^2}{2\sigma^2\omega_m^2}\right] \tag{5}$$

$$\omega_m = 0.32 + \frac{1.8}{H_S + 0.6}$$

while $\sigma = 0.08$ for $\omega \le \omega_m$ and $\sigma = 0.1$ for $\omega > \omega_m$.

However, the JONSWAP spectrum is generally employed as a well-established and widely accepted model for partially developed sea states, and it is given by:

$$S_J(\omega) = A_\gamma \frac{5}{16}\frac{H_S^2\omega_m^4}{\omega^5} exp\left[-\frac{5}{4}\left(\frac{\omega_m}{\omega}\right)^4\right] \gamma^{exp\left(-0.5\left(\frac{\omega-\omega_m}{\sigma\omega_m}\right)^2\right)}, \tag{6}$$

where γ is the peak enhancement factor, $A_\gamma = 1 - e_0 \ln(\gamma)$ is a normalization constant, and σ is the spectral width parameter.

The one-parameter JONSWAP-Adriatic wave spectrum is recently developed, based on the JONSWAP formulation combined with Tabain's modal frequency models, with parameters optimized for the Adriatic Sea and all sea state conditions [24]:

$$S_J(\omega) = 0.8626 \frac{5}{16} \frac{H_S^2 \omega_m^4}{\omega^5} exp\left[-\frac{5}{4}\left(\frac{\omega_m}{\omega}\right)^4\right] 1.78^{exp\left(-0.5\left(\frac{\omega-\omega_m}{\sigma\omega_m}\right)^2\right)}, \tag{7}$$

where:

$$\omega_m = 0.52 + \frac{1.4}{H_S + 0.7} \tag{8}$$

while $\sigma = 0.06$ for $\omega \leq \omega_m$ and $\sigma = 0.08$ for $\omega > \omega_m$.

2.1.3. Ship response in short term irregular waves

The general expression for the ship's response spectrum in short-term irregular waves is given as:

$$S_R(\bar{\omega}) = |\Phi(\bar{\omega})|^2 S_J(\bar{\omega}), \tag{9}$$

where $\bar{\omega}$ is the encounter frequency and $S_J(\bar{\omega})$ is the encounter wave spectrum.

Zeroth moment of the response spectrum represents the area under the response spectrum:

$$m_{0R} = \int_0^\infty S_R(\bar{\omega}) \cdot d\bar{\omega}. \tag{10}$$

Higher order response spectra for $n = 1,2$ ... read:

$$m_{nR} = \int_0^\infty \bar{\omega}^n \cdot S_R(\bar{\omega}) \cdot d\bar{\omega}. \tag{11}$$

The moments can also be determined in the wave frequency domain, i.e., it is not necessary to calculate encounter frequencies for this purpose [25].

2.1.4. Model uncertainty of transfer functions

Model uncertainty in transfer functions can be evaluated by comparing seakeeping calculations with experimental measurements. In this context, transfer functions obtained using CFE are benchmarked against data of experimental measurements in towing tanks reported in the literature. Since most published experiments include comparisons with strip theory or 3D panel theory, the associated model uncertainties of these approaches can also be assessed. CFE are employed to calculate transfer functions for heave, pitch, and VWBM amidships for 13 different ships: Canadian frigate (CF), RNLI's lifeboat, 6750 TEU container ship (CS), Chemical tanker (CT), LNG carrier (LNGC), Large containership (LC), Cruise ship (C), Container ship (CS), S175 container ship (CS), 6500 TEU container ship (CS), DTMB 5415 hull, Fast monohull (FM), and Panamax oil product tanker (OT) [1].

Epistemic uncertainty of the transfer functions is introduced through the Frequency Independent Model Error, proposed firstly by Guedes Soares [26]. The mean value of FIME is estimated by regression analysis and then used together with an assumed standard deviation to define normal random variables representing model uncertainty. Operability limits for pitch and roll angles, vertical acceleration at the forward perpendicular and slamming, and propeller emergence frequencies are also treated as random variables with assigned coefficients of variation.

The core idea of FIME is based on scaling transfer functions by a constant fitting factor φ:

$$\varphi = \frac{\sum_i \hat{H}_i H_i}{H_i^2} \tag{12}$$

where $\hat{H}_i$ and H_i are measured and calculated transfer functions at the frequency ω_i, respectively. This allows the transfer function to be adjusted to match, on average, with the experimental results at all frequencies. According to its geometrical meaning, φ is the slope of the regression line passing through the origin when comparing experimental and calculated transfer functions. The theory overestimates the experimental results when φ is less than 1, whereas it underestimates readings when φ is more than 1 [4].

The mean trend of the FIME is described by the multivariate linear-regression expression:

$$\varphi = \mathrm{A} + \mathrm{B}\beta + \mathrm{C}C_b + \mathrm{D}F_n \tag{13}$$

where A is an intercept, while B, C, and D are the regression coefficients, β is the heading angle, C_b is the block coefficient, and F_n is the Froude number. The heading angle β is expressed in degrees in Eq. (13), where $\beta = 180°$ indicates head seas. This relation comes directly from the FIME analysis summarised in Article 1 and is then reused in Article 2 as an input to reliability calculations. In practical applications, regression equations are used to adjust seakeeping predictions by multiplying the transfer functions for heave, pitch, and VWBM by the result of the regression expression for the given parameters (*Cb, β, F*n). The resulting value provides the best estimate of the FIME for correcting the transfer functions for epistemic uncertainty.

Uncertainty associated with predictions based on regression analysis can be expressed through the standard deviation of the data around the regression lines. Standard deviations are determined as the square root of squares of deviations of FIME from the regression line.

Results of the regression analysis are shown in Section 3.1.

2.2. Seakeeping criteria

Most seakeeping criteria relate to operability, i.e., the crew's ability and willingness to operate the vessel and its equipment under given sea state conditions. These criteria are typically defined in terms of roll and pitch angles, roll motion, vertical and lateral acceleration, deck wetness, propeller emergence, and slamming. Additionally, some criteria account for human responses, as motion sickness incidence (MSI), weighted average motion sickness incidence (WAMSI), and motion-induced interruptions (MII).

However, limiting values of these criteria vary across standards for the same vessel type. For instance, the allowable vertical acceleration at the forward perpendicular is 0.2 g RMS according to NATO, compared to 0.275 g RMS specified by the U.S. Coast Guard for merchant ships under 100 m.

Given these discrepancies and variations in operational judgment, operability limits are inherently uncertain and are therefore treated as random variables. Their mean values are provided in Table 1, with a coefficient of variation (CoV) of 0.05 assumed in all cases, and the uncertainty is modelled using a Gaussian (normal) distribution.

Table 1. Mean values of operability criteria limits [23]

Criteria	Statistical property	Mean value
Pitch angle (°)	RMS	1.5
Vertical acceleration at FP (m/s^2)	RMS	0.05g
Roll angle (°)	RMS	2.5
Slamming frequency	Probability	0.03
Propeller emergence frequency	Probability	0.25

2.3. Reliability Problem Formulation

Uncertainties in seakeeping predictions and limiting values, which are typically neglected, are incorporated into the ship operability analysis. The deterministic concept of operability is extended by considering both response predictions and operability limits as uncertain quantities. Consequently, seakeeping criteria may be exceeded with a certain probability, which is evaluated using limit state functions.

The general limit state function is written as:

$$g(x_1, x_2, \ldots x_n) < 0 \tag{14}$$

where $x_1, x_2, \ldots x_n$ is a vector of random variables and g takes negative value when the limiting criterion is exceeded. In the thesis, random variables are epistemic uncertainties of the seakeeping results and limiting operability values.

For pitch angle, the random limit x_θ is compared with the RMS value obtained from the uncertainty-modified transfer function:

$$x_\theta - \sqrt{\int_0^\infty |\varphi_\theta \Phi_\theta(\omega)|^2 S_J(\omega) \cdot d\omega} < 0. \tag{15}$$

x_θ in Equation (15) is a normally distributed random variable representing pitch angle criterion, with a mean value equal to 1.5°, and CoV of 0.05 (Table 1). φ_θ is also normally distributed with the mean value calculated by Equation (13), depending on the heading angle and ship speed, and a standard deviation of 0.19 which is obtained in Article 1. $\Phi_\theta(\omega)$ is a transfer function of pitch, given by Equation (2), and $S_J(\omega)$ represents the wave energy spectrum. The same principle of probabilistic modelling is extended to other criteria.

2.4. Reliability Analysis

The reliability analysis is performed using the Second-Order Reliability Method (SORM) implemented in Comrel [27]. The First-Order Reliability Method (FORM), which is commonly used in ship structural reliability analysis (SRA), may not provide accurate results due to strongly nonlinear limit state functions. The results obtained using SORM are validated by Monte Carlo (MC) simulations and are found to be sufficiently accurate.

The practical implementation of the procedure within Comrel program is as follows. Firstly, the limit state functions $g(x_1, x_2, \dots x_n)$ are formulated as described in Section 2.3. A stochastic model for the variables was then defined separately. The stochastic modelling consists of selecting type of the distribution and its parameters or the mean and standard deviation. Next, the calculation method was selected, where the user has choice between FORM, SORM or different versions of the Monte Carlo simulation. The reliability calculations can be automatized using the multirun option, in the case when the range of reliability parameters are to be considered. This option is used for calculating the probabilities of exceeding the specified criteria for the range of H_s and β.

2.5. Risk-based perspective

In maritime applications, risk (*R*) is commonly defined as the product of the probability of an event (*P*) and its consequence (*C*) [28]. The total risk for a set of N uncorrelated serial events is given by:

$$R = \sum_{i=1}^{N} R_i = \sum_{i=1}^{N} P_i C_i. \tag{16}$$

The economic losses necessary for risk estimation can be expressed as:

$$C_{tot} = C_c + C_{eq} + C_s + C_d + C_{rp}, \tag{17}$$

where:

- C_c represents damage to cargo,
- C_{eq} accounts for damage to equipment,
- C_s represents damage to ship,
- C_d are costs related to delays,
- C_{rp} represents costs associated with loss of reputation.

The latter component, C_{rp}, includes factors such as passenger seasickness, reduced crew performance, and the consequences of delays [29].

The primary risk control parameters for a ship sailing in waves are forward speed and heading relative to the waves. For each combination, the probability of exceeding seakeeping criteria is evaluated through reliability analysis, and the total risk is calculated using Equation (16).

The risk criterion is expressed as the ratio of the potential cost ΔR and the related certain cost Δc, i.e. [29],

$$\frac{\Delta R}{\Delta c} = \frac{R_{current} - R_{alter}}{\Delta c} > M, \tag{18}$$

where:

- $R_{current}$ and R_{alter} represent the risk of the current and alternative combination of speed and heading, respectively,
- Δc are the increased costs because of choosing alternative sailing parameters,
- M is the risk control ratio, typically greater than 1, which serves as the decision criterion for the ship master when making maneuvering choices in heavy weather.

The physical meaning of the equation (18) is that the risk reduction should be higher than corresponding risk reduction measures.

A specific example of an attempt to determine the costs for a route in the Adriatic Sea can be found in Section 4.1 of Article 2.

2.6. Extreme wave loads

The contribution of this section is the method for the extreme values of wave loads using the hindcast wave database and accounting for ship operational restrictions.

2.6.1. Wave statistics

The WorldWaves hindcast database, containing numerically simulated wave data calibrated with satellite observations at 39 locations in the Adriatic Sea over a 23-year period (Figure 1), is used. Data from four points along the sailing route (locations 10, 12, 15, and 18) are considered. Each location includes 12 parameters recorded every 6 hours from January 1997 to January 2020, resulting in 33,600 records. The analysis focuses on significant wave height, peak period, mean wave direction, and time data [30].

Figure 1. 39 evenly distributed locations in the Adriatic Sea [31]

2.6.2. Method for the prediction of extreme wave loads

The transfer function of the vertical wave-induced bending moment (VWBM) at midship is calculated using the closed-form expression given in Equation (3). The response spectrum of VWBM is obtained by multiplying the squared transfer function by the wave energy spectrum given in Equation (6). The zero-th and second spectral moments of the response spectrum are determined using Equations (10) and (11), respectively.

The most probable extreme value (MPEV) of VWBM in the short-term sea state depends on the sea state duration T_d:

$$\text{MPEV(VWBM)} = \sqrt{m_{0_M} \cdot 2ln\left(\frac{T_d}{T_z}\right)}. \tag{19}$$

T_z is the average zero-crossing period of the response and it is defined as:

$$T_z = 2\pi\sqrt{\frac{m_{0_M}}{m_{2_M}}}, \tag{20}$$

where m_{0_M} and m_{2_M} are the zeroth and second moments of the response spectrum of wave bending moment [32].

For the period of data availability (January 1997 to January 2020), all MPEV of VWBM are calculated and then annual maximum MPEV of VWBM are extracted for all sea states at four locations along the route. When calculating the short-term MPEV, it is necessary to define the wave encounter angle. In the database, the wave direction is available for a given sea state, and with the known ship course, the wave encounter angle was calculated. The resulting histograms are fitted using the Gumbel distribution, commonly applied in extreme value analysis. The distribution parameters are estimated by the method of moments [33, 34].

The probability of exceedance of the long-term extreme VWBM can be written as:

$$Q = \frac{1}{RP} \tag{21}$$

and the probability of non-exceedance is:

$$F = 1 - Q \tag{22}$$

where RP is the return period in years [30].

To obtain the extreme value distribution along the route, distributions at individual locations are statistically combined. Exceedance at any location implies exceedance along the entire route, which can be modelled as a series system. Upper and lower bounds are defined by assuming statistical independence or full correlation between locations, respectively, following the approach of Mansour and Preston [35]. The data analyzed in the present study indicate that extreme values at different locations tend to occur simultaneously, suggesting a strong spatial correlation of sea states along the route.

If sea states along the location are assumed statistically independent, the system probability of non-exceedance of the extreme vertical bending moment along the sailing route $P_{ne,SI}$ reads:

$$P_{ne,SI} = \prod_{i=1}^{n} \left(P_{ne_i}\right)^{k_i}, \tag{23}$$

while the system probability of non-exceedance of extreme vertical bending moment valid for fully correlated sea states along the route $P_{ne,FC}$ is [36]:

$$P_{ne,FC} = \min_i \left(P_{ne_i}\right)^{k_i}. \tag{24}$$

The parameter k_i in Equations (23) and (24) represents the fraction of time the ship spends at each of the n wave locations along the route. Neglecting port time, the sum satisfies $\sum_{i=1}^{n} k_i = 1$. In this study, equal time distribution is assumed across locations.

Combined probability distributions along the route, defined by Equations (23) and (24), are evaluated numerically. They are presented on the VWBM-P_{ne} diagram, from which vertical bending moments corresponding to a 20-year return period are determined.

3. Selected results with discussion

This section presents selected results together with their discussion. The results are structured progressively, starting with model uncertainty of CFE, followed by probabilistic operability assessment on a representative route in the Adriatic Sea, while the final part addresses long-term extreme wave loads and the influence of operational conditions.

3.1. Modelling uncertainty of CFE

Building on the methodology described in section 2.1.4., the proposed FIME formulation and regression-based modelling of epistemic uncertainty are here applied to quantify and compare the performance of different prediction approaches. The following results therefore provide a direct evaluation of how well CFE, ST, and 3D methods reproduce experimental transfer functions, as well as the associated levels of bias and variability.

FIME is evaluated using Eq. (12) for 13 ships based on transfer functions from CFE, ST, 3D panel methods, and experiments. The ship models are listed in Section 2.1.4. and described in detail in Article 1. Histograms of FIME results obtained for heave, pitch, and VWBM amidships are shown in Figures 2-4, with corresponding statistics summarized in Table 2. Figures 2-4 and the results in Table 2 refer to FIME considering all ships together as well as all speeds and headings.

CFE exhibits the lowest bias and variability for pitch and the highest for VWBM amidships (Figure 2). Overall, CFE exhibit significantly higher uncertainty compared to ST and 3D methods. By comparing Figures 2-4, one finds out that, among three methods considered, the 3D methods tend to provide the lowest bias and variability for prediction of ship motion. By comparing Figures 2 and 3, it follows that, for VWBM amidships, ST shows slightly lower bias than 3D methods, although variability remains high in both cases.

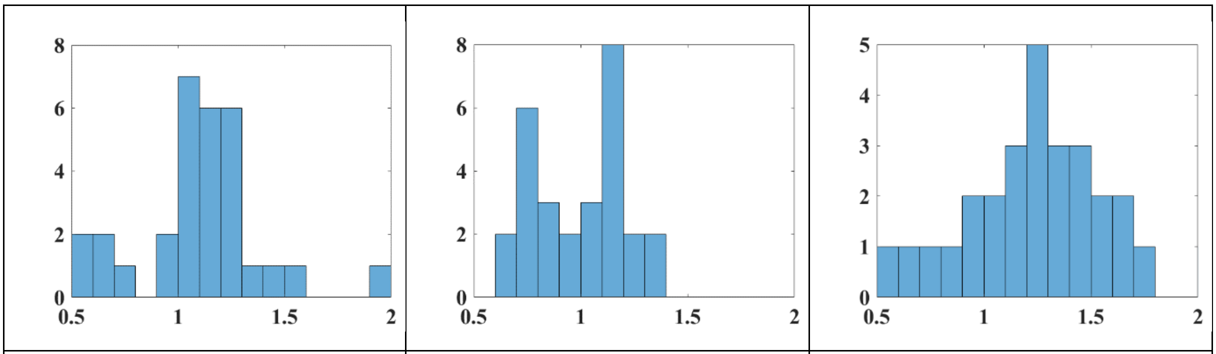

FIME for heave (CFE)	FIME for pitch (CFE)	FIME for VWBM (CFE)

Figure 2. Histograms of FIME for heave, pitch, and vertical bending moment (VWBM) calculated with CFE

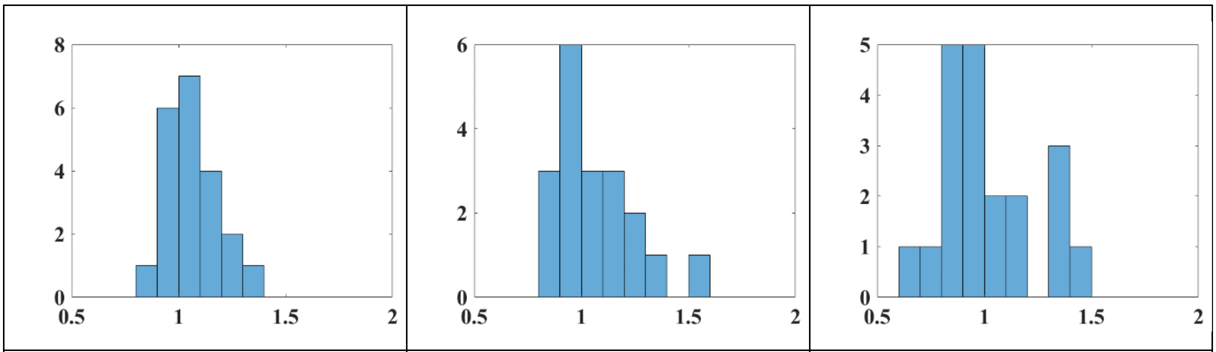

FIME for heave (ST)	FIME for pitch (ST)	FIME for VWBM (ST)

Figure 3. Histograms of FIME for heave, pitch, and vertical bending moment (VWBM) calculated in accordance with strip theory

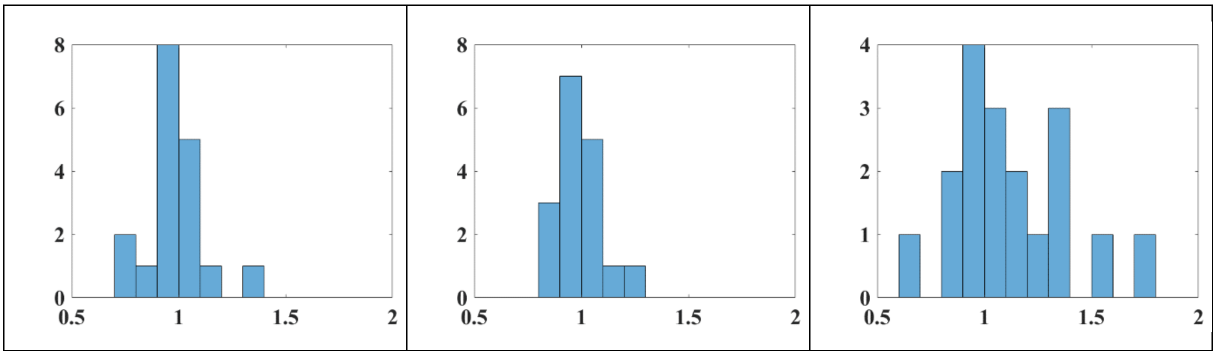

FIME for heave (3D)	FIME for pitch (3D)	FIME for VWBM (3D)

Figure 4. Histograms of FIME for heave, pitch, and vertical bending moment (VWBM) calculated with the 3D panel method

Table 2. Statistics (mean value and standard deviation) of data presented in Figures 2-4

	CFE		**ST**		**3D**	
	Mean value	σ	**Mean value**	σ	**Mean value**	σ
Heave (m)	1.09	0.30	1.05	0.12	0.98	0.14
Pitch (°)	0.99	0.22	1.06	0.18	0.98	0.10
VWBM (MNm)	1.25	0.33	1.00	0.22	1.12	0.26

Within the regression-based framework introduced for modelling epistemic uncertainty, the FIME data obtained for the considered set of ships are used to derive the corresponding regression parameters and to quantify the associated scatter. This step enables a practical implementation of the obtained results, linking the theoretical formulation of FIME with its statistical representation in terms of mean trends and standard deviations.

Regression analysis of FIME is carried out using the Real Statistics package in Excel, with intercepts and coefficients given in Table 3. The standard deviations, listed in Table 4, are calculated as the root mean square of the FIME deviations from the regression lines, as described in Section 2.1.4.

The results show that the uncertainty, expressed as the standard deviation, is highest for CFE and significantly lower for ST and 3D methods. For all methods, the largest uncertainty is observed for VWBM amidships, compared to heave and pitch, which is expected since VWBM is obtained by integrating local loads influenced by ship motions, leading to accumulation of errors.

Table 3. Intercepts and regression

	CFE			
	A	**B**	**C**	**D**
Heave	0.623	-0.000447	0.076	0.990
Pitch	0.540	-0.000527	0.135	0.950
VWBM	1.149	0.000040	0.640	-0.003
	ST			
	A	**B**	**C**	**D**
Heave	1.383	-0.000366	-0.107	-0.549
Pitch	1.033	0.000086	0.540	-0.159
VWBM	0.497	-0.000446	0.637	0.859
	3D			
	A	**B**	**C**	**D**
Heave	1.098	0	-0.177	0
Pitch	0.686	-0.000313	-0.184	0.589
VWBM	1.100	-0.000418	1.602	-0.151

Table 4. Standard deviations around regression lines for data presented in Figs. 2-4

	σ_{CFE}	σ_{ST}	σ_{3D}
Heave (m)	0.27	0.09	0.13
Pitch (°)	0.19	0.13	0.08
VWBM (MNm)	0.31	0.16	0.20

By comparing Table 4 and Table 2, one may conclude that the results are consistent, showing that more advanced methods (ST and 3D) yield lower uncertainty than CFE, while global loads exhibit higher variability than motions. No clear difference is observed between ST and 3D methods, in line with previous benchmark studies [37].

The application of multiple linear regression improves FIME estimates by removing bias and reducing standard deviations, although uncertainty remains relatively high for CFE. Part of the observed variability in ST and 3D methods arises from grouping different method subtypes; a more detailed, method-specific analysis would provide more accurate estimates but is difficult to implement.

The limitations of CFE follow those of the ordinary linear strip theory, including assumptions related to frequency range, Froude number, hull slenderness, and simplified hydrodynamic effects. Despite these limitations, CFE are applied here beyond their strict validity.

The presented results have practical application, as regression-based corrections can improve the accuracy of the transfer functions, while probabilistic modelling of FIME enables uncertainty quantification. Further developments may include frequency-dependent models and advanced techniques such as nonlinear regression or machine learning methods.

3.2. Probabilistic operability analysis

As a case study, the thesis considers a liner vessel operating in the Adriatic Sea (Figure 5). The ship design is based on a passenger vessel like those currently used on coastal and international routes in the Adriatic Sea. Its principal particulars, provided in Table 5 [38], are representative of vessels within the "larger ferry" category. The passenger ship operates between the Croatian port of Split and the Italian port of Ancona across the Adriatic Sea. The sailing headings are 275° from Split to Ancona and 95° in the opposite direction (0° corresponding to North). Operability criteria and ship loads are evaluated at four locations along the route (Figure 6). The four locations shown in Figure 6 correspond to points 10, 12, 15, and 18 in Figure 1. The vessel and the considered route are the same for Articles 2 and 3.

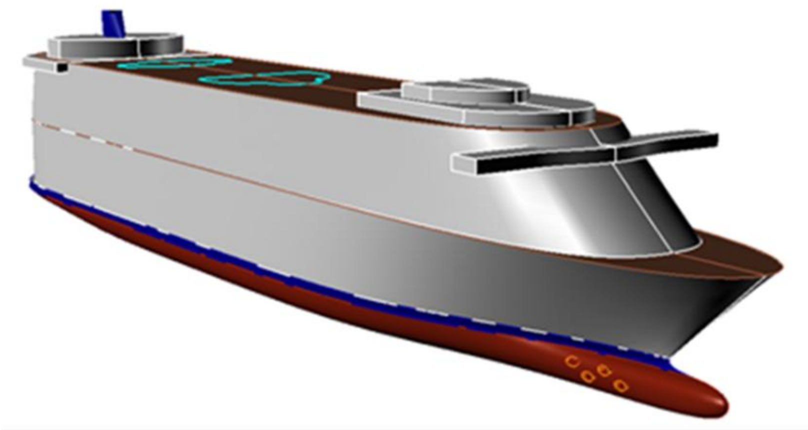

Figure 5. Model of the liner ship [38]

Table 5. Main particulars of the ship [38]

Feature	Value	Measuring unit	Description
L_{OA}	114	m	Length over all
L_{PP}	103.2	m	Length between perpendiculars
B	18.7	m	Breadth
T	5	m	Draft
V	17	kn	Maximum ship speed

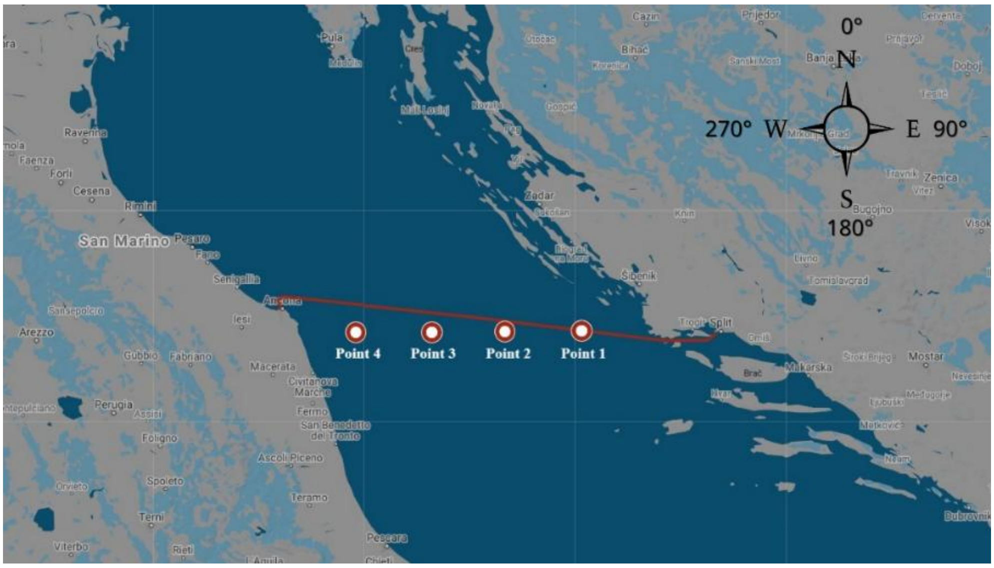

Figure 6. Points near the route Split-Ancona

3.2.1. Probabilistic operability diagrams

Cumulative probability distributions for each seakeeping limiting criterion in Table 1 are obtained using the procedure described in Section 2.2. For the nominal ship speed, and for each sea state defined by the significant wave height H_S and the wave spectrum presented in Article 2, as well as for each heading angle β, the probabilities of not satisfying the limit state functions given in Section 2.3 are calculated. Probability distribution functions for pitch, vertical acceleration at the forward perpendicular, slamming, and propeller emergence at a heading angle of 180°, as well as roll angle in beam seas ($\beta = 90°$), are presented in Figure 7.

Horizontal lines indicate exceedance probabilities of 5%, 50%, and 95%, corresponding to different values of H_S depending on the seakeeping criterion.

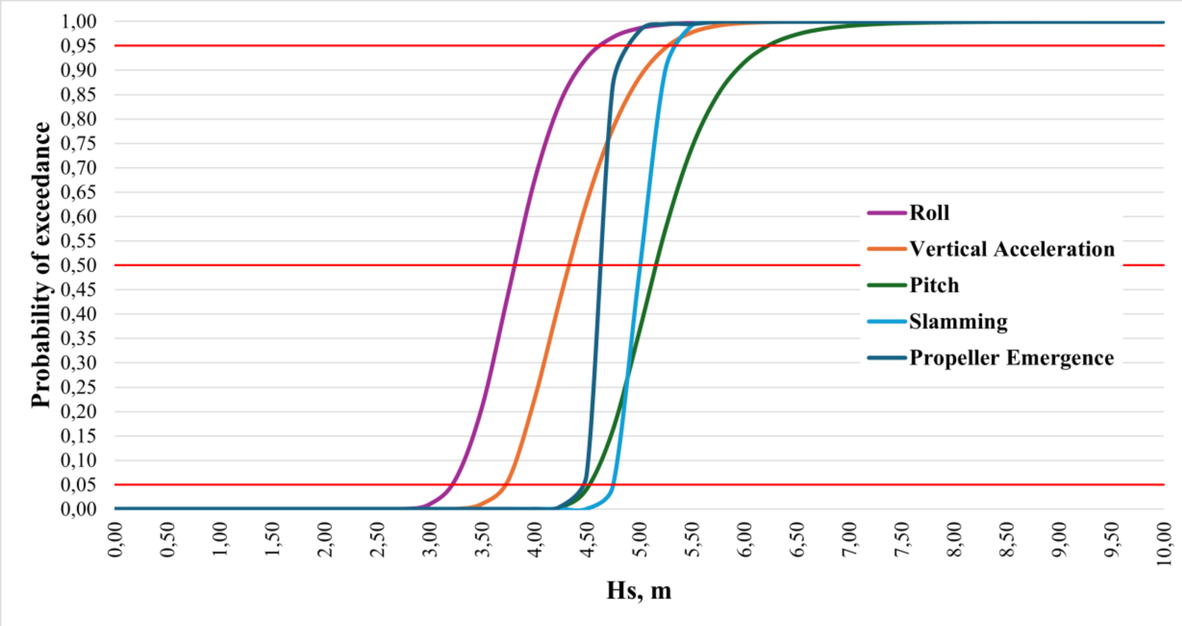

Figure 7. Cumulative probability distributions of exceedance of operability criteria in Table 1

Figure 7 shows that roll is the most critical criterion, as it reaches high exceedance probabilities at the lowest significant wave heights (H_s), indicating that it governs operability in milder sea states. In contrast, pitch is the least restrictive criterion, requiring the highest H_s values to reach the same probability levels. The differences between the criteria are most pronounced at the 50% exceedance level, where the spread in H_s is largest, while at 5% and 95% the spread of the curves is slightly reduced, indicating smaller relative sensitivity at very low and very high probabilities.

The results are further presented in the form of probabilistic operability diagrams. Separate diagrams are generated for 5%, 50%, and 95% exceedance probabilities, as shown in Figure 8, thereby transforming a single deterministic boundary into a family of probability-conditioned operability maps. The radial coordinate represents the sea state according to the Douglas scale shown in Table 6, while the angular coordinate denotes the heading angle between the ship and the waves, with 180° corresponding to head seas.

Table 6. Douglas scale of sea states

Degree	Wave height (m)	Description
0	0	Calm (glassy)
1	0-0.1	Calm (rippled)
2	0.1-0.5	Smooth (wavelets)
3	0.5-1.25	Slight
4	1.25-2.5	Moderate
5	2.5-4	Rough
6	4-6	Very rough
7	6-9	High
8	9-14	Very high
9	>14	Phenomenal

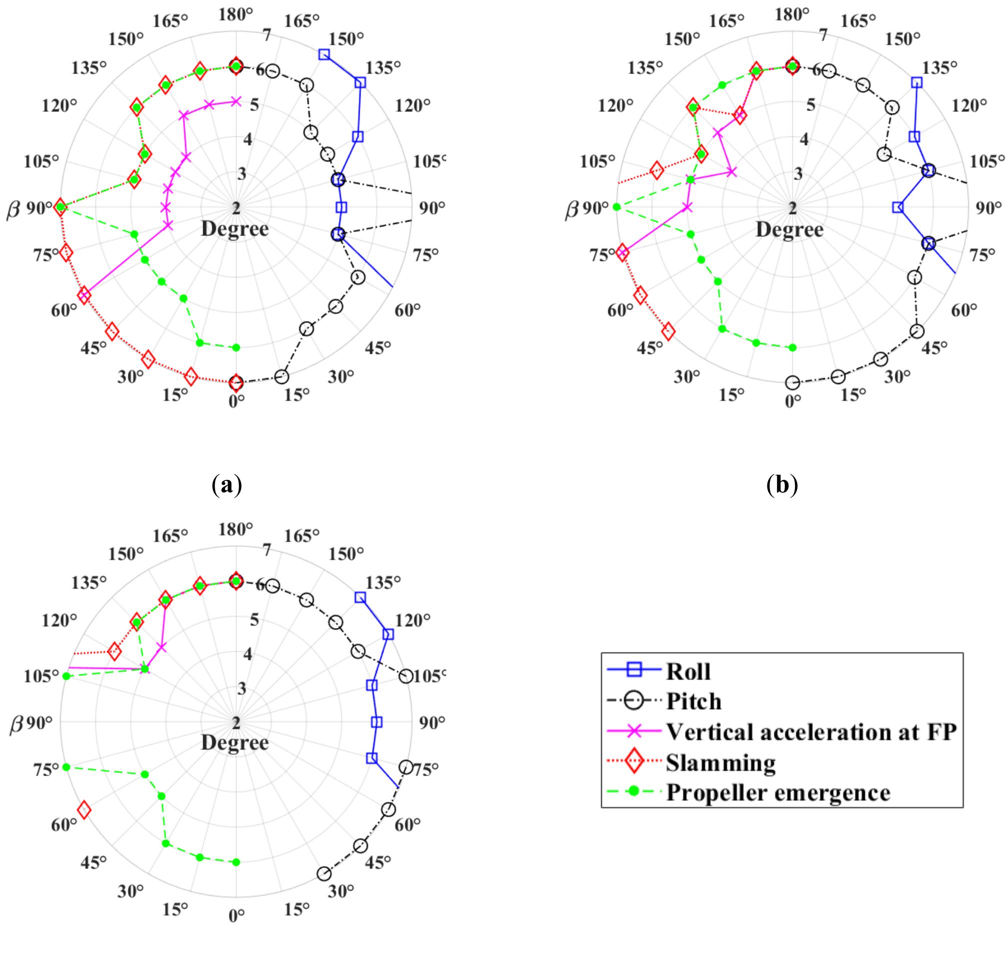

(a) (b) (c)

Figure 8. Polar plots for probabilities of exceeding limit states of: (a) 5%; (b) 50%; (c) 95%

The diagrams indicate that, as the probability level increases, more severe sea states, characterized by larger significant wave heights, are required to exceed the criteria. In the first diagram (5% exceedance probability), there is only a small likelihood of exceeding each criterion, representing the most conservative scenario. Such a diagram is relevant for risk-averse decision-makers, such as ship owners or masters who prefer to minimize operational risk. Conversely, at higher probability levels (e.g., 95%), the criteria are exceeded under less restrictive conditions, and the corresponding diagram may be considered by those willing to accept a higher level of risk, as the indicated operability limits are more likely to be exceeded. Overall, these results support the hypothesis that conventional deterministic operability diagrams should be extended using the proposed probabilistic approach to enable risk-based decision making.

3.2.2. Practical application of probabilistic approach

The probabilistic approach to operability diagrams can be used in ship design as a decision-making tool. The commonly used Operability Index (OI) is defined as the percentage of sea states in which the limiting significant wave height is not exceeded:

$$OI\ (\%) = \frac{\sum_{H_{\frac{1}{3}},T_P} n_{ss,\beta}\left(H_s < H_s^{lim}\right)}{N} \cdot 100, \tag{25}$$

where $n_{ss,\beta}$ is the number of sea states satisfying the operability criterion and N is the total number of sea states.

A probabilistic extension, the Probabilistic Operability Index (POI), accounts for both the occurrence frequency of sea states and the probability of satisfying the criteria:

$$POI\ (\%) = \sum\nolimits_{H_{1/3},T_P} f_{H_{1/3},T_p} P\left(H_s < H_s^{lim}\right) \cdot 100 \tag{26}$$

where f_{H_s,T_p} is the relative frequency of a sea state defined by H_s and T_p, given by:

$$f_{H_s,T_P} = \frac{n_{H_s,T_p}}{N} \tag{27}$$

with n_{H_s,T_p} being the number of occurrences of that sea state, and $P(H_s < H_s^{lim})$ the probability that the operability limit is not exceeded.

For the analyzed Adriatic route, POI = 98.7% and OI = 98.9% at 17 kn indicating minor difference between two approaches in this case. While POI is suitable for risk-based decision-making, incorporating corresponding operational costs is a complex task remaining beyond the scope of this study.

This approach can also support ship operation as a tactical decision tool. In heavy weather, operability plots allow the master to evaluate the effects of speed and course changes, as illustrated by the comparison of 17 kn and 5 kn conditions (Figure 9).

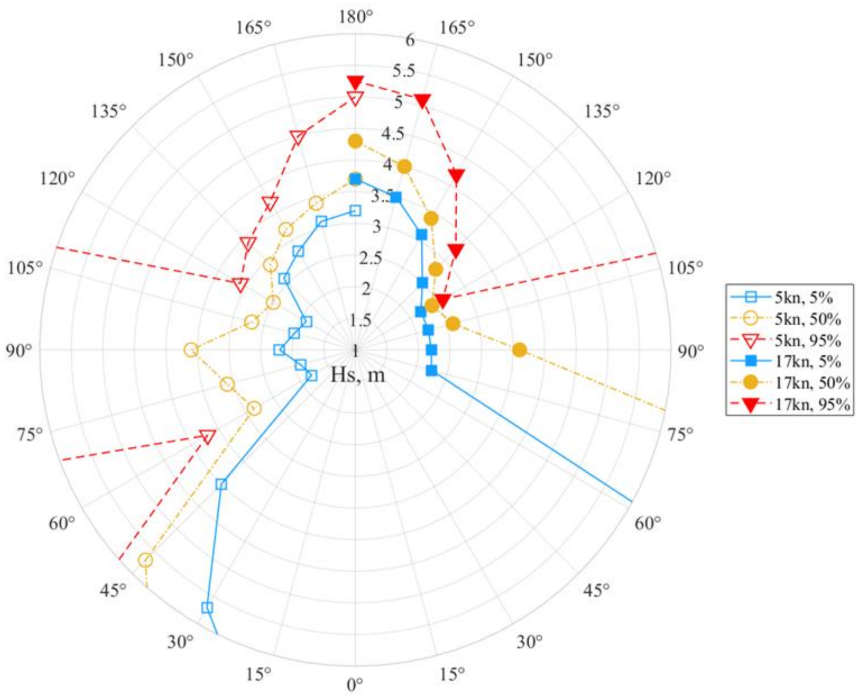

Figure 9. Polar plots representing the effect of ship speed on probabilities of exceeding limit states (Left: Ship speed 5 knots; Right: Ship speed 17 knots)

Operability diagrams enable the master to compare alternative actions, such as route adjustments or speed reduction, and assess their implications. This is demonstrated in Figure 9, where results for nominal (17 kn) and reduced speed (5 kn) are presented, illustrating how different operating conditions influence ship response and support informed maneuvering decisions. To fully exploit probabilistic nature of these diagrams within the risk-based framework, costs related to different maneuvers should be incorporated in the analysis.

3.2.3. Correlation with the experience on the shipping route

The vessel analyzed in this study is representative of ferries operating on the Ancona–Split route. Although detailed operational data are not available, insight can be obtained from documented heavy weather events in the Adriatic. Severe conditions are typically associated with the "jugo" wind, a south-easterly wind known to generate the highest waves in the region.

A notable incident occurred on November 1, 2012, when a ferry sailing from Ancona to Split experienced large roll motions during a storm, resulting in damage to 70 vehicles due to cargo shifting. The significant wave height reached 5.31 m, corresponding to Sea State 6 on the Douglas scale. Another event on December 23, 2024, caused a delay of approximately 6 hours, with reconstructed wave conditions indicating a maximum significant wave height of about 3.13 m (Sea State 5).

Long-term data show a maximum recorded wave height of 6.12 m (February 1, 1986). Sea State 5 occurs relatively frequently along the route, while more severe conditions (Sea State 6, $H_s >$ 4 m) occur on average once per year. These observations can be related to the operability diagrams in Figure 8, particularly for heading angles of 45° and 135°. The 5% exceedance level appears overly conservative, identifying even Sea State 4 as critical for vertical acceleration at the FP. In contrast, the 50% and 95% levels provide more realistic predictions, indicating reduced operability in Sea States 5 and 6. In Sea State 5, the most critical criteria are vertical acceleration at the FP and propeller emergence, while in Sea State 6 most operability limits are exceeded.

3.3. The long-term extreme wave loads

The method for the long-term extreme wave loads developed in Article 3 applies the seakeeping framework to a passenger ship, described in Section 3.2., sailing on the Split - Ancona route in the Adriatic Sea (Figure 5). Wave data are taken from a hindcast database at four points near the route for the period from January 1997 to January 2020, with a six-hour time step (Figure 6). For each recorded sea state and short-term most probable extreme values of the vertical wave bending moment are evaluated. The annual maxima are then extracted and fitted with the Gumbel distribution, which allows the determination of long return-period extreme values at each location.

The section is structured as follows: first, extreme VWBM distributions are analyzed at individual locations, considering the influence of operability criteria; this is followed by a system-level probabilistic assessment to establish bounds of extreme VWBM along the route. The effect of operational restrictions, such as speed reduction in severe sea states, is then examined, and the chapter concludes with a discussion of the results and their practical implications.

3.3.1. Probability distributions of extreme VWBM at individual locations

Short-term annual extreme VWBMs are evaluated at four locations along the route, considering both all sea states and only those satisfying operability criteria. Gumbel distributions are fitted to the VWBM histograms (Appendix A in [3]), although some deviations from the fitted distributions are observed. Nevertheless, the Gumbel model is retained due to its common use for extreme wave-induced responses [39].

For a 20-year return period ($F = 0.95$), the most probable long-term extreme VWBM is obtained from the fitted Gumbel distributions and presented in Table 7. The results show similar extreme values across locations when operability criteria are satisfied, while significantly higher values occur when these criteria are neglected.

Table 7. The most probable long-term extreme values of VWBM for 20 years-long return period at individual locations along the route [MNm]

Point (Figure 6)	**Long-term extreme VWBM for 20 years-long return period [MNm]**		
	All sea states	Sea states satisfying operability criteria	
		Split - Ancona 275°	Ancona – Split 95°
1	124	76	68
2	139	76	73
3	152	78	73
4	150	77	68

3.3.2. System probabilities

System probabilities of extreme VWBM for all sea states and for only those satisfying operability criteria are presented in Figure 10a and 10b respectively. The corresponding curves are obtained numerically using the procedure described in Section 2.6.3.

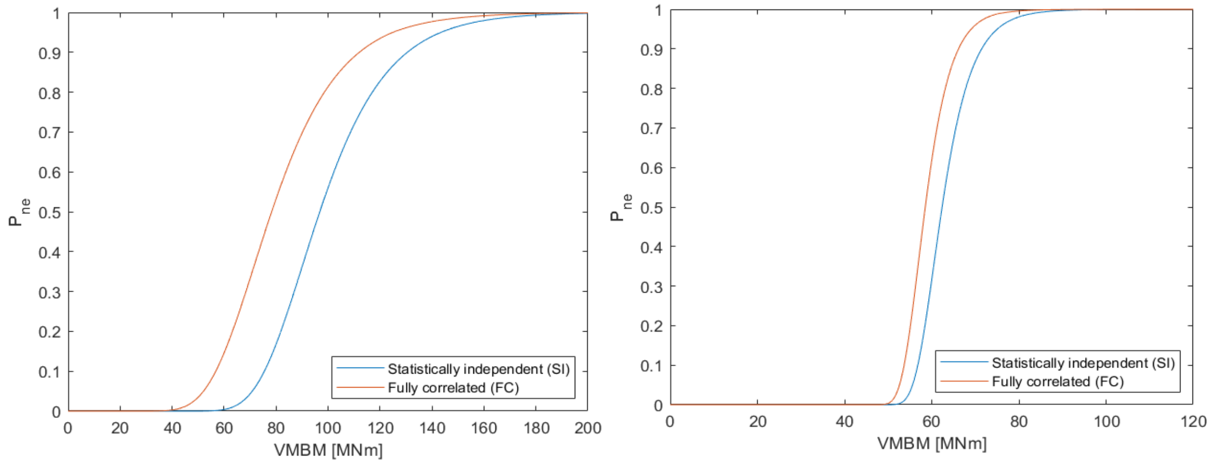

(a) **(b)**

Figure 10. System probabilities of non-exceedance of extreme VWBM calculated for: (a) all sea states; (b) sea states satisfying operability criteria

For the long return period of 20 years, system probability bounds of extreme VWBM can be determined from diagrams in Figure 10. These values are presented in Table 8, where the left column represents values determined from fully correlated system probabilities, and the right column represents statistically independent system probabilities.

Table 8. System probability bounds of extreme VWBM (left column – fully correlated extremes, right column – statistically independent extremes)

	VWBM [MNm] determined from $P_{ne,FC}$	**VWBM [MNm] determined from $P_{ne,SI}$**
All sea states	125	143
Sea states satisfying operability criteria	69	75

As shown in Table 8, operational restrictions have a significant impact, reducing extreme VWBMs by approximately half when applied. In addition, the assumption of statistical independence results in values that are about 10% higher than those obtained under the assumption of full correlation of extreme VWBM between locations. The assumption of the full correlation seems to be more realistic, as extreme VWBM at different locations along the route, are likely to occur during the same voyage.

3.3.3. The effect of the speed reduction in severe sea states

In Sections 3.3.1 and 3.3.2, extreme VWBMs are evaluated for a constant nominal ship speed of 17 knots. To assess the effect of speed reduction, the speed is decreased to 5 knots only for those sea states in which operability limits are exceeded. Histograms of annual maximum VWBMs for headings of 275° and 95°, together with the fitted Gumbel distributions, are provided in Appendix B in Article 3.

The most probable long-term extreme VWBMs for a 20-year return period at each location are presented in Table 9. System probabilities of non-exceedance are shown in Figure 11, while Table 10 summarizes the corresponding bounds of the most probable extreme values.

Table 9. The most probable long-term extreme values of VWBM for 20 years-long return period calculated for a speed of 5 knots on sea states exceeding operability criteria

	Long-term extreme VWBM for 20 years-long return period [MNm]	
Point (Figure 2)	Split – Ancona	Ancona - Split
	275°	95°
1	104	103
2	116	117
3	126	126
4	124	125

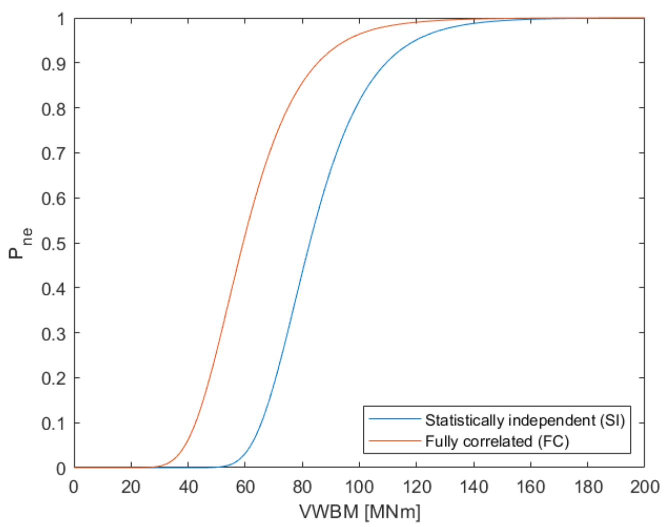

Figure 11. System probabilities of non-exceedance of extreme VWBM for reduced speed

Table 10. Bounds of extreme vertical bending moments calculated for speed of 5 kn on sea states exceeding operability criteria

VWBM [MNm] determined from $P_{ne,FC}$	VWBM [MNm] determined from $P_{ne,SI}$
95	120

The extreme values corresponding to a ship speed of 17 knots are shown in Table 8, determined from the diagrams shown in Figure 10. While Table 10 presents the results obtained for a reduced ship speed of 5 knots in sea states that do not satisfy the operability criteria. As can be seen, the extreme VWBM values given in Table 10 lie between the values obtained in Table 8.

The results indicate that reducing ship speed to 5 knots in sea states that do not satisfy the operability criteria leads to VWBM values that are intermediate between the two limiting cases: complete avoidance of all non-operable sea states and operation at full speed in all sea states. This behaviour is illustrated in Figure 12.

3.3.4. Discussion on extreme wave loads and limitations of the study

The most probable 20-year extreme VWBM along the route is summarized in Figure 12 for different assumptions regarding operability limitations and statistical correlation among the extremes along the shipping route. Operating at full speed in all sea states yields the highest VWBM, while excluding sea states that violate operability criteria reduces extremes by about 50%. If such states are not avoided but speed is reduced, extremes decrease by roughly 20%. Assuming full correlation between locations further lowers predicted extremes compared to the assumption of statistical independence.

The results are consistent with the conventional long-term analysis conducted, which produces similar extreme values, i.e. 145 MNm for a speed of 17 kn and 123 MNm for a speed of 5 kn. [40].

Although direct validation through full-scale measurements is limited, comparison with real incidents supports the findings. For example, a 2012 ferry accident under Sea State 6 conditions confirms that operability limits can be exceeded, particularly for roll, while other criteria may also be violated.

The methodology can be applied to other ship types and routes, although different operability limits and wave environments must be considered. While the Gumbel distribution is adopted for extreme value modelling, alternative distributions may be more appropriate in some cases. Reliable analysis requires sufficiently long wave records, and results may be sensitive to data length.

Finally, the study is based on linear wave loads; nonlinear effects, such as differences between sagging and hogging moments, may be significant and can be included through simplified corrections.

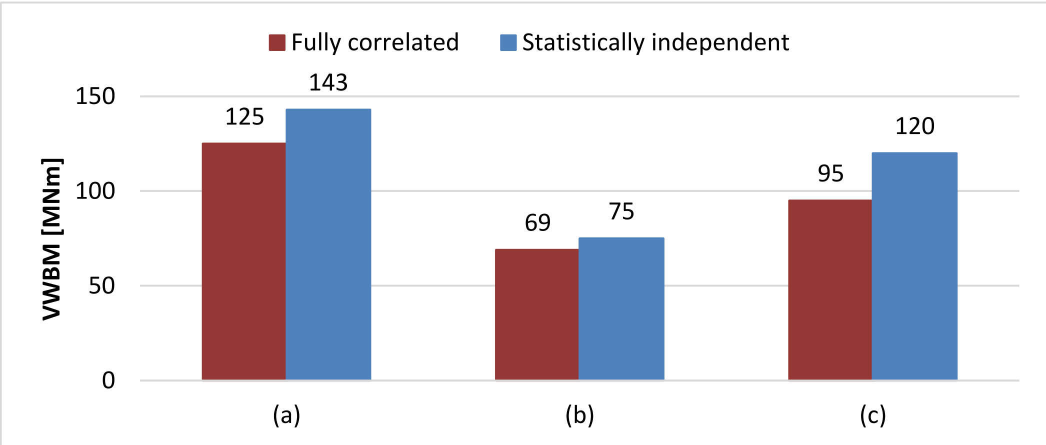

Figure 12. Comparison of extreme VWBMs determined from fully correlated and statistically independent system probabilities for (a) all sea states; (b) only sea states satisfying operability criteria with speed of 17 knots; (c) a case when ship speed is reduced to 5 knots on sea states not satisfying operability criteria

4. Conclusions

This thesis addresses uncertainties in seakeeping predictions and its implications for ship operability and wave load assessment. It combines model error quantification, probabilistic operability analysis, and long-term extreme load estimation into a unified framework applicable to both ship design and operation. In addition, knowledge and methods commonly used in ship structural reliability assessment are extended to probabilistic ship operability analysis. The work is based on three interconnected journal articles.

In Article 1, frequency-independent model errors of transfer functions obtained from closed-form expressions are quantified through comparison with experimental data for a diverse set of ships. The analysis shows that closed-form equations exhibit higher bias and variability than strip theory and 3D panel methods, while no clear difference is observed between the latter two. Uncertainty is consistently higher for global wave loads than for ship motions. The application of multivariate linear regression significantly improves predictions by removing bias and reducing variability, although uncertainty levels remain relatively high for closed-form expressions. The resulting probabilistic model of transfer function error enables correction of predictions and provides a basis for uncertainty-aware seakeeping analysis.

In Article 2, the uncertainties from Article 1 are incorporated into probabilistic operability assessment by treating both response predictions and limiting criteria as random variables. This leads to probabilistic operability diagrams, which describe the likelihood of exceeding seakeeping limits under given wave conditions. Compared to commonly used deterministic approaches, these diagrams provide a more informative basis for decision-making. The method is applicable both in early-stage ship design, through the introduction of a probabilistic operability index, and in ship operation, where it supports tactical decisions in heavy weather. Validation using numerical wave databases demonstrates the practical applicability of the approach.

Article 3 provides the framework for the estimation of long-term extreme wave loads along a shipping route. The method combines hindcast wave data at multiple locations with operability analysis and probabilistic modelling of extremes. Annual maxima are described using the Gumbel distribution for individual locations and then combined along the route under different assumptions regarding spatial correlation. The results show that operational constraints have a strong influence on extreme loads: avoiding non-operable conditions reduces extreme values of vertical wave bending moments by approximately half, while speed reduction leads to more moderate decreases. Accounting for spatial correlation further reduces predicted extremes. The proposed method is consistent with conventional long-term approach, while offering additional insight into the effects of operational decisions and environmental variability.

Overall, the thesis demonstrates that incorporating uncertainty into seakeeping and operability analysis leads to more realistic and practically relevant results. The developed methods enable improved assessment of ship performance, support risk-based decision-making, and provide a foundation for further extensions, including frequency-dependent uncertainty models and advanced data-driven approaches.

4.1. Future research

Several challenges remain in the development of a fully consistent probabilistic framework for ship operability. In particular, the definition of probabilistic models for operability limit criteria remains difficult. Initial attempts to address this issue through interviews with seafarers have not yet yielded satisfactory results, revealing notable differences in how operability is perceived and assessed by ship designers compared to those responsible for operating vessels in practice [41].

Further work should also focus on validation of seakeeping methods through full-scale measurements, which are essential for a more reliable quantification of modelling uncertainty. Previous studies conducted on smaller vessels have shown encouraging agreement between numerical predictions and measurements, except under specific conditions, such as stern-quartering seas, where discrepancies suggest that certain effects, such as Doppler shift, may not be adequately captured [42].

In addition, differences between spectral descriptions of sea states and their statistical representations require further investigation. Full-scale measurements have shown that statistically and spectrally derived parameters, such as mean zero up-crossing periods and significant wave heights, do not always coincide as it would be expected. [42].

Future research should also address economic and risk-based aspects related to operability criteria and voyage delays. Although the proposed Probabilistic Operability Index (POI) provides a suitable framework for risk-informed decision-making, its practical application requires estimating the consequences of non-fulfilment of operational criteria. These include delay-related costs such as additional fuel consumption, crew overtime, port penalties, and passenger compensation. Since such costs strongly depend on the operator and route characteristics, reliable data remains limited in the available literature. Integrating probabilistic operability assessment with cost models would therefore represent an important step toward practical decision-support risk-based tools for ship design and operation.

Bibliography

[1] Petranović, T.; Mikulić, A.; Gledić, I.; Parunov, J. Comparative analysis of closed-form expressions and other commonly used seakeeping methods. *Ocean Eng*. **2023**, *281*, 114977. [CrossRef]

[2] Petranović, T.; Parunov, J. Incorporating Epistemic Uncertainties in Ship Operability Study. *Appl. Sci.* **2025**, *15*, 4268. [CrossRef]

[3] Petranović, T.; Mikulić, A.; Katalinić, M.; Ćorak, M.; Parunov, J. Method for Prediction of Extreme Wave Loads Based on Ship Operability Analysis Using Hindcast Wave Database. *J. Mar. Sci. Eng.* **2021**, *9*, 1002. [CrossRef]

[4] Parunov, J.; Guedes Soares, C.; Hirdaris, S.; Wang, X. Uncertainties in modelling the low-frequency wave-induced global loads in ships. *Mar. Struct*. **2022**, *86*, 103307. [CrossRef]

[5] van Essen, S.; Bernardino, M.; Franz von Bock und Polach, R.U.; Martins Campos, R.; de Hauteclocque, G.; Dong, S.; Johannessen, T.B.; Vanem, E.; Bitner-Gregersen, E.M.; Lataire, E.; Soo Moon, J.; Polojärvi, A.; Prpić-Oršić, J.; Zhu, T. Committee I.1: Environment. In: Wu, W.; Ding, J. (eds) Proceedings of the 22nd International Ship and Offshore Structures Congress (Volume 3). ISSC 2025. Lecture Notes in Mechanical Engineering. Springer, Singapore. pp 1-27. [CrossRef]

[6] Abbasnia, A.; Coppola, T.; Diebold, L.; Dimitrios, K.; Fujarra, A.; Gaggero, T.; Hirdaris, S.; Jeon, G.Y.; Marcollo, H.; Oka, M.; Rodrigues, M.; Sazidy, M.; Sprenger, F.; Wellens, P.; Zhang, G. Committee I.2: Loads. In Proceedings of the 22nd International Ship and Offshore Structures Congress (Volume 3). ISSC 2025. Lecture Notes in Mechanical Engineering. Springer: Singapore, 2025; pp. 28–48. [CrossRef]

[7] Soares, C.G.; Bitner-Gregersen, E.; Brizzolara, S.; Ould el Moctar, B.; Papanikolaou, A.; Parunov, J.; Qiu, W.; Solomon, Y.; Tomoki, T.; Wang, X.; Waseda, T.; Zhang, H. Committee V.8: Uncertainty Modelling in Waves and Wave Responses. In: Proceedings of the 22nd International Ship and Offshore Structures Congress (Volume 3). ISSC 2025. Lecture Notes in Mechanical Engineering. Springer: Singapore, 2025; pp. 323–334. [CrossRef]

[8] Huges, O.F.; Paik, J.K., 2010. Ship structural analysis and design. SNAME: USA, 2010.

[9] de Hauteclocque, G.; Vitali Maretic, N.; Derbanne, Q. Hindcast based global wave statistics. *Appl. Ocean Res.* **2023**, *130*, 103438. [CrossRef]

[10] Bitner-Gregersen, E.M.; Waseda, T.; Parunov, J.; Yim, S.; Hirdaris, S.; Ma, N.; Guedes Soares, C. Uncertainties in long-term wave modelling. *Mar. Struct*. **2022**, *84*, 103217. [CrossRef]

[11] IACS Rec. No. 34. Rev. 2. Standard wave data. 2022

[12] IACS Rec. No. 34. Rev. 1. Standard wave data. 2001

[13] Austefjord, H.N.; de Hauteclocque, G.; Johnson, M.C.; Zhu, T. Update of wave statistics standards for classification rules. In Advances in the Analysis and Design of Marine Structures; Ringsberg, J.W., Soares, C.G., Eds.; CRC Press Balkema: Oxon, UK, 2023; pp. 95–205.

[14] Moan, T.; Shu, Z.; Drummen, I.; Amlashi, H. Comparative reliability analysis of ships-considering different ship types and the effect of ship operations on loads. In Proceedings of the International Conference on Maritime Safety and Operations, Glasgow, UK, 2006.

[15] Tezdogan, T.; Incecik, A.; Turan, O. Operability assessment of high speed passenger ships based on human comfort criteria. *Ocean Eng*. **2014**, *89*, 32–52. [CrossRef]

[16] Papanikolaou, A.; Mohammed, E.A.; Hirdaris, S.E. Stochastic uncertainty modelling for ship design loads and operational guidance. *Ocean Eng*. **2014**, *86*, 47–57. [CrossRef]

[17] Temarel, P.; Bai, W.; Bruns, A.; Derbanne, Q.; Dessi, D.; Dhavalikar, S.; Fonseca, N.; Fukasawa, T.; Gu, X.; Nestegård, A.; Papanikolaou, A.; Parunov, J.; Song, K.H.; Wang, S. Prediction of wave-induced loads on ships: Progress and challenges. *Ocean Eng*. **2016**, *119*, 274–308. [CrossRef]

[18] Hirdaris, S.E.; Bai, W.; Dessi, D.; Ergin, A.; Gu, X.; Hermundstad, O.A.; Huijsmans, R.; Iijima, K.; Nielsen, U.D.; Parunov, J.; Fonseca, N.; Papanikolaou, A.; Argyriadis, K.; Incecik, A. Loads for use in the design of ships and offshore structures. *Ocean Eng*. **2014**, *78*, 131–174. [CrossRef]

[19] Jensen, J.J.; Mansour, A.E.; Olsen, A.S. Estimation of ship motions using closed-form expressions. *Ocean Eng*. **2004**, *31*, 61–85. [CrossRef]

[20] Jensen, J.J.; Pedersen, P.T.; Shi, B.; Wang, S.; Petricic, M.; Mansour, A.E. Wave induced extreme hull girder loads on containerships. In Proceedings of the SNAME Maritime Convention, Houston, TX, USA, October 2008. [CrossRef]

[21] Nielsen, U.D.; Iseki, T. Prediction of first-order vessel responses with applications to decision support systems. In Proceedings of the SNAME Maritime Convention and 5th

World Maritime Technology Conference, Providence, RI, USA, November 2015. [CrossRef]

[22] Nielsen, U.D.; Mounet, R.E.G.; Brodtkorb, A.H. Tuning of transfer functions for analysis of wave–ship interactions. *Mar. Struct*. **2021**, *79*, 103029. [CrossRef]

[23] Ghaemi, M.H.; Olszewski, H. Total ship operability - review, concept and criteria. *Pol. Marit. Res*. **2017**, *24*, 74-81. [CrossRef]

[24] Katalinić, M.; Ćorak, M.; Parunov, J. Optimized wave spectrum definition for the Adriatic Sea. *Naše More*. **2020**, *67*, 19-23. [CrossRef]

[25] Cramer, E.H.; Hansen, P.F. Stochastic modeling of long term wave induced responses of ship structures. *Mar. Struct*. **1994**, *7*, 537–566. [CrossRef]

[26] Guedes Soares, C. Effect of transfer function uncertainty on short-term ship responses. *Ocean Eng*. **1991**, *18*, 329–362. [CrossRef]

[27] STRUREL, version 2021; Structural Reliability Analysis Programs - COMREL, SYSREL, COSTREL User Manual; RCP Consult GmbH: München, Germany, 2021.

[28] Bitner-Gregersen, E.M.; Skjong, R. Concept for a risk based navigation decision assistant. *Mar. Struct*. **2009**, *22*, 275–286. [CrossRef]

[29] Spanos, D.; Papanikolaou, A.; Papatzanakis, G. Risk-based onboard guidance to the master for avoiding dangerous seaways. In Proceedings of the 6th Osaka Colloquium on Seakeeping and Stability of Ships, Osaka, Japan, 26-28 March 2008.

[30] Katalinić, M.; Parunov, J. Comprehensive Wind and Wave Statistics and Extreme Values for Design and Analysis of Marine Structures in the Adriatic Sea. *J. Mar. Sci. Eng*. **2021**, *9*, 522. [CrossRef]

[31] Katalinić, M.; Parunov, J.; Mikulić, A. Toward operability analysis of a passenger ship in the Adriatic Sea based on the JONSWAP-Adriatic wave spectrum. In Proceedings of the 24th Symposium on Theory and Practice of Shipbuilding SORTA 2020, Malinska, Krk Island, Croatia, 15–17 October 2020.

[32] DNV GL. Class Guideline DNVGL-CG-0130: Wave Loads; Det Norske Veritas Germanischer Lloyd: Oslo, Norway, 2018.

[33] Mansour, A.; Liu, D. The Principles of Naval Architecture Series: Strength of Ships and Ocean Structures; The Society of Naval Architects and Marine Engineers: Jersey City, NJ, USA, 2008; pp. 4–56.

[34] Katalinić, M.; Parunov, J. Uncertainties of estimating extreme significant wave height for engineering applications depending on the approach and fitting technique - Adriatic Sea case study. *J. Mar. Sci. Eng*. **2020**, *8*, 259. [CrossRef]

[35] Mansour, A.E.; Preston, D.B. Return periods and encounter probabilities. *Appl. Ocean Res.* **1995**, *17*, 127–136. [CrossRef]

[36] Mikulić, A.; Katalinić, M.; Ćorak, M.; Parunov, J. The effect of spatial correlation of sea states on extreme wave loads of ships. *Ships Offshore Struct*. **2021**. [CrossRef]

[37] Parunov, J.; Guedes Soares, C.; Hirdaris, S.; Iijima, K.; Wang, X.; Brizzolara, S.; Qiu, W.; Mikulić, A.; Wang, S.; Abdelwahab, H.S. Benchmark study of global linear wave loads on a container ship with forward speed. *Mar. Struct*. **2022**, *84*, 103162. [CrossRef]

[38] Petranović, T.; Gledić, I.; Katalinić, M.; Matić, P.; Vujičić, S.; Parunov, J. Wave measurement in the Adriatic Sea using floating buoy. In Proceedings of the 25th Symposium on Theory and Practice of Shipbuilding SORTA 2022, Malinska, Croatia, 7-10 September 2022.

[39] DNV GL. Recommended Practice DNVGL-RP-C205: Environmental Conditions and Environmental Loads; Det Norske Veritas Germanischer Lloyd: Oslo, Norway, 2017; pp. 64-66.

[40] Ćorak, M.; Parunov, J.; Guedes Soares, C. Long-term prediction of combined wave and whipping bending moments of container ships. *Ships Offshore Struct*. **2015**, *10*, 4-19. [CrossRef]

[41] Ćorak, M.; Vujičić, S.; Petranović, T.; Parunov, J. Critical overview of the operability limiting criteria of passenger ships in the Adriatic Sea. In Trends in Maritime Technology and Engineering: Proceedings of the 6th International Conference on Maritime Technology and Engineering (MARTECH 2022), Lisbon, Portugal, 24–26 May 2022; Guedes Soares, C., Santos, T.A., Eds.; CRC Press: Boca Raton, FL, USA, 2022; pp. 1-7. [CrossRef]

[42] Petranović, T.; Katalinić, M.; Mihanović, H.; Parunov, J. Statistical and spectral description of full-scale measurements of ship motion in waves. In Theory and Practice of Shipbuilding: Proceedings of the 26th Symposium (SORTA 2024), Zadar, Croatia, 2-5 October 2024; Degiuli, N., Valčić, M., Bucci, V., et al., Eds.; IOS Press: Amsterdam, The Netherlands, 2024; pp. 126–138. [CrossRef]

Curriculum Vitae

Tamara Petranović was born on June 23, 1992, in Banja Luka, Bosnia and Herzegovina. She completed her secondary education at the Aeronautical Technical School "Rudolf Perešin". She earned a degree in Mechanical Engineering from the Faculty of Mechanical Engineering and Naval Architecture at the University of Zagreb (FAMENA UNIZG), specializing in Engineering Modelling and Computer Simulations. Her thesis topic was "Vehicle aerodynamics on bridges equipped with roadway wind barriers".

Since October 1, 2020, she has been employed as an Assistant at the Chair for Ship Structure Design at FAMENA UNIZG.

Tamara is also a co-author of 14 scientific papers published in journals and conference proceedings (ResearchGate profile, CroRIS profile, ORCID).

List of publications

Article 1

Petranović, T.; Mikulić, A.; Gledić, I.; Parunov, J. Comparative analysis of closed-form expressions and other commonly used seakeeping methods. *Ocean Eng*. **2023**, *281*, 114977. [CrossRef]

Article 2

Petranović, T.; Parunov, J. Incorporating Epistemic Uncertainties in Ship Operability Study. Appl. Sci. 2025, 15, 4268. [CrossRef]

Article 3

Petranović, T.; Mikulić, A.; Katalinić, M.; Ćorak, M.; Parunov, J. Method for Prediction of Extreme Wave Loads Based on Ship Operability Analysis Using Hindcast Wave Database. *J.* Mar. Sci. Eng. 2021, 9, 1002. [CrossRef]

Other publications

Parunov, J.; Petranović, T.; Ćatipović, I.; Katalinić, M.; Mihanović, H.; Prpić-Oršić, J. Amended comparison of full-scale measurements and seakeeping calculation for research vessel motion in the Adriatic Sea. In Innovations in the Analysis and Design of Marine Structures; Garbatov, Y., Guedes Soares, C., Eds.; CRC Press: London, UK, 2025; pp. 21–28. [CrossRef]

Petranović, T.; Katalinić, M.; Mihanović, H.; Parunov, J. Statistical and spectral description of full-scale measurements of ship motion in waves. In Theory and Practice of Shipbuilding: Proceedings of the 26th Symposium (SORTA 2024), Zadar, Croatia, 2-5 October 2024; Degiuli, N., Valčić, M., Bucci, V., et al., Eds.; IOS Press: Amsterdam, The Netherlands, 2024; pp. 126–138. [CrossRef]

Gledić, I.; Petranović, T.; Katalinić, M.; Vujičić, S.; Matić, P.; Ćatipović, I.; Parunov, J. Comparison of full-scale measurements and seakeeping calculations for two research vessels in the Adriatic Sea. *Ocean Eng*. **2022**, *266*, 113135. [CrossRef]

Petranović, T.; Parunov, J.; Guedes Soares, C. Concept of the probability-based ship operability analysis. In Advances in the Analysis and Design of Marine Structures: Proceedings of the 9th

International Conference on Marine Structures (MARSTRUCT 2023); Ringsberg, J.W., Ed.; CRC Press: London, UK, 2023; pp. 885–890.

Petranović, T.; Gledić, I.; Mikulić, A.; Parunov, J. Frequency independent model error of closed-form expressions for calculating wave-induced ship motions in vertical plane. In PRADS 2022 Proceedings; Fakultet strojarstva i brodogradnje Sveučilišta u Zagrebu: Zagreb, Croatia, 2022; pp. 883–893.

Vujičić, S.; Petranović, T.; Parunov, J.; Katalinić, M. The seaworthiness of a training ship "Naše more" in heavy seas. In Proceedings of the International Association of Maritime Universities (IAMU) Conference; Batumi State Maritime Academy: Batumi, Georgia, 2022; pp. 63–71.

Ćorak, M.; Vujičić, S.; Petranović, T.; Parunov, J. Critical overview of the operability limiting criteria of passenger ships in the Adriatic Sea. In Trends in Maritime Technology and Engineering: Proceedings of the 6th International Conference on Maritime Technology and Engineering (MARTECH 2022), Lisbon, Portugal, 24–26 May 2022; Guedes Soares, C., Santos, T.A., Eds.; CRC Press: Boca Raton, FL, USA, 2022; pp. 1-7. [CrossRef]

Katalinić, M.; Petranović, T.; Matić, P.; Parunov, J. Full-scale measurements of ship motion in rough seas in the Adriatic Sea. In Trends in Maritime Technology and Engineering, Vol. 1; CRC Press: London, UK; Delhi, India, 2022; pp. 365–371. [CrossRef]

Petranović, T.; Mikulić, A.; Katalinić, M.; Parunov, J. Operability study of passenger ship in the Adriatic Sea using a hindcast database. In Developments in the Analysis and Design of Marine Structures; CRC Press: London, UK; Delhi, India, 2021; pp. 10–17.

Petranović, T.; Gledić, I.; Katalinić, M.; Matić, P.; Vujičić, S.; Parunov, J. Wave measurement in the Adriatic Sea using floating buoy. In Proceedings of the 25th Symposium on Theory and Practice of Shipbuilding SORTA 2022, Malinska, Croatia, 7-10 September 2022.

Ćorak, M.; Vujičić, S.; Parunov, J.; Petranović, T. Practice-based operability limiting criteria in the Adriatic Sea. In International Conference on Sustainable Transport: Book of Abstracts; Pomorski fakultet Sveučilišta u Rijeci: Rijeka, Croatia, 2022; pp. 35–35.

Article 1

Article published by Elsevier in Ocean Engineering on 1 August 2023.
DOI: 10.1016/j.oceaneng.2023.114977

Ocean Engineering 281 (2023) 114977

Contents lists available at ScienceDirect

Ocean Engineering

journal homepage: www.elsevier.com/locate/oceaneng

Comparative analysis of closed-form expressions and other commonly used seakeeping methods

Tamara Petranović, Antonio Mikulić, Ivana Gledić, Joško Parunov *

University of Zagreb, Faculty of Mechanical Engineering and Naval Architecture, Ivana Lučića 5, 10002, Zagreb, Croatia

A R T I C L E I N F O

Handling Editor: Prof. A.I. Incecik

Keywords:
Seakeeping
Closed-form expressions
Strip theory
3D panel codes
Frequency independent model error
Multivariate linear regression

A B S T R A C T

Closed-form expressions (CFE) are semi-analytical transfer functions for ship wave-induced responses based only on main ship particulars. They are useful in an early stage of ship design and situations when hull lines for seakeeping analysis are not available. As the accuracy of CFE remains an open subject, the aim of the present study is to quantify the frequency independent model error (FIME) of CFE. Measured transfer functions of the heave, pitch, and vertical wave bending moment at midship for 13 ships are acquired from literature, together with calculated transfer functions using the strip theory and the 3D panel method, where several speeds and heading angles are available. FIME is determined by comparing transfer functions calculated by CFE, strip theory, and 3D panel codes with model-scale experiments. Multivariate linear regression analysis is performed for three seakeeping methods to indicate a dependence of FIME on the main parameters of the analysis. Dispersion of the FIME around the regression line is determined, enabling a relative comparison of the uncertainty of seakeeping methods of different complexity. The results of this study may improve the practical applicability of CFE and provide an uncertainty quantification of commonly used seakeeping methods, which is important for probability-based applications.

1. Introduction

Seakeeping refers to a ship's ability to withstand rough sea conditions. It is used as a part of a ship design spiral and to enhance the efficiency of operation for ships in service (Lloyd, 1998). As ships operate in a random wave environment, their wave-induced responses are usually determined by spectral analysis. Due to the request for reasonable computational efficiency, spectral analysis is performed, using transfer functions calculated by linear seakeeping methods, such as strip theory (ST) or 3D panel methods (Hirdaris et al., 2014; Temarel et al., 2016). The correction for non-linear effects may be imposed upon linear results (IACS Ltd, 2000). Evidently, on account of their importance, it becomes clear why there is a great interest in the engineering and research community regarding the uncertainty of predictions of transfer functions (Parunov et al., 2022a).

Closed-form expressions (CFEs) developed by Jensen et al. (2004) represent a rapid and simple method for calculating transfer functions of wave-induced motions and global loads of the monohull ship. These expressions only require the main ship particulars as input data, i.e., ship length, breadth, draught, block coefficient, forward speed, and heading angle. The formulae are semi-analytical, so they can be easily calculated using a usual spreadsheet application. CFEs are particularly suitable for seakeeping predictions in the conceptual design, enabling a rapid sensitivity analysis of the concept ship regarding operating profile and the wave scatter diagram (Jensen and Mansour, 2002). CFEs have been also used in studies of hydro-elastic responses (Jensen et al., 2008) and for the development of a method for the extreme values of wave loads using the hindcast wave database and accounting for ship operational restrictions (Petranović et al., 2021). Furthermore, CFEs are suitable for ships in service when hull lines are unavailable, yet ship operations must be optimized. Such applications include the development of decision support systems (DSS) (Nielsen and Toshio, 2015) and the tuning of the transfer function for the prediction of ship responses (Nielsen et al., 2021). CFEs can be potentially used for other applications where rapid seakeeping computations are required, e.g., for the development of the risk-based ship DSS for heavy weather manoeuvring. For such a software tool, where probabilistic methods are to be used for decision-making onboard the ship on heavy seas, numerical efficiency is obviously crucial (Papanikolaou et al., 2014).

In this paper, transfer functions of heave, pitch, and vertical wave

* Corresponding author.
E-mail address: josko.parunov@fsb.hr (J. Parunov).

https://doi.org/10.1016/j.oceaneng.2023.114977
Received 21 September 2022; Received in revised form 16 May 2023; Accepted 27 May 2023
0029-8018/© 2023 Elsevier Ltd. All rights reserved.

bending moment (VWBM) at midship calculated by CFEs are systematically compared to the transfer functions obtained from model-scale experiments, enabling the definition of the model uncertainty of the method. Furthermore, all the model-scale experiments chosen from the literature include comparisons with common methods for seakeeping analysis, such as ST and 3D panel methods, also allowing for uncertainty quantification with respect to these methods.

The approach used herein for the uncertainty assessment of ST and 3D panel methods is not fully consistent as there are different versions of ST and 3D panel methods (Hirdaris et al., 2014). The results used in the present comparison comprise ST and 3D methods formulated in the frequency and temporal domain. Moreover, some ST codes represent the so-called 2.5 strip theory, which is the method used for fast ships (DNV GL, 2018). Individual codes implementing the same theoretical method may also result in differences between transfer functions (Parunov et al., 2022b). To account for differences among seakeeping codes, uncertainty is divided into the uncertainty of each individual code with respect to the average of all codes to which the method pertains and the uncertainty of the method average with reference to the experimental results (Parunov et al., 2022b). Such an approach is difficult to perform in the present study as all ships should be analysed with the same seakeeping code. Therefore, the present study considers that all ST codes pertain to the same method and that all 3D codes also belong to the same method. This will result in a greater uncertainty as a mix of different theories is referred to, however such an approach is still adopted herein despite the relative inconsistency. For CFEs, however, such a consideration is not applicable, as this is a unique method which may be consistently employed in this comparison.

In this paper, the Frequency independent model rrror (FIME) is used as the uncertainty measure of transfer functions of vertical ship motions (heave and pitch) and vertical wave bending moments (VWBM) at midship. The FIME was initially developed by Guedes Soares (1991), however it has been recently used by Parunov et al. (2020, 2022b) in benchmark studies of ship global wave-induced responses. Furthermore, FIME is expressed as a linear function of main parameters which influence transfer functions, such as the block coefficient, Froude number, and the relative heading angle. Multiple linear regression analysis is used for this purpose, and it is adopted separately for all three methods (CFE, ST, and 3D). FIME calculated by the regression analysis may be used to improve the accuracy of the prediction by eliminating the bias of methods, i.e., results acquired by regression analysis represent the best estimate of each method. However, there is still a dispersion of FIME around the regression line, which may be described using the standard deviation. Such a full uncertainty description may be used in probabilistic-based approaches and represents the main contribution of the present study.

The rest of this paper is structured as follows. To provide an understanding of the methods used, Section 2 describes CFEs, and Section 3 explains FIME. The ships which constitute the subject of research are described in Section 4. Comparisons of transfer functions are presented in Section 5, while FIME results are provided in Section 6. In Section 7, multivariate linear regression is performed, and its results are presented. Finally, the discussion and conclusions are given in Sections 8 and 9, respectively.

2. Closed-form expressions

Frequency response functions of wave-induced motions and loads for monohull ships can be calculated by Closed-form expressions as developed by Jensen et al. (2004) and Jensen and Mansour (2002).

Semi-analytical CFEs are derived for the motion of the prismatic barge in the vertical plane, using common assumptions of the linear strip theory and, furthermore, by neglecting the coupling terms between heave and pitch, and finally assuming a constant sectional added mass equal to the displaced water (Jensen et al., 2004). In addition to the ship speed and heading angle, only basic ship particulars are required in CFEs, such as ship length, breadth, draught, and the block coefficient. The sectional hydrodynamic damping is approximated using a dimensionless ratio between the incoming and the diffracted wave amplitudes, with regard to which details are provided in the work of Jensen et al. (2004).

Table 1
Terms of Eqs. (2.1) and (2.2).

Term	Unit	Description
a	–	Wave amplitude
A	–	Approximation of the sectional hydrodynamic damping given in Jensen et al. (2004)
B	m	Ship breadth
F	–	Heave forcing function, given in Jensen et al. (2004)
G	–	Pitch forcing function, given in Jensen et al. (2004)
k	1/m	Wave number
t	s	Time
T	m	Ship draught
w	m	Heave amplitude
α	–	Parameter
θ	rad	Pitch amplitude
ω	rad/s	Wave frequency
$\overline{\omega}$	rad/s	Encounter frequency

Heave and pitch motions in regular waves with amplitude a are described by equations:

$$2\frac{kT}{\omega^2}\ddot{w}+\frac{A^2}{kB\alpha^3\omega}\dot{w}+w=aFcos(\overline{\omega}t), \tag{2.1}$$

$$2\frac{kT}{\omega^2}\ddot{\theta}+\frac{A^2}{kB\alpha^3\omega}\dot{\theta}+\theta=aGcos(\overline{\omega}t), \tag{2.2}$$

the terms of which are described in Table 1.

The encounter frequency $\overline{\omega}$ is given as:

$$\overline{\omega}=\omega-kVcos\beta\equiv\alpha\omega, \tag{2.3}$$

Parameter α is defined as

$$\alpha=1-Fn\sqrt{kL}cos\,\beta. \tag{2.4}$$

β in Eq. (2.3) is the heading angle, L is ship length, and Fn in Eq. (2.4) is a Froude number. Analytical solutions of Eqs. (2.1) and (2.2) lead to the transfer functions of heave (H_H) and pitch (H_P):

$$H_H=\eta F, \tag{2.5}$$

$$H_P=\eta G \tag{2.6}$$

where:

$$\eta=\left(\sqrt{\left(1-2kT\alpha^2\right)^2+\left(\frac{A^2}{kB\alpha^2}\right)^2}\right)^{-1}. \tag{2.7}$$

A corresponding formula for a transfer function H_M for the wave-induced vertical bending moment amidships has been derived and validated in Jensen and Mansour (2002):

$$H_M=\kappa\frac{1-kT}{\left(k_eL\right)^2}\left[1-cos\left(\frac{k_eL}{2}\right)-\frac{k_eL}{4}sin\left(\frac{k_eL}{2}\right)\right]F_V(Fn)F_C(Cb)\sqrt[3]{|cos\,\beta|}. \tag{2.8}$$

The correction factor for the block coefficient $F_C(Cb)$ reads:

$$F_C(Cb)=\left[(1-\vartheta)^2+0.6\alpha(2-\vartheta)\right]\ \vartheta=2.5(1-C_b)C_b=\max\,(0.6,C_b), \tag{2.9}$$

and the correction factor for speed, which is validated for $Fn<0.3$ only, reads:

$$F_V(Fn) = 1 + 3Fn^2. \quad (2.10)$$

The Smith correction factor κ from Eq. (2.8) is approximated by:

$$\kappa = \exp(-k_e T), \quad (2.11)$$

where the effective wave number k_e is:

$$k_e = |k\cos\beta|. \quad (2.12)$$

3. Frequency independent model error

The model uncertainty in transfer functions can be assessed by a comparison of seakeeping calculations with the results of experimental measurements. Transfer functions calculated with CFE are compared to experimental measurements in towing tanks obtained from the literature. As most of the published experiments contain comparisons of measurements to strip theory or 3D panel theory, it is also possible to assess the model uncertainty of those seakeeping methods.

Comparisons of different seakeeping calculation methods to experimental results are usually made only visually, with intuitive conclusions about the precision of linear seakeeping theories. So, the Frequency independent model error (FIME) φ is proposed by Guedes Soares (1991) for the formulation of the model uncertainty of transfer functions, and it presents a quantitative approach to exclude intuitive conclusions regarding uncertainties. If the computed transfer functions were multiplied by a constant factor φ, the transfer functions could be altered to match, on average, the experimental measurements. As a result, the FIME reflects a systematic error, so the bias of the computational method may be reduced (Parunov et al., 2022a). The random dispersion of the experimental results relating to altered transfer function would then represent the uncertainty.

Thus, the measurement $\widehat{H}_i$ of the i-th transfer function can be expressed as:

$$\widehat{H}_i = \varphi H_i + \varepsilon_i, \quad (3.1)$$

where H_i is the calculated value of the transfer function at the frequency ω_i and ε_i is a random error in the measurement made at the same frequency. In Eq. (3.1), it is assumed that measurement errors are independent of wave frequency. The value of FIME, i.e., φ can be approximated by minimizing the sum of the squares of the errors:

$$Q = \sum_i (\widehat{H}_i - \varphi H_i)^2 = \sum_i \varepsilon_i^2. \quad (3.2)$$

The equation for FIME is obtained by differentiating Q with respect to φ and equating it to zero:

$$\varphi = \frac{\sum_i \widehat{H}_i H_i}{\sum_i H_i^2}. \quad (3.3)$$

FIME φ represents the slope of the regression line of experimental vs. computed transfer functions, which is forced to pass through the origin, and it provides information on whether the seakeeping method overestimates or underestimates measurements. FIME larger than 1 suggests that theory underestimates measurements, whereas FIME less than 1 shows that theory overestimates experimental values.

4. Database of ship models

CFEs are employed to calculate transfer functions for heave, pitch, and VWBM amidships for 13 different ships, for which model scale experiments of ship motions and global loads are available in the literature. For most of the models, transfer functions obtained by ST and/or the 3D panel method are also available in addition to the experimental results. Ships and their scaled models used in this study are described below. Lengths of the ships between perpendiculars (L_{pp}), their block coefficients (C_b), Froude numbers (F_n), and headings (β) used in the paper are presented in Table 2.

Table 2
Ships and their lengths between perpendiculars, block coefficients, Froude numbers, and headings.

Ship	*Lpp* [m]	*Cb*	*Fn*	*β* [°]
Canadian frigate (CF) (McTaggart et al., 1997)	124.5	0.50	0.12	180
			0.21	180
RNLI's lifeboat (Prini et al., 2021)	15.57	0.37	0	180
			0.2	180
			0.4	180
			0.6	180
			0.8	180
			0	135
			0	90
			0	45
			0	0
6750 TEU container ship (CS) (Kim and Kim, 2016)	286.6	0.61	0	180
Chemical tanker (CT) (Ley and Moctar, 2021)	161	0.75	0	180
LNG carrier (LNG) (Ley and Moctar, 2021)	186.9	0.73	0	180
Large containership (LC) (Ley and Moctar, 2021)	333.44	0.62	0.13	180
Cruise ship (C) (Ley and Moctar, 2021)	216.8	0.65	0.07	180
Container ship (CS) (Parunov et al., 2022b)	2	0.60	0.245	45
			0.245	135
	70		0.245	180
S175 container ship (CS) (ITTC, 2011)	175	0.57	0.275	120
6500 TEU container ship (CS) (Graefe et al., 2014)	286.3	0.62	0.05	0
			0.05	180
			0	180
			0.1	180
			0.15	180
DTMB 5415 hull (Parunov et al., 2020; Lee et al., 2012)	142.04	0.49	0	180
			0	135
			0	90
			0	45
Fast monohull (FM) (Guedes Soares et al., 2004)	122	0.489	0.2	180
Panamax oil product tanker (OT) (Ćatipović et al., 2018)	174.73	0.795	0.087	180

A warship Canadian Patrol Frigate (CPF) has a length between perpendiculars of 124.5 m and a displacement of 4655 tonnes. A scaled model of the CPF with a scale of 1/20 was used in the experimental measurements, which were taken at The Institute for Marine Dynamics (IMD) in St. John's, Newfoundland. The Clearwater Towing Tank (200 m long x 12 m wide x 7 m water depth) was used for tests in head seas, and the Offshore Engineering Basin (75 m long x 32 m wide x 3.5 m water depth) was used for oblique seas tests and a few head seas tests to ensure consistency with towing tank tests. The model tests are provided for regular and irregular waves. Regular and irregular wave tests were conducted at different Froude numbers (0.06, 0.12, 0.21, 0.25) and headings (180°, 165°, 150°, 135°) (McTaggart et al., 1997).

A lifeboat is a high-speed vessel that operates in heavy conditions. The United Kingdom and the Republic of Ireland use the Royal National Lifeboat Institution's (RNLI's) Severn Class lifeboat as a 24-h maritime search and rescue service. The Severn is a monohull with a maximum speed of 25 knots and with a displacement of 42 tonnes. The model scale used for the study was 1/13.5. All experiments were performed in the towing tank at Newcastle University (37 m long x 3.7 m wide x 1.25 m depth of water). The experiment was divided into two groups of tests. The forward speed tests ($\beta = 180°$) are comprised in the first group at Froude numbers 0.2, 0.4, 0.6, and 0.8, and zero speed tests ($F_n = 0$) at headings 0°, 45°, 90°, 135°, 180°, 225°, 270°, and 315° (Prini et al., 2021) are present in the second group of tests.

The experiments on the 6750 TEU container ship were performed by the Korea Research Institute of Ships and Ocean Engineering/Korea Institute of Ocean Science and Technology (KRISO/KIOST) using the model scale of 1/70. Conditions of the experiments were adjusted differently for linear transfer functions and nonlinear responses, so for

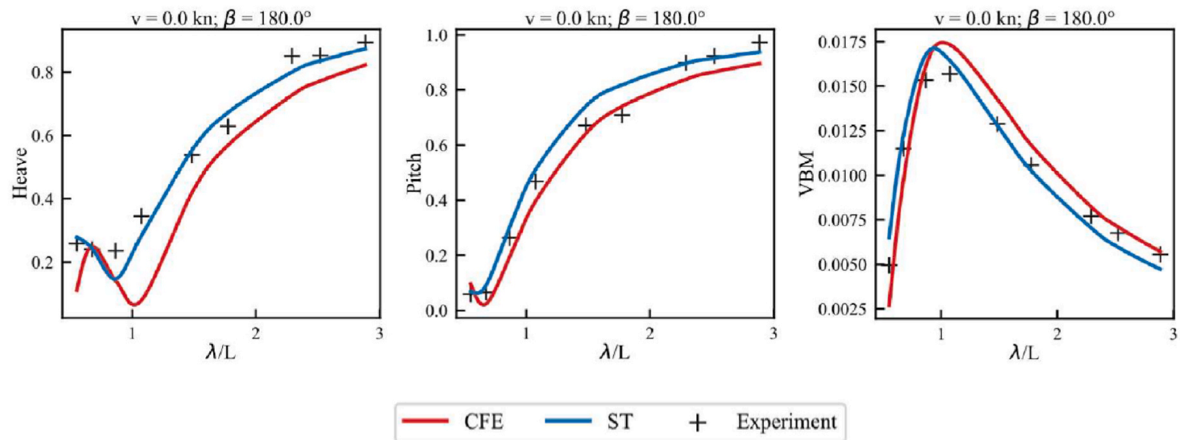

Fig. 1. Transfer functions for heave (left), pitch (centre), and vertical bending moment (right) of the 6750 TEU container ship.

linear response $\beta = 180^\circ$ and $F_n = 0$, and for nonlinear responses $\beta = 180^\circ$ and $F_n = 0.5$, 0.12 (Kim and Kim, 2016).

Model tests with a scale of 1/80 for the large post-Panamax container ship were conducted at Canal de Experencias Hidrodinámicas Del Pardo (CEHIPAR) (150 m long x 30 m wide x 5 m depth of water), and the model was tested at two full-scale speeds of 15 knots ($F_n = 0.13$) and 22 knots ($F_n = 0.2$) in head seas ($\beta = 180^\circ$) (Ley and Moctar, 2021).

Model tests of the Flokstra container ship were conducted in the Seakeeping Basin of Marin (170 × 40 × 5 m) at a scale of 1/55. Measurement results were reported for Froude number $F_n = 0.245$ and headings $\beta = 180^\circ$, 135°, and 45° (Parunov et al., 2022b, Abdelwahab et al., 2023).

Experiments for the S175 containership were conducted for linear analysis at headings $\beta = 0^\circ$, 90°, 120°, 180°, and Froude number $F_n = 0.275$, and for nonlinear analysis at heading $\beta = 180^\circ$ and Froude numbers $F_n = 0.2$, 0.25, 0.275 (ITTC, 2011).

In the collaborative industrial project WILS, a 1/55 scaled model of the 6500 TEU container ship was evaluated by the Maritime and Ocean Engineering Research Institute (MOERI). Tests were conducted in head seas at Froude numbers $F_n = 0$, 0.05, 0.1, 0.15, and in the following seas at Froude number $F_n = 0.05$ (Graefe et al., 2014).

Experimental model tests for the chemical tanker and the liquified natural gas (LNG) carrier were conducted at the Technical University of Berlin (100 m long x 8 m wide x 1 m water depth) at head seas and zero speeds on the 1/70 scaled models (Ley and Moctar, 2021).

Experimental measurements of the model of the cruise ship were conducted at CEHIPAR at head seas and $F_n = 0.07$. The model was scaled to 1/50 (Ley and Moctar, 2021).

Model tests of the fiberglass model of the DTMB 5415 hull were conducted at the Newcastle University Towing Tank (37 × 4 × 1.2 m). A model was scaled 1/100, and tests were conducted at zero speeds and headings $\beta = 180^\circ$,135°, 90°, 45° (Lee et al., 2012; Parunov et al., 2020).

A fast monohull with a length between perpendiculars of 122 m and a maximum speed of 27 knots has been tested as a segmented model in experimental measurements at CEHIPAR. The model is tested at head seas and Froude number $F_n = 0.02$ (Guedes Soares et al., 2004).

The ship model of the Panamax oil product tanker was made of wood at a scale of 1/28.8, and it was tested at the Brodarski Institut in Zagreb at head seas and Froude number $Fn = 0.087$. The towing tank is 276.3 m long, 12.5 m wide, and has a water depth of 6.0 m (Ćatipović et al., 2018).

The present study targets ocean-going ships with more than 90 m in length, sailing with low Froude number (less than 0.4). One of ships from the database is a lifeboat of 15.57 m in length and operating with large Froude numbers, which is clearly outside the range of ships covered by this study. However, as majority of experiments on this high-speed vessel are performed for low, or even zero Froude number, and since the experiments are well documented and performed recently, the vessel is included in the database. Rare data points outside the main intended range of parameters will not affect significantly results of the multiple regression analysis, described in Section 6. It is also to mention that in engineering practice, potential theory valid for low Froude numbers is often extended for smaller vessels and for higher Froude numbers, although this is not theoretically consistent.

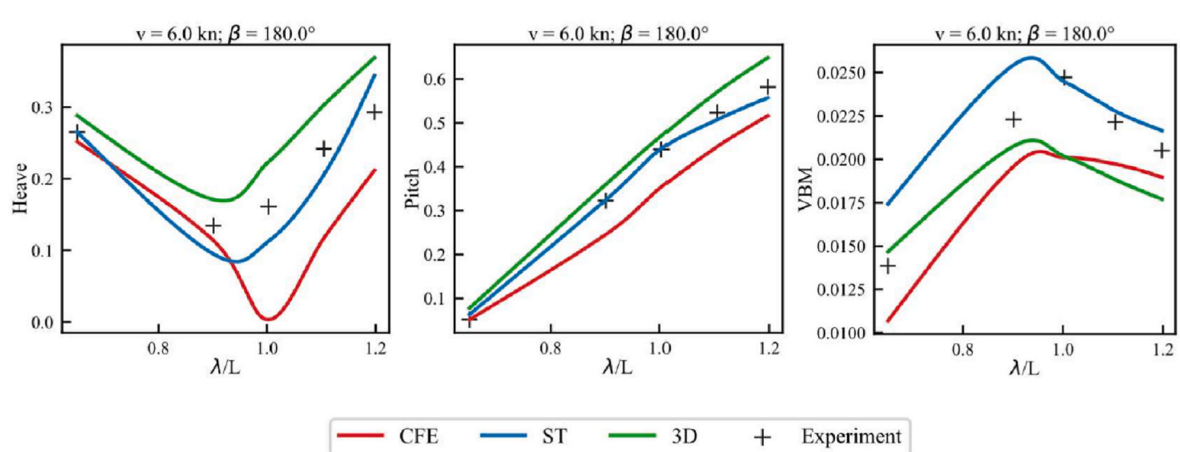

Fig. 2. Transfer functions for heave (left), pitch (centre), and VWBM (right) of the cruise ship.

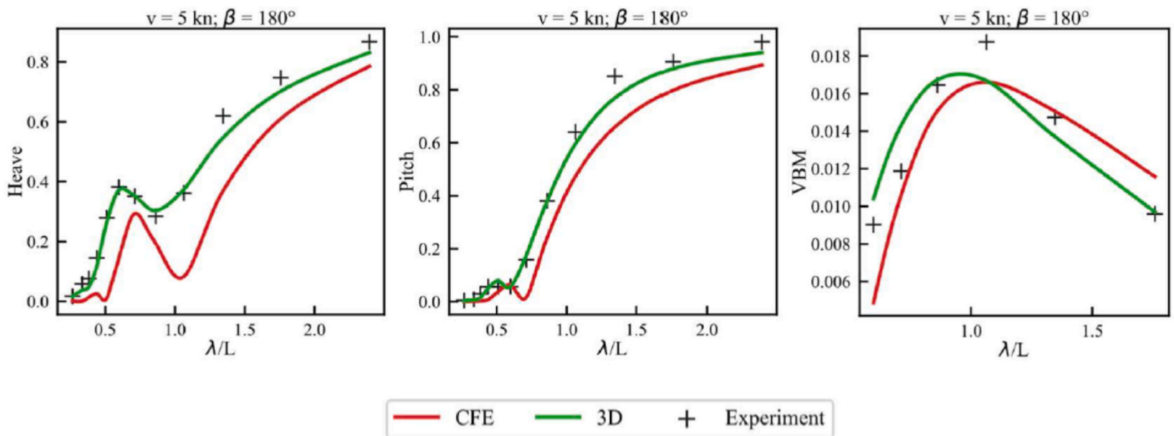

Fig. 3. Transfer functions for heave (left), pitch (centre), and VWBM (right) of the 6500 TEU container ship.

Table 3
FIME for transfer functions of heave φ_h, pitch φ_p, and VWBM φ_M calculated with CFEs, strip theory (ST), and the 3D panel method (3D).

Ship	β [°]	F_n	*CFE*			ST			3D		
			φ_h	φ_p	φ_M	φ_h	φ_p	φ_M	φ_h	φ_p	φ_M
CF (McTaggart et al., 1997)	180	0.12	1.32	0.92	1.06	1.12	0.97	0.76	1.03	0.97	0.89
	180	0.21	–	–	0.93	–	–	0.83	–	–	0.93
RNLI (Prini et al., 2021)	180	0	1.22	0.92	1.42	1.21	0.99	0.85	–	–	–
	180	0.2	0.66	0.71	1.55	1.01	1.22	0.82	–	–	–
	180	0.4	0.53	0.64	1.75	1	1.23	0.92	–	–	–
	180	0.6	0.62	0.66	1.61	1.06	1.31	1.17	–	–	–
	180	0.8	1.22	1.39	1.28	1.1	1.58	1.12	–	–	–
	135	0	1.06	0.71	1.23	1.31	0.84	0.63	–	–	–
	90	0	0.56	–	–	0.98	–	–	–	–	–
	45	0	1.03	0.76	1.34	1.25	1.1	0.85	–	–	–
	0	0	1.21	0.88	1.33	1.15	1.05	0.94	–	–	–
CS (Kim and Kim, 2016)	180	0	1.14	1.06	0.95	1.02	0.97	0.97	–	–	–
CT (Ley and Moctar, 2021)	180	0	1.05	1.08	1.33	0.94	1.1	1.09	1.03	1.02	0.97
LNG (Ley and Moctar, 2021)	180	0	1.02	1.17	1.14	0.92	1.14	0.94	0.97	1	1.02
LC (Ley and Moctar, 2021)	180	0.13	1.98	1.26	1.25	–	–	–	1.15	0.98	1.06
C (Ley and Moctar, 2021)	180	0.07	1.28	1.18	1.16	1	1.02	0.93	0.81	0.91	1.13
CS (Parunov et al., 2022b)	45	0.245	1.59	1.23	1.24	1.14	0.94	1	1.37	1.14	1.5
	135	0.245	0.91	0.73	1.47	0.81	0.84	1.3	0.74	0.8	1.25
	180	0.245	1.48	0.87	1.44	0.9	0.91	1.31	0.78	0.89	1.35
CS (ITTC, 2011)	120	0.275	1.13	0.79	2.08	–	–	–	0.9	0.88	1.71
CS (Graefe et al., 2014)	0	0.05	1.11	1.1	0.86	–	–	–	0.98	0.97	0.84
	180	0.05	1.27	1.19	1.06	–	–	–	1.05	1.05	0.99
	180	0	1.18	1.11	1.1	–	–	–	0.98	0.98	1.01
	180	0.1	1.21	1.11	1.52	–	–	–	1	1.02	1.36
	180	0.15	1.15	1.01	1.6	–	–	–	0.97	1	1.37
DTMB (Parunov et al., 2020; Lee et al., 2012)	180	0	1.09	1.17	0.69	0.97	0.85	1.31	0.97	0.93	0.99
	135	0	0.91	0.73	–	–	–	–	–	–	–
	90	0	0.74	–	–	1.02	–	–	0.96	–	–
	45	0	1.11	1.37	0.79	1.07	1	0.8	1.08	0.97	1.11
FM (Guedes Soares et al., 2004)	180	0.2	1.04	0.86	0.55	0.99	0.99	1.43	–	–	–
OT (Ćatipović et al., 2018)	180	0.087	1	1.15	1.22	–	–	–	0.93	1.22	0.69

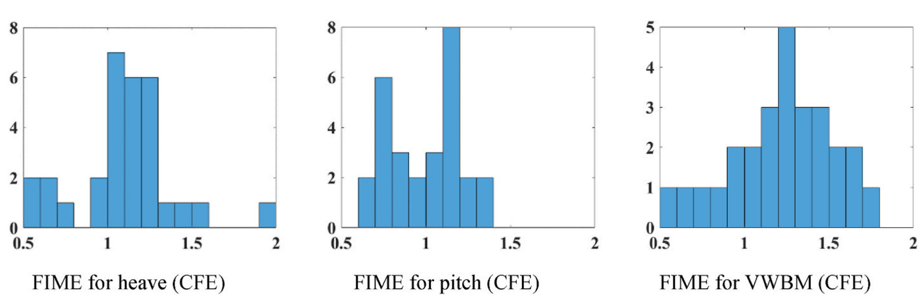

Fig. 4. Histograms of FIME for heave, pitch, and vertical bending moment (VWBM) calculated with CFEs.

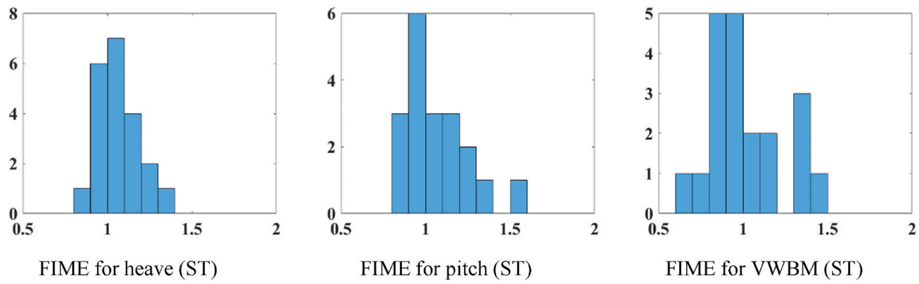

Fig. 5. Histograms of FIME for heave, pitch, and vertical bending moment (VWBM) calculated in accordance with strip theory, the results of which are obtained from literature.

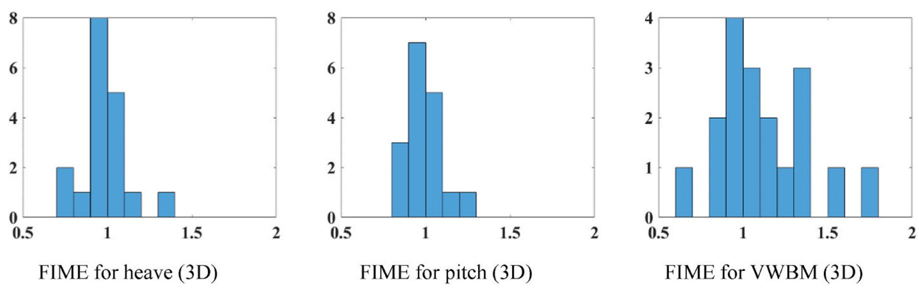

Fig. 6. Histograms of FIME for heave, pitch, and vertical bending moment (VWBM) calculated with the 3D panel method, the results of which are obtained from literature.

Table 4
Statistics (mean value and standard deviation) of data presented in Figs. 4–6.

	CFE		ST		3D	
	Mean value	σ	Mean value	σ	Mean value	σ
Heave	1.09	0.30	1.05	0.12	0.98	0.14
Pitch	0.99	0.22	1.06	0.18	0.98	0.10
VWBM	1.25	0.33	1.00	0.22	1.12	0.26

5. Comparison of transfer functions

Transfer functions for heave, pitch, and a vertical wave bending moment amidships of 13 ships are compared. To provide an illustration of the situation, comparisons of the transfer functions are shown in Figs. 1–3 for three different vessels. Transfer functions calculated using CFEs and those available in the literature from the ST and 3D panel method are compared to measured transfer functions.

The comparison of the heave, pitch, and VWBM amidships of the 6750 TEU container ship is presented in Fig. 1, highlighting the high level of accordance between CFEs, experiments, and the strip theory. Fig. 2 presents a comparison of transfer functions for the cruise ship, and one may see that, although curve trends correspond to each other, there are significant discrepancies between the results. In Fig. 3, a satisfying agreement of CFEs, experiments, and the 3D panel method may be noted regarding the 6500 TEU container ship.

6. FIME results

FIME is calculated by Eq. (3.3) for 13 ships, using transfer functions obtained by CFEs, ST, 3D panel codes, and experiments. Detailed results are presented in Table 3, while overall FIME histograms for heave, pitch, and VWBM amidships are shown in Figs. 4–6.

Statistics (mean value and standard deviation) of FIME data presented in Figs. 4–6 are available in Table 4. Both the bias (mean value) and standard deviation of CFEs are the lowest for pitch motion, while the highest results are obtained, as expected, for VWBM amidships. The mean values and standard deviations of the ST and 3D panel method present different results. One may see from Table 4 that the lowest bias and standard deviation of ST are for VWBM amidships and heave, respectively, and the lowest bias and standard deviation of the 3D panel method related to the pitch and heave, respectively.

Comparing FIME statistics of CFE and the commonly adopted ST and 3D panel method, one may conclude that the lowest biases for ship motion are obtained for 3D methods. The standard deviation of FIME is the lowest for pitch motion calculated by 3D methods. The bias of FIME for VWBM amidships is, on average, lower for ST than for 3D methods, although standard deviations are high in both cases. As may be expected, as noted in Table 4, the uncertainty of CFE is much larger compared to the ST and 3D methods.

7. Multivariate linear regression analysis

Although the variability of FIME shown in Figs. 4–6 may be attributed to the statistical variability of the experiments and inconsistencies

Table 5
Intercepts and regression coefficients.

	CFE				ST				3D			
	A	**B**	**C**	**D**	**A**	**B**	**C**	**D**	**A**	**B**	**C**	**D**
Heave	0.623	−0.000447	0.076	0.990	1.383	−0.000366	−0.107	−0.549	1.098	0	−0.177	0
Pitch	0.540	−0.000527	0.135	0.950	1.033	0.000086	0.540	−0.159	0.686	−0.000313	−0.184	0.589
VBM	1.149	0.000040	0.640	−0.003	0.497	−0.000446	0.637	0.859	1.100	−0.000418	1.602	−0.151

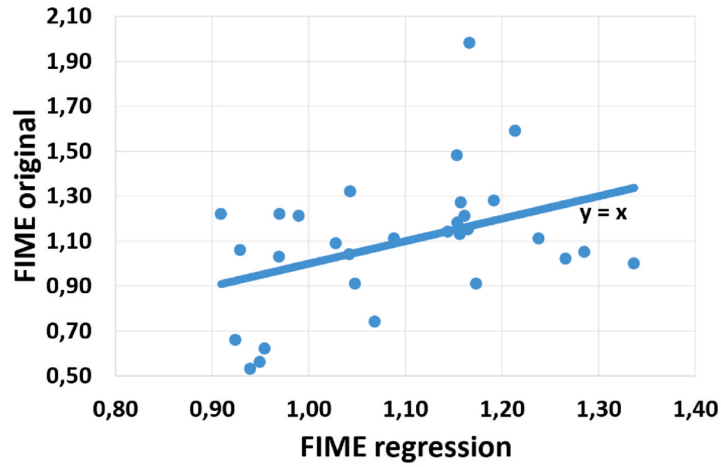

(a)

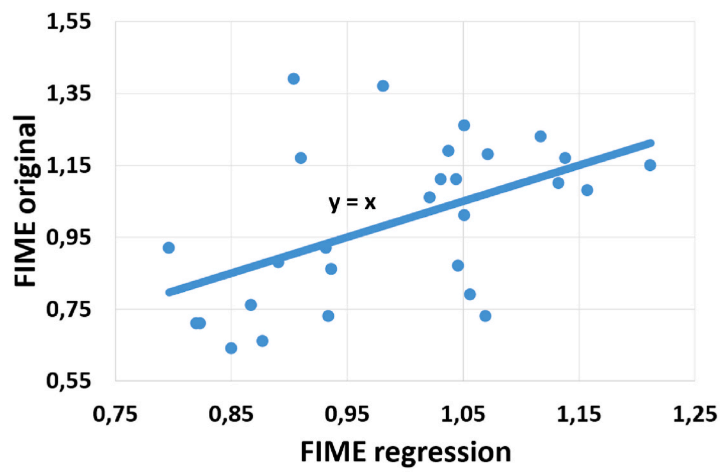

(b)

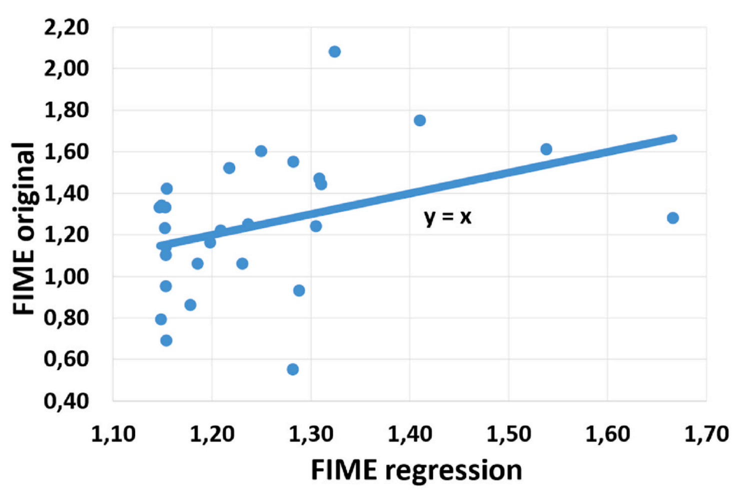

(c)

Fig. 7. Comparison of original FIMEs from Table 3 and results of the MLR analysis for (a) heave, (b) pitch, and (c) VWBM calculated with CFEs.

of employed methods, it is expected that the FIME depends on relative heading, ship speed, and block coefficient (Guedes Soares, 1991). The dependency of FIME on these primary parameters is expressed using the multivariate linear regression (MLR) analysis, which enables the calculation (prediction) of FIME for other ships that are not presented in Table 3.

The dependency of the FIME on Froude number F_n, block coefficient C_b, and heading β is given by the following formula:

$$\varphi_{reg} = \mathrm{A} + \mathrm{B}\beta + \mathrm{C}C_b + \mathrm{D}F_n, \tag{7.1}$$

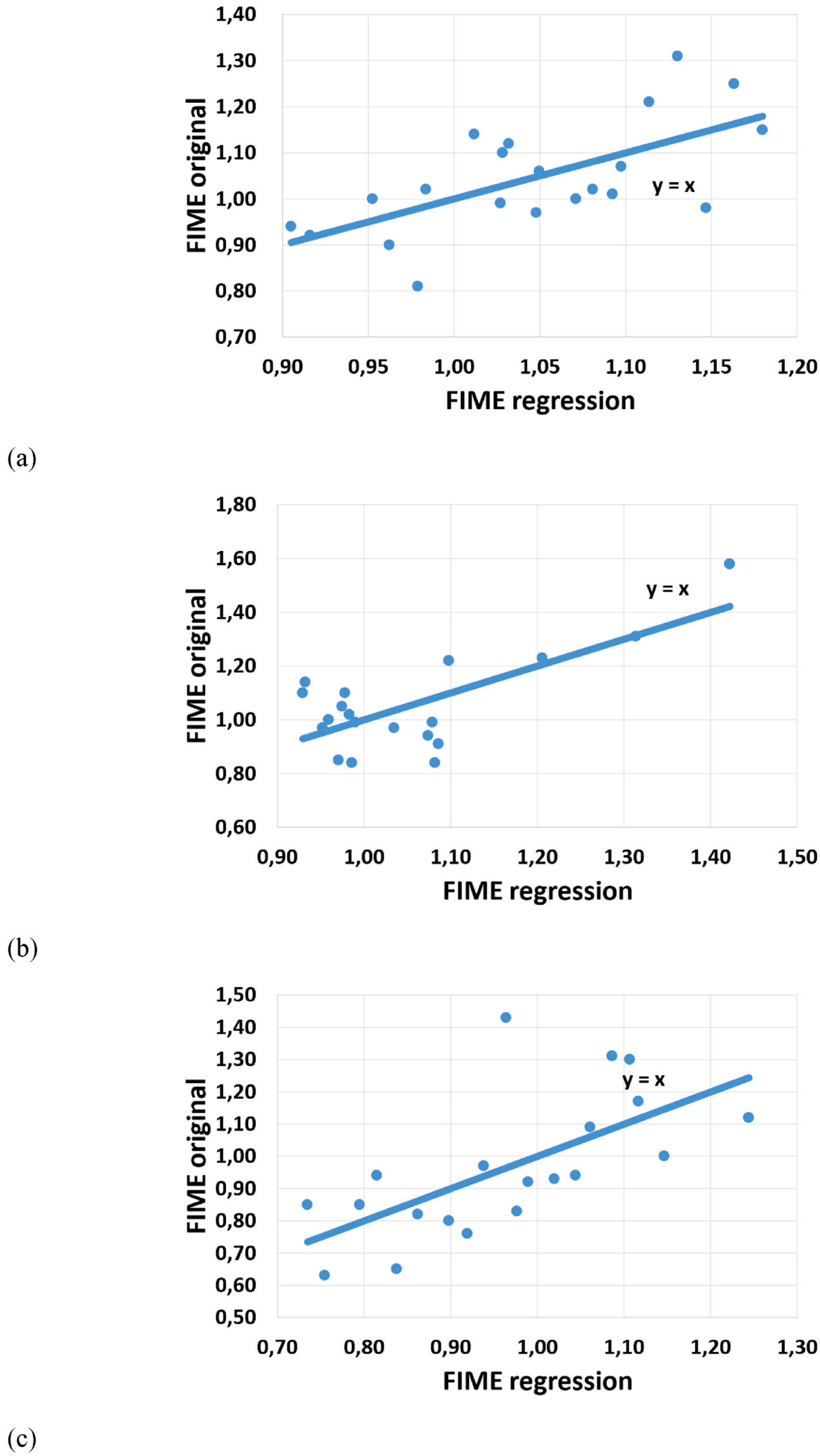

Fig. 8. Comparison of original FIMEs from Table 3 and results of the MLR analysis for (a) heave, (b) pitch, and (c) VWBM calculated with ST.

where A is an intercept, and B, C, and D, are the regression coefficients. The heading angle β is expressed in degrees in Eq. (7.1), where $\beta = 180^\circ$ indicates head seas.

Regression analysis is performed using the software package Real Statistics, using Excel (n.d.). The intercepts and regression coefficients are presented in Table 5.

Graphs with a comparison of the FIME obtained through MLR (Eq. (7.1)) and the original FIME given in Table 3 are shown in Figs. 7–9. The

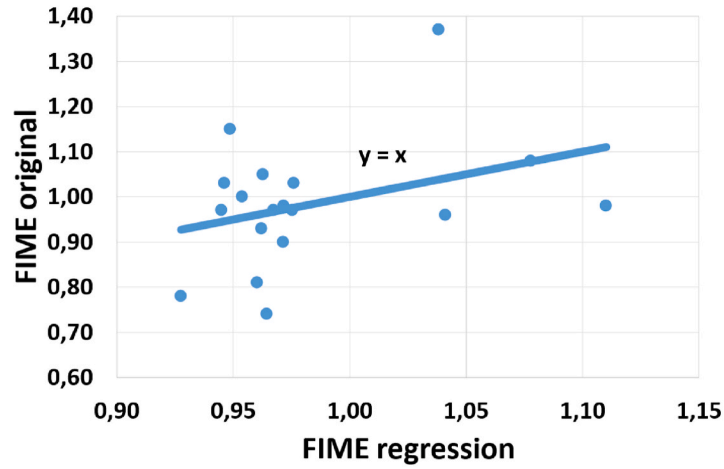

(a)

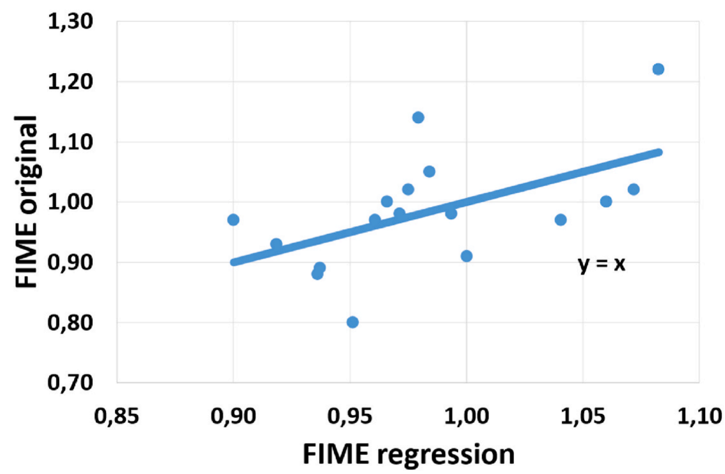

(b)

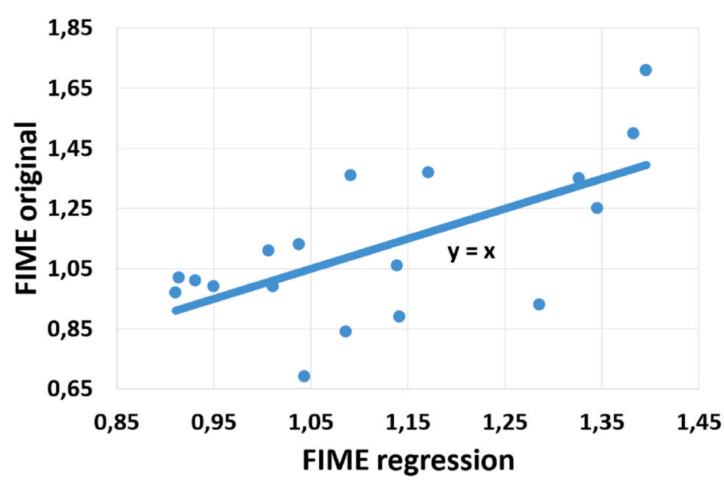

(c)

Fig. 9. Comparison of original FIMEs from Table 3 and results of the MLR analysis for (a) heave, (b) pitch, and (c) VWBM calculated with the 3D panel method.

linear regression lines for heave, pitch, and VWBM amidships are given by equation $y = x$, indicating that MLR represents, as expected, the best estimate for the FIME. However, there is an uncertainty in predictions made based on regression analysis, which may be expressed as the standard deviation of data presented in Figs. 7–9 around regression lines. Standard deviations are given in Table 6 for calculation cases presented in Figs. 7–9.

Standard deviations in Table 6 are determined as the square root of

Table 6
Standard deviations around regression lines for data presented in Figs. 7-9.

	σ_{CFE}	σ_{ST}	σ_{3D}
Heave	0.27	0.09	0.13
Pitch	0.19	0.13	0.08
VBM	0.31	0.16	0.20

squares of deviations of FIME from the regression line. It may be seen from Table 6 that the uncertainty of the regression analysis is the largest in the case of CFEs, and much lower with respect to the ST and 3D methods. Furthermore, for each of the methods, the greatest uncertainty occurs for VWBM at midship compared to the heave and pitch motions, which is expected behaviour. More specifically, as the VWBM is, in principle, obtained by integrating local loads, which depend on ship motion, errors in heave and pitch motion along the ship are summed up in the larger errors of the VWBM.

8. Discussion

Results presented in Section 7 are theoretically consistent and in accordance with experience, as more complex methods (ST and 3D) provide lower uncertainty compared to simple CFEs. Also, greater uncertainty arises with respect to global loads, compared to motion, which is a theoretically justified result. There is no clear distinction in the uncertainty between ST and 3D methods, which is also found in the benchmark studies, (Schellin et al., 1996; Bunnik et al., 2010), including the study performed most recently (Parunov et al., 2022b).

The benefits of performing an MLR analysis may be clearly observed in Fig. 10, where uncertainties (standard deviations) are compared before (Table 4) and after MLR analysis (Table 6). Not only is the bias eliminated, as MLR results in the best estimate of FIME, but standard deviations are also reduced in all the cases analysed. However, despite the reduction following the MLR analysis, the levels of uncertainty regarding CFE are still rather high.

The uncertainties in FIME with respect to the ST and 3D methods are greater than expected, because, in some cases, different method subtypes are grouped. For example, 2.5 ST is considered together with ordinary ST, while time-domain and frequency-domain methods are grouped as the same method. To obtain a more realistic uncertainty estimate, each code should be considered separately, as there is an uncertainty of the individual code with respect to the average of all codes belonging to the same theoretical method (Parunov et al., 2022 a,b). Moreover, the uncertainty of the theoretical method average with respect to the experiments should be calculated separately. Such detailed uncertainty analysis is, however, difficult to organise. The present study provides a rough and conservative estimate of the uncertainty of ST and 3D methods.

The limitations of the CFEs are like those of the ordinary linear ST. ST is considered as the high frequency theory, meaning that better accuracy is expected for head and bow waves than for following and stern quartering waves, as the encounter frequency decreases in the latter case. It is also known as the theory of low Froude numbers ($F_n < 0.4$), as the flow variation in the transverse plane is much larger compared to the longitudinal direction. ST is a slender body theory, more appropriate for slender ship hulls with large length-to-breadth ratio. Other assumptions are also used in derivation of CFEs, as neglecting the coupling terms between heave and pitch, and assuming a constant sectional added mass equal to the displaced water. Former assumption may be primordial when dealing with the forward speed. Details of other limitations of CFEs may be found in Jensen et al. (2004). CFEs are considered in the present study for large Froude numbers, which is theoretically inconsistent, as CFEs are based on the assumptions of the ordinary ST. This inconsistency is ignored in the present analysis, and CFEs are employed even beyond the scope of their validity.

The analysis presented may have several practical applications in cases when transfer functions are used based on CFE. Transfer functions may be corrected by the Linear Regression Equation using the parameters given in Table 4 to obtain their best estimate and thus improve seakeeping predictions. Furthermore, a probabilistic representation of FIME, using the Gaussian distribution with a mean value equal to the linear regression estimate and the standard deviation from Table 6, may be used in various probability-based applications.

The present analysis may be extended to the Frequency Dependent Model Error (FDME) by including frequency as another argument in the regression analysis. Moreover, it would be possible to use the non-linear regression analysis to better describe the model error. Artificial Neural Networks (ANN) and similar deep learning methods may be used for the improvement of the FIME predictions and for FDME computation.

9. Conclusion

The Frequency independent model error of transfer functions defined by Closed-form expressions for heave, pitch, and vertical wave bending moment amidships is determined in the study. The model error is calculated by comparing predicted transfer functions with measurements taken from the model-scale experiments published in the literature. Thirteen ships of different sizes and types, with various speeds and heading angles, are considered. The same type of model error calculations is performed for the results obtained by different versions of Strip theory and 3D panel methods, available in the literature together with the measurements. Calculated model errors are subjected to multivariate linear regression analysis, providing the best estimates of the model error based on the heading angle, ship speed, and block coefficient.

The main results of the study are:

– Both bias and standard deviation of the model error are larger for Closed-form expressions compared to the commonly used seakeeping methods.
– There is no clear evidence of a possible reduction in uncertainty if the 3D panel codes are used instead of the strip theory.

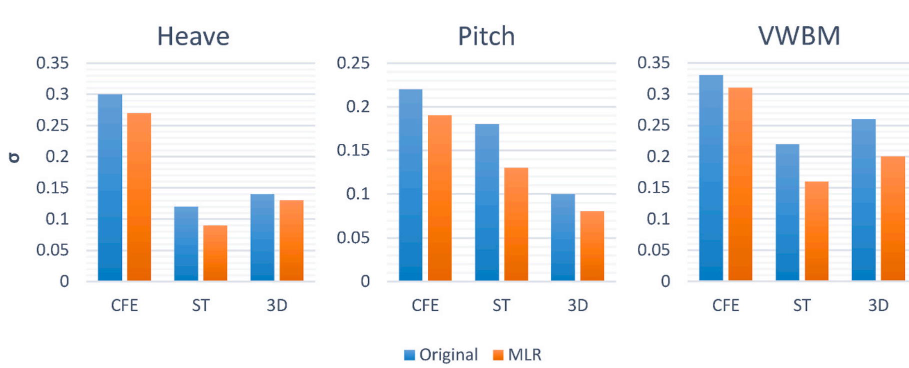

Fig. 10. Comparison of standard deviation before and after multivariate linear regression analysis.

– For all methods, uncertainties of ship motions are lower compared to the uncertainty of global wave loads.
– Application of the multivariate linear regression analysis leads to the elimination of the bias and reduction of the standard deviation for all methods. However, the level of uncertainty with respect to Closed-form expressions still remains rather high.

The quantification of the uncertainties presented in the paper enables a more efficient practical application of seakeeping methods by correcting transfer functions for the bias. The introduction of the probabilistic uncertainty model, consisting of both bias and standard deviation, enables the advancement of probabilistic formulations in the risk-based methods for ship design and operation. Thus, the results of the study are immediately applicable for optimizing ship operations when hull lines are unavailable, as in the conceptual ship design or for ships in service. Probabilistic description of model error in transfer functions is required for wave loads in ship structural reliability analysis and for seakeeping criteria in probabilistically based ship decision support system.

CRediT authorship contribution statement

Tamara Petranović: Software, Data curation, Writing – original draft. **Antonio Mikulić:** Software, Visualization. **Ivana Gledić:** Software, Data curation, Formal analysis, Writing – original draft. **Joško Parunov:** Conceptualization, Methodology, Validation, Writing – original draft, Writing – review & editing, Supervision, Project administration, Funding acquisition.

Declaration of competing interest

The authors declare that they have no known competing financial interests or personal relationships that could have appeared to influence the work reported in this paper.

Data availability

Data will be made available on request.

Acknowledgment

This work has been fully supported by the Croatian Science Foundation under the project IP-2019-04-2085.

References

Bunnik, T., van Daalen, E., Kapsenberg, G., Shin, Y., Huijsmans, R., Deng, G.B., Delhommeau, G., Kashiwagi, M., Beck, B., 2010. A Comparative study on state-of-the-art prediction tools for seakeeping. In: 28th Symposium on Naval Hydrodynamics Pasadena, California, 12-17 September 2010.
Ćatipović, I., Ćorak, M., Parunov, J., Alujević, N., 2018. Seakeeping experiments on damaged ship. Ships Offshore Struct. 14, 1–12. https://doi.org/10.1080/17445302.2018.1559911.
DNV, G.L., 2018. Class Guideline DNVGL CG 0130: Wave Loads. Det Norske Veritas Germanischer Lloyd, Oslo.
Graefe, A., Moctar, O., Oberhagemann, J., Shigunov, V., 2014. Linear and nonlinear sectional loads with potential and field methods. J. Offshore Mech. Arctic Eng. 136, 31602. https://doi.org/10.1115/1.4026885, 1.
Guedes Soares, C., 1991. Effect of transfer function uncertainty on short-term ship responses. Ocean Eng. 18, 329–362.
Guedes Soares, C., Fonseca, N., Pascoal, R., 2004. Long term prediction of non-linear vertical bending moments on a fast monohull. Appl. Ocean Res. 26 (6), 288–297. https://doi.org/10.1016/j.apor.2005.08.002.
Hirdaris, S.E., Bai, W., Dessi, D., Ergin, A., Gu, X., Hermundstad, O.A., Huijsmans, R., Iijima, K., Nielsen, U.D., Parunov, J., Fonseca, N., Papanikolaou, A., Argyriadis, K., Incecik, A., 2014. Loads for use in the design of ships and offshore structures. Ocean Eng. 78, 131–174. https://doi.org/10.1016/j.oceaneng.2013.09.012.
IACS Ltd, 2000. Rec. No. 34 Standard Wave Data.
ITTC, 2011. Report of the seakeeping committee in. In: Proceedings of the 26th International Towing Tank Conference, vol. 1, pp. 219–225 (Rio de Janeiro).
Jensen, J.J., Mansour, A.E., 2002. Estimation of ship long-term wave-induced bending moment using closed-form expressions. Int. J. Maritime Eng. 41–55.
Jensen, J.J., Mansour, A.E., Olsen, A.S., 2004. Estimation of ship motions using closed-form expressions. Ocean Eng. 31, 61–85.
Jensen, J.J., Pedersen, P.T., Shi, B., Wang, S., Petricic, M., Mansour, A.E., 2008. Wave induced extreme hull girder loads on containerships. Trans. SNAME 116, 128–151.
Kim, Y., Kim, J., 2016. Benchmark study on motions and loads of a 6750-TEU containership. Ocean Eng. 119, 262–273. https://doi.org/10.1016/j.oceaneng.2016.04.015.
Lee, Y., Chan, H., Pu, Y., Incecik, A., Dow, R.S., 2012. Global wave loads on a damaged ship. Ships Offshore Struct. 7 (3), 237–268. https://doi.org/10.1080/17445302.2011.588081.
Ley, J., Moctar, O., 2021. A comparative study of computational methods for wave-induced motions and loads. J. Mar. Sci. Eng. 9 (1), 83. https://doi.org/10.3390/jmse9010083.
Lloyd, A.R.J.M., 1998. Seakeeping: ship behavior in rough weather. A.R.J.M. Lloyd. ISBN: 0953263401.
McTaggart, K., Datta, I., Stirling, A., Gibson, S., Glen, I., 1997. Motions and loads of a hydroelastic frigate model in severe seas. In: Paper Presented at the SNAME Annual Meeting, 1997. Ottawa, Canada.
Nielsen, U.D., Toshio, I., 2015. Prediction of first-order vessel responses with applications to decision support systems. In: Paper Presented at the SNAME Maritime Convention and 5th World Maritime Technology Conference, Providence, Rhode Island, USA, November 2015. https://doi.org/10.5957/WMTC-2015-127.
Nielsen, U.D., Mounet, R.E.G., Brodtkorb, A.H., 2021. Tuning of transfer functions for analysis of wave-ship interactions. Mar. Struct. 79, 103029 https://doi.org/10.1016/j.marstruc.2021.103029.
Papanikolaou, A., Mohammed, E.A., Hirdaris, S.E., 2014. Stochastic uncertainty modelling for ship design loads and operational guidance. Ocean Eng. 86, 47–57. https://doi.org/10.1016/j.oceaneng.2014.01.014.
Parunov, J., Ćorak, M., Guedes Soares, C., Jafaryeganeh, H., Kalske, S., Lee, Y., Liu, S., Papanikolaou, A., Prentice, D., Prpić-Oršić, J., Ruponen, P., Vitali, N., 2020. Benchmark study and uncertainty assessment of numerical predictions of global wave loads on damaged ships. Ocean Eng. 197, 106876 https://doi.org/10.1016/j.oceaneng.2019.106876.
Parunov, J., Guedes Soares, C., Hirdaris, K., Wang, 2022a. Uncertainties in modelling the low-frequency wave-induced global loads in ships. accepted in Marine Structures.
Parunov, J., Guedes Soares, C., Hirdaris, S., Iijima, K., Wang, X., Brizzolara, S., Qiu, W., Mikulić, A., Wang, S., Abdelwahab, H.S., 2022b. Benchmark study of global linear wave loads on a container ship with forward speed. Mar. Struct. 84, 103162 https://doi.org/10.1016/j.marstruc.2022.103162.
Petranović, T., Mikulić, A., Katalinić, M., Ćorak, M., Parunov, J., 2021. Method for prediction of extreme wave loads based on ship operability analysis using hindcast wave database. J. Mar. Sci. Eng. 9 (9), 1002. https://doi.org/10.3390/jmse9091002.
Prini, F., Benson, S., Dow, R.S., Phillips, H.J., Sheppard, P.J., Birmingham, R.W., 2021. Model scale prediction of seakeeping and global bending moment on a high-speed craft. Eng. Struct. 231, 111738 https://doi.org/10.1016/j.engstruct.2020.111738.
Real statistics using Excel. https://www.real-statistics.com/free-download. (Accessed 12 April 2022).
Schellin, T.E., Östergaard, C., Guedes Soares, C., 1996. Uncertainty assessment of low frequency load effects for containerships. Mar. Struct. 9 (3–4), 313–332. https://doi.org/10.1016/0951-8339(95)00039-9.
Temarel, P., Bai, W., Bruns, A., Derbanne, Q., Dessi, D., Dhavalikar, S., Fonseca, N., Fukasawa, T., Gu, X., Nestegård, A., Papanikolaou, A., Parunov, J., Song, K.H., Wang, S., 2016. Prediction of wave-induced loads on ships: progress and challenges. Ocean Eng. 119, 274–308. https://doi.org/10.1016/j.oceaneng.2016.03.030.
Abdelwahab, H., Wang, S., Parunov, J., Guedes Soares, C., 2023. A New Model Uncertainty Measure of Wave-Induced Motions and Loads on a Container Ship with Forward Speed. J. Mar. Sci. Eng. 11 (5), 1042 https://doi.org/10.3390/jmse11051042, 28.

Article 2

Article published by MDPI in Applied Sciences on 12 April 2025.
DOI: 10.3390/app15084268

applied sciences

Article

Incorporating Epistemic Uncertainties in Ship Operability Study

Tamara Petranović * and Joško Parunov *

Faculty of Mechanical Engineering and Naval Architecture, University of Zagreb, 10000 Zagreb, Croatia
* Correspondence: tamara.petranovic@fsb.unizg.hr (T.P.); josko.parunov@fsb.unizg.hr (J.P.)

Abstract: Ship operability diagrams are commonly defined based on the seakeeping analysis, showing which course and speed can safely be taken at the sea state to satisfy predefined seakeeping limiting values. Although ship operability diagrams are inherently probabilistic, because of the random nature of the environmental loads, their outcome is deterministic, showing if the seakeeping criteria are satisfied or not for a certain combination of environmental and operational parameters. In the present study, uncertainties in seakeeping predictions and limiting values, which are usually neglected, are integrated into the ship operability analysis. This results in probabilistic operability diagrams, where the seakeeping criteria are exceeded with certain probabilities. The approach is demonstrated in the example of the passenger ship on a route in the Adriatic Sea. Semi-analytical closed-form expressions are used for seakeeping analysis, while limiting values for vertical bow acceleration, pitch, slamming, roll, and propeller emergence are analyzed. The second-order reliability method is used to calculate probabilities of the exceedance of the seakeeping criteria, and the results are presented as probabilistic operability diagrams. The method enables the determination of a new probabilistic operability index applicable to the ship design and represents a prerequisite for risk-based decision making in ship operation. It is also presented how the method can be validated for the existing shipping route using numerical wave databases.

Keywords: seakeeping analysis; operability criteria; uncertainties

check for updates

Academic Editor: José A. Orosa

Received: 11 March 2025
Revised: 6 April 2025
Accepted: 9 April 2025
Published: 12 April 2025

Citation: Petranović, T.; Parunov, J. Incorporating Epistemic Uncertainties in Ship Operability Study. *Appl. Sci.* **2025**, *15*, 4268. https://doi.org/10.3390/app15084268

Copyright: © 2025 by the authors. Licensee MDPI, Basel, Switzerland. This article is an open access article distributed under the terms and conditions of the Creative Commons Attribution (CC BY) license (https://creativecommons.org/licenses/by/4.0/).

1. Introduction

The prediction of the seakeeping behavior of ships for a variety of probable environmental and operational conditions has wide application in the shipping industry, providing important information about the design and efficient/safe operation of modern ships. For a ship sailing in waves, the basic controllable parameters are the forward speed and the heading to the waves, so the ship operability study aims to determine in which sea states, described by a significant wave height (H_S) and peak spectral periods (Tp), the ship can maintain a given course and speed.

In ship design, ship operability studies could be utilized to determine the operability index (OI), which represents basically the proportion of time a ship is accessible for perfect operation [1]. The OI considers simultaneously the wave characteristics of the sailing area, the dynamic ship response to the waves, and the ship mission. The ship OI may be used as a decision-making tool when acquiring a new ship for a specific service, to compare the comfort level of different ships [2], and for ship form optimization [3]. There are variations of the OI, such as the operability robustness index (ORI), a performance criterion used to assess the robustness of a vessel in different sea states [4]. The Habitability Index (HI) refers to the assessment of onboard comfort and livability, particularly for passenger vessels [5]. The Comfort Index (CI) is used to assess passenger comfort aboard vessels, especially on longer journeys. This index considers factors like motion sickness, noise levels, and vibrations, using probabilistic methods to predict comfort levels under various sea conditions. It allows operators to anticipate discomfort and optimize routes to minimize passenger distress [6].

In ship operations, operability studies are used for real-time decisions in Decision Support Systems (DSS), where the time frame may be hours (tactical decisions) or days (strategic decisions relating to route planning) [7]. Tactical decisions are made at the navigation bridge, related to the choice of ship speed and course having an impact on the ship motions and loads due to the wave action. In that respect, the following commands could be given: no change is required, speed reduction, course change, or speed and course change [8]. The strategic decision is to determine, before the mission, which route the ship may take, duly accounting for structural safety, the total travel time, fuel consumption, etc. A strategic decision about ship routing is, therefore, a multi-attribute decision-making process [9]. Examples of operational decision-making include predicting first-order vessel responses as a key component of decision support systems, examining the effects of uncertainties in sea state descriptions on operational limits, and presenting a new model for adaptive weather routing based on seakeeping analysis and optimization, aimed at reducing operational risks [10–12]. Operability analysis as a part of weather routing is presented in [13].

In the common ship operability studies, the seakeeping calculations and assessments are based on specific ship-inherent and environmental data and assumptions. Thus, seakeeping tools are employed assuming their results as ground truth, while seakeeping limiting values are also considered as fixed, prescribed values. However, different seakeeping theories may result in rather different outcomes of the operability studies [14]. The uncertainties associated with the sea state descriptions used in the numerical analysis influence the operational limits (in terms of H_S and Tp) [11]. The effect of the seakeeping criteria on the seakeeping performance assessment for passenger vessels shows that the OI is strongly affected by the chosen limiting values [15].

It becomes evident from this review that operability studies are dependent not only on inherent (or aleatory) uncertainties of random sea surface elevation and wave environmental variations in ship operating zones, but also on the knowledge-based (or epistemic) uncertainties, encompassing modeling uncertainties of seakeeping theories and tools and uncertainties of seakeeping limiting values [16]. Obviously, both uncertainty types need to be included in the consistent probabilistic ship operability analysis [17].

The concept of the risk-based Navigation Decision Assistant (NDA) was proposed initially in [7]. The concept described the evaluation of probabilities and consequences, accounting for the uncertainties of the input variables. Another concept of the risk-based DSS was introduced, incorporating aleatory and epistemic uncertainties related to the parameters of the problem of ship motions in waves [18]. It is concluded that the system can be applied to both the ship's operational assessment and the design procedure, but there is a need to improve the efficiency of the probabilistic assessment for practical onboard applications [19]. A procedure to incorporate random variables and associated uncertainties in the calculations of the outcrossing rates that are the basis for risk-based DSS is suggested in [20].

The present study aims to continue this development of the risk-based DSS by formulating and solving the probabilistic problem of ship operability analysis for different seakeeping limiting criteria. Epistemic uncertainties are included in this operability study, resulting in probabilistic operability polar plots being more informative compared to the "deterministic" polar plots. While previous studies (e.g., [18,19]) included seakeeping uncertainties in operability analysis, the present work extends these studies by incorporating uncertainties in operability limiting values. The limit state equations are formulated and solved using Comrel 2021 software for structural reliability analysis. This study also proposes extending the conventional OI for ship design to the Probabilistic Operability Index (POI) as a more rational measure of ship operability. The potential application of probabilistic operability diagrams for tactical DSS is also shown.

An examination of probabilistic operability is provided for a passenger ship traveling on the actual sailing route across the Adriatic Sea. Fuel consumption and corresponding CO_2 emissions along common ferry routes in the Adriatic have recently been studied in [21]. To demonstrate the concept of probabilistic operability analysis, a simplified seakeeping approach is used, where transfer functions of heave, pitch, and roll are calculated by closed-form expressions (CFE), formulated in [22]. The model uncertainty of CFE for heave and pitch is defined by comparison to the model-scale experiments for a relatively large number of ships [23]. In previous studies, model uncertainties in seakeeping methods were assumed. In contrast, this study consistently employs a seakeeping method while explicitly defining the corresponding modeling uncertainty. For the sake of simplicity, a single-parameter wave spectrum, which is representative for the Adriatic Sea, defined only by a significant wave height, is used for the description of short-term sea conditions. A histogram of sea states along the sailing route is obtained from the wave hindcast database, described in [24]. The seakeeping limiting criteria of roll, pitch, vertical acceleration on forward perpendicular, slamming, and propeller emergence are considered as random variables to illustrate the procedure. The second-order reliability method (SORM) is used to calculate probabilities of exceedance of the seakeeping criteria, and the results are presented in probabilistic polar plots.

This paper is organized as follows. The seakeeping method, wave spectrum model, uncertainty model of CFE based on a frequency-independent model error, reliability analysis, and risk-based decision making are described in Section 2. The results of the operability analysis for the case ship are given in Section 3. The discussion section includes the application of the POI in ship design, potential usage of probabilistic operability plots in ship operation, correlation of the results with past experience on the sailing route concerned, and limitations of the developed model. Conclusions and recommendations for future development are given in the last section of this paper.

2. Methods

2.1. Seakeeping Analysis

Linear seakeeping analysis is used in the present study. The analysis consists of the computation of transfer functions in the frequency domain and the definition of the wave energy spectrum. Then, the response spectrum is calculated by multiplying the square of transfer functions by the wave spectrum. Spectral moments are then obtained by integrating the response spectrum.

2.1.1. Transfer Functions

Transfer functions for heave and pitch are calculated using semi-analytical closed-form expressions (CFE) [22]. These simple formulas are determined for the motion of a prismatic barge in the vertical plane using standard linear strip theory assumptions, assuming a constant sectional added mass equal to the displaced water volume and ignoring the coupling components between pitch and heave. The main ship attributes—length L, breadth B, draft T, block coefficient Cb, and speed V—are the only necessary input data for the procedure.

In this section, the procedure is briefly outlined, while details may be found in the original reference [22].

The frequency response functions for heave (Φ_w) and pitch (Φ_θ) are given as:

$$\Phi_w = \eta F, \quad (1)$$

$$\Phi_\theta = \eta G, \quad (2)$$

where F and G are heave and pitch forcing function, and:

$$\eta = \left(\sqrt{(1 - 2kT\alpha^2)^2 + \left(\frac{A^2}{kB\alpha^2} \right)^2} \right)^{-1}, \quad (3)$$

where k is the wave number, T is draft, A is approximation of the sectional hydrodynamic damping, B is breadth of ship, and α is parameter:

$$\alpha = 1 - F_n \sqrt{kL} \cos\beta, \quad (4)$$

where F_n is Froude number, L is the ship length, and β is heading of the ship.

The transfer functions of vertical motion Φ_u and vertical acceleration Φ_v at the forward perpendicular are given as:

$$\Phi_u = \sqrt{\Phi_w^2 + x_{\mathrm{FP}}^2 \Phi_\theta^2}, \quad (5)$$

$$\Phi_v = \overline{\omega}^2 \Phi_u, \quad (6)$$

where x_{FP} is the longitudinal distance of the forward perpendicular from the center of gravity, and $\overline{\omega}$ is the encounter frequency.

The transfer function for roll motion is obtained by solving the equation of the motion for roll in regular waves, and it can be written as:

$$\Phi_\varphi = \frac{|M|}{\left(\left[-\overline{\omega}^2 (\mathrm{T_N}/2\pi)^2 + 1 \right]^2 \mathrm{C}_{44}^2 + \overline{\omega}^2 B_{44}^2 \right)^{1/2}}, \quad (7)$$

where $|M|$ is the amplitude of the excitation moment; T_N is the natural roll period; C_{44} is the restoring moment coefficient; and B_{44} is the hydrodynamic roll damping for the ship which is considered 20% in this study.

The CFEs are semi-analytical formulae, so they can be easily calculated using a usual spreadsheet application. CFEs have been used for seakeeping predictions in conceptual design, enabling an efficient sensitivity analysis regarding operational profiles and different wave environments [25]. CFEs have also been used in hydro-elastic studies [26], for the computation of extreme wave loads using the hindcast wave database, and for tuning the transfer function for the prediction of ship responses [27].

In the present paper, CFEs are considered for the development of the risk-based ship DSS for heavy weather maneuvering. The numerical efficiency of DSS could be crucial if DSS is used for decision making onboard the ship on heavy seas [19]. CFEs have already been considered for DSS application in [28].

2.1.2. Wave Spectrum

Short-term stationary irregular sea states are for engineering purposes traditionally described by wave energy spectrum. The formulation of the wave energy spectrum depends on the geographical area under consideration with local bathymetry and the severity of the sea state. The Pierson–Moskowitz spectrum and JONSWAP spectrum are frequently applied for wind seas. The former was originally proposed for a fully developed sea in the open ocean, while the latter is appropriate for fetch limited seas, describing developing sea states.

The shipping route in the Adriatic Sea is considered in the present study. For such an enclosed sea, modification of the JONSWAP type of wave spectrum is used. Tabain's single-parameter wave spectrum, developed specifically for the Adriatic, has been used for naval architecture and marine engineering applications [29]. Recently, Tabain's spectrum was optimized using a wave database obtained by combining satellite measurements and numerical re-analysis [30]. Thus, the following one-parameter spectral formulation relevant to the Adriatic Sea is used:

$$S(\omega) = 0.8626 \frac{5}{16} \frac{H_s^2 \omega_m^4}{\omega^5} exp\left[-\frac{5}{4} \left(\frac{\omega_m}{\omega} \right)^4 \right] 1.78^{\, exp\left[-\frac{1}{2} \left(\frac{\omega - \omega_m}{\sigma\, \omega_m} \right)^2 \right]}, \tag{8}$$

$$\omega_m = 0.52 + \frac{1.4}{H_s + 0.7}, \tag{9}$$

$$\sigma \begin{cases} \sigma_a = 0.06 \; za \; \omega \; \leq \; \omega_m \\ \sigma_b = 0.08 \; za \; \omega > \omega_m \end{cases}. \tag{10}$$

where $\omega_m = 2\pi/Tp$ is the peak of the wave energy spectrum.

Obviously, that one-parameter formulation cannot cover all combinations of significant wave heights and zero-crossing periods occurring in the Adriatic [24].

2.1.3. Ship Response in Short-Term Irregular Waves

The ship's response spectrum's general equation is expressed as:

$$S_R(\overline{\omega}) = |\Phi(\overline{\omega})|^2 S_J(\overline{\omega}) \;, \tag{11}$$

where $\overline{\omega}$ is the encounter frequency and $S_J(\overline{\omega})$ is the encounter wave spectrum.

The variance of the ship response represents the area under the response spectrum:

$$m_{0R} = \int_0^\infty S_R(\overline{\omega}) \cdot d\overline{\omega} \;. \tag{12}$$

The root mean square (RMS) represents the standard deviation, and it is obtained as the square root of the response variance.

2.1.4. Model Uncertainty of Transfer Functions

The Frequency Independent Model Error (FIME) is developed and utilized to formulate the model uncertainty of transfer functions [31]. The fundamental concept of FIME involves multiplying transfer functions by a constant fit factor φ, which is expressed as follows:

$$\varphi = \frac{\sum_i \hat{H}_i H_i}{\sum_i H_i^2}, \tag{13}$$

where $\hat{H}_i$ and H_i are measured and calculated transfer functions at the frequency ω_i, respectively. This allows the transfer function to be adjusted to match, on average, with the experimental results at all frequencies.

According to its geometrical meaning, φ is the slope of the regression line that must pass through the origin when comparing experimental and calculated transfer functions. The theory overestimates the experimental results when φ is less than 1, whereas it underestimates readings when φ is more than 1 [17].

By comparing transfer functions computed by CFEs with model-scale experiments for 13 ships of various types, speeds, and relative heading angles, the parameter φ was found for heave and pitch in [23]. Using linear multivariate regression analysis, the dependence of φ on the main parameters was expressed as:

$$\varphi = \mathrm{A} + \mathrm{B}\beta + \mathrm{C}C_b + \mathrm{D}F_n, \quad (14)$$

where F_n, C_b, and β are Froude number, block coefficient, and heading angle, respectively. Table 1 provides the regression coefficients and intercept [23].

Table 1. Intercept and regression coefficients for the regression Equation (14).

	A	**B**	**C**	**D**
Heave	0.623	−0.000447	0.076	0.990
Pitch	0.540	−0.000527	0.135	0.950

Values in Table 1 represent a mean value for each speed and heading angle and a standard deviation of 0.19 and 0.27 is determined for pitch and heave, respectively, in [23]. Due to the lack of relevant comparisons with experiments, mean value and standard deviation for the model uncertainty of the roll angle are assumed in the present study as 2.5 and 0.2, respectively. The normal distribution is used to represent the model uncertainty of the seakeeping calculations.

2.2. Seakeeping Criteria

Most seakeeping criteria are concerned with operability, i.e., crew ability and willingness to operate a vessel and all its installed equipment in a specified seaway. Operability criteria are typically expressed in terms of roll and pitch angles, roll motion, vertical and lateral acceleration, deck wetness, propeller emergence, and slamming. In addition, there is a group of criteria expressing the interaction between ship motion and human reactions, such as motion sickness incidence and motion-induced interruptions. Limiting values of these criteria are not standardized and do not cover all vessel types, but there are well-established criteria sets referring to the overall vessel system's operability or habitability of the vessel. There are different reasons for discrepancies in criteria between different sources, even if they refer to the similar ship types, such as complexities and inaccuracies of motion prediction methods and discrepancies in the definition of seakeeping amongst naval architects and how vessel owners viewed seakeeping. A critical review of currently used standards and criteria is provided in [32].

An example of discrepancies of limiting values among different operability standards is given for the case of vertical acceleration at forward perpendicular in [8]. The limiting values read from 0.2 g RMS according to NATO and US Coast Guard Standards, to 0.275 g RMS according to NORDFORSK for Merchant ships less than 100 m in length. There are also other options to express the limiting value of vertical acceleration at the forward perpendicular, such as the probability of exceeding individual acceleration amplitudes and Subjective Magnitude (SM) values [33]. Limiting values for some criteria are less scattered, e.g., limiting value for RMS of the pitch angle of 1.5° is often found [8].

The brief review in the preceding paragraph indicates that limiting values are uncertain and that captains could have a different attitude against limiting values for operability criteria. In other words, it is reasonable to consider limiting operability values as random variables. The definition of parameters of probability distributions of such random variables is a challenging task. Performing a questionnaire among experienced seafarers, such as the one presented in [34], could be the right way to define these parameters. The main problem found was the lack of onboard measurements, thus preventing clear quantification of the seakeeping limiting criteria. A large spread among answers to some of the questions, e.g., estimation of pitch angle, was found. That finding about the uncertainty of operability limiting values supports the necessity of their probabilistic description, as proposed in the present study.

For illustration of the procedure, the mean values of the operability limiting value are taken from those given in Table 2, while their coefficient of variation (CoV) is assumed as 0.05 in all cases. Gaussian distribution is used to model this uncertainty.

Table 2. Mean values of operability criteria limits [8].

Criteria	Statistical Property	Mean Value
Pitch	RMS	1.5°
Vertical acceleration at FP	RMS	0.05 g
Roll	RMS	2.5°
Slamming	Probability	0.03
Propeller emergence	Probability	0.25

2.3. Reliability Problem Formulation

As explained in the preceding section, the accuracy of the seakeeping calculations is uncertain, as well as limiting values of seakeeping criteria. Therefore, the seakeeping criteria are exceeded with a certain probability, which is calculated based on the limit state functions. In general, the limit state function $g(X)$ is given as:

$$g(x_1, x_2, \ldots x_n) < 0, \tag{15}$$

where $x_1, x_2, \ldots x_n$ is a vector of random variables and g takes negative value when the limiting criterion is exceeded. In the present study, the random variables are epistemic uncertainties of the seakeeping results and criteria.

To describe the procedure, let us consider the simplest limit state function, which is for pitch angle. The limit state function, in this case, reads:

$$x_\theta - \sqrt{\int_0^\infty |\varphi_\theta \Phi_\theta(\overline{\omega})|^2 S_J(\overline{\omega}) \cdot d\overline{\omega}} < 0 \tag{16}$$

x_θ in Equation (16) is a normally distributed random variable representing pitch criterion, with a mean value equal to 1.5°, according to Table 2, and CoV of 0.05. φ_θ is also normally distributed with the mean value calculated by Equation (14), depending on the heading angle and ship speed, and a standard deviation of 0.19. $\Phi_\theta(\overline{\omega})$ is a transfer function of pitch, given by Equation (2), while the wave energy spectrum $S_J(\overline{\omega})$ is defined by Equations (8)–(10). The limit state function for the roll is defined in similar way, only that the random variable representing criterion uncertainty x_{roll} with a mean value of 2.5° is used. The transfer function of roll motion is $\Phi_\varphi(\overline{\omega})$, defined by Equation (7).

The limit state function for vertical acceleration at FP is a bit more complicated, as the transfer function for vertical acceleration at FP (Equation (6)) depends on heave and pitch transfer functions (Equation (5)). Each of these transfer functions is multiplied by the corresponding epistemic uncertainty, calculated by Equation (14), using parameters from Table 1. The limit state function is then readily defined using an expression like Equation (16).

The limit state function for propeller emergence requires the calculation of the probability of the propeller emergence:

$$p_{pe} = \exp\left[-\left(\frac{D_p^2}{2m_{0\_r}}\right)\right] \quad (17)$$

where D_p is the propeller blade tips' depth, while m_{0_r} is the variance of the relative motion at the location of the propeller. The transfer function of the relative motion is given by an expression analogous to Equation (5). Transfer functions of heave and pitch are multiplied by corresponding modeling uncertainties. The limit state function for propeller emergence is then given as:

$$x_{pe} - p_{pe} < 0 \quad (18)$$

where x_{pe} is normal distribution with a mean value of 0.25, according to Table 2, and with assumed CoV of 0.05.

The slamming probability, p_s, employed in the slamming limit state function, is given as:

$$p_s = \exp\left[-\left(\frac{T_e^2}{2m_{0\_r}} + \frac{v_{kr}^2}{2m_{0\_v}}\right)\right], \quad (19)$$

where T_e is the effective draft; m_{0_r} is the variance of the relative vertical motion at ship FP; v_{kr} is the critical vertical velocity; and m_{0_v} is the variance of the relative velocity at FP. Critical velocity is calculated from Ochi's equation:

$$v_{kr} = 0.093\sqrt{gL_P}, \quad (20)$$

where LP is a ship length between perpendiculars.

The limit state function for bow slamming is then given as:

$$x_s - p_s < 0, \quad (21)$$

where x_s is a normal distribution with a mean value of 0.03, according to Table 2, and with assumed CoV of 0.05. Model uncertainties in heave and pitch are used in the definition of the variances of the ship relative motion and velocity.

2.4. Reliability Analysis

The software program Comrel is used for reliability analysis, and the basic steps to perform the analysis are [35]:

1. Formulating the limit state functions in standard mathematical notation;
2. Preparation of the stochastic model for the variables;
3. Selecting computation options;
4. Performing the reliability analysis with embedded Symbolic Processor;
5. Analysis of the results and graphical post-processing.

Second-Order Reliability Method (SORM) is chosen as the computational option for reliability analysis. First-Order Reliability Method (FORM), which is often used in ship structural reliability analysis, is not performing well in all cases, as some of the limit state functions are complex, including integration, and are formulated in several lines.

The Multiple Runs option was used for calculation over different periods, and in one pass, the calculation was made for all significant wave heights H_S, and each pass calculated for different angles β.

Except for Comrel, other commercial and in-house software tools have been used for risk-based DSS concepts. Specifically, the commercial probability analysis program

PROBAN was used in [18], while the in-house structural system reliability analysis program RELSYS was used in [36].

2.5. Risk-Based Perspective

A review and analysis of general risk definitions, perspectives, and scientific approaches to risk analysis in the maritime transportation application area are provided in [37]. The results indicate that risk is strongly associated with probability, though alternative views exist. Additionally, various scientific approaches to risk analysis have been identified. More recently, a multi-attribute-based assessment model has been proposed in [38] to support decision making on risk control options. A discussion on risk assessment and key risk factors affecting ferry navigation safety is presented in [39].

The prevailing approach to risk analysis in maritime defines the risk (R) as the product of the probability of an event (P) and its associated consequence (C), e.g., [7]. The total risk for a combination of N uncorrelated serial events is given as:

$$R = \sum_{i=1}^{N} R_i = \sum_{i=1}^{N} P_i C_i \tag{22}$$

while the expression for the case of correlated events may be found in [7]. In addition, each individual risk R_i may be multiplied by the company-specific aversion factor A_i.

While the probabilities of an adverse event P_i are obtained through reliability analysis, the associated consequences are determined via consequence analysis, categorized as follows:

- Safety of people (loss of life, injuries, and health);
- Risk to the maritime environment;
- Economic risk (damage to ship structure, equipment and cargo, including total loss, and loss of reputation).

Quantifying the first two categories in monetary terms is controversial and typically beyond the scope of risk-based DSS. Events related to these risk categories generally have a low probability of occurrence (less than 10^{-3}). Such extremely hazardous situations are classified as "intolerable" risks that must be mitigated regardless of cost. These risks may be considered at the ship design stage and addressed through proper masters' training or qualitative guidance [18].

Additionally, due to the well-known "tail sensitivity" issue in structural reliability analysis, the probabilities of such rare events are highly dependent on the uncertainty model used and cannot be applied universally [7]. In risk terminology, DSS is used in the "As Low as Reasonably Practicable" (ALARP) region, which lies between "intolerable" and "negligible" (broadly acceptable) risk levels [40].

The economic losses necessary for risk estimation can be expressed as:

$$C_{tot} = C_c + C_{eq} + C_s + C_d + C_{rp} \tag{23}$$

where

- C_c represents damage to cargo;
- C_{eq} accounts for damage to equipment;
- C_s represents damage to ship;
- C_d is costs related to delays;
- C_{rp} represents costs associated with loss of reputation.

The latter component, C_{rp}, includes factors such as passenger seasickness, reduced crew performance, and the consequences of delays, all of which directly impact the economic viability and reputation of maritime services [18]. Estimates of economic losses should ideally be provided by the owner or operator, preferably supported by data from insurance companies [7].

An example of a consequence analysis for an oil tanker, including specific costs associated with potential hull failure or the exceedance of specific limit states, is presented in [36]. In that study, total consequences are divided into:

- Direct consequences, i.e., losses due to damage or failure itself;
- Indirect consequences, i.e., losses related to system failures or malfunctions that result in external monetary impacts.

The primary risk control parameters for a ship sailing in waves are forward speed and heading relative to waves. For each combination of these parameters, the probability of exceeding seakeeping criteria is determined through reliability analysis, while the total risk is calculated using Equation (22).

Some alternative combinations of ship speed and heading angles will likely result in lower total risk compared to the current settings, suggesting that risk reduction can be achieved. However, at the same time, altering speed and/or course will certainly increase anticipated voyage costs, such as higher fuel consumption due to a longer route.

The risk criterion is expressed as the ratio of the potential cost ΔR and the related certain cost Δc, i.e.,

$$\frac{\Delta R}{\Delta c} = \frac{R_{current} - R_{alter}}{\Delta c} > M \tag{24}$$

where

- $R_{current}$ and R_{alter} represent the risk of the current and alternative combination of speed and heading, respectively;
- Δc is the increased costs because of choosing alternative sailing parameters;
- M is the risk control ratio, typically greater than 1, which serves as the decision criterion for the ship master when making maneuvering choices in heavy weather.

More elaborated discussion on the risk control options using Equation (24) is provided in [18].

3. Results

3.1. Example Ship Description

This study is presented for a model of a liner ship operating in the Adriatic Sea (Figure 1). The main particulars of the ship are given in Table 3. The main particulars of the ship model correspond to the features of the vessels within the "larger ferry category".

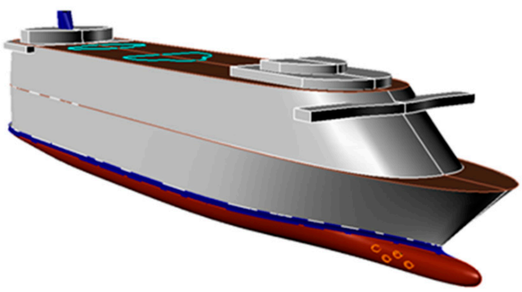

Figure 1. Three-dimensional model of the ship used in this study.

Table 3. Main particulars of the ship.

Feature	Value	Measuring Unit	Description
L_{OA}	114	m	Length overall
L_{PP}	103.2	m	Length between perpendiculars
B	18.7	m	Breadth
T	5	m	Draft
V	17	kn	Nominal ship speed

The shipping route between Ancona (Italy) and Split (Croatia) is assumed (Figure 2).

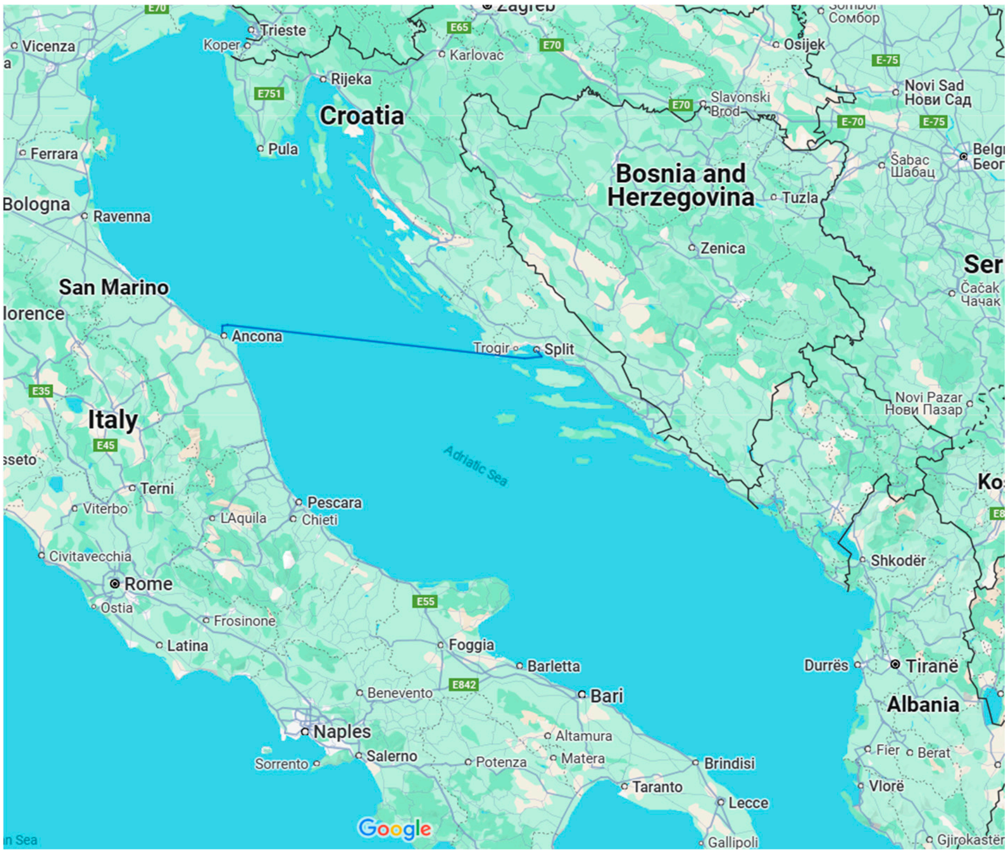

Figure 2. Shipping route: Split (right)–Ancona (left).

The histogram of sea states along this shipping route is presented in Figure 3. Data in Figure 3 are obtained from the extensive analysis of sea states in the Adriatic Sea, using a reanalysis database [24].

Based on the prior study of the shipping route, it is expected that the ship would only face waves from 45° and 135° directions, which correspond to the routes from Split to Ancona and vice versa.

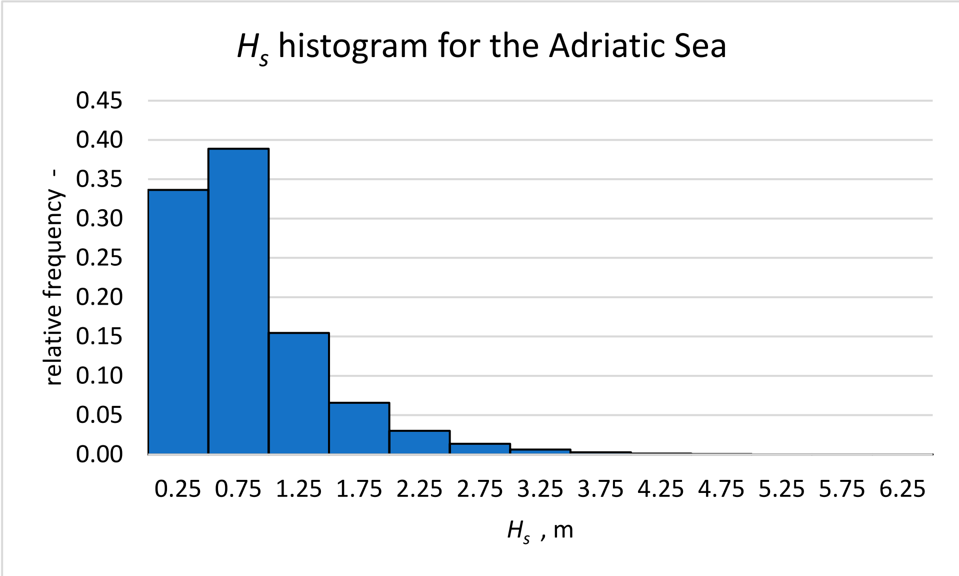

Figure 3. Histogram of the sea states along the assumed shipping route in the Adriatic Sea.

3.2. Probabilistic Operability Diagrams

Cumulative probability distributions for each criterion are obtained by the procedure presented in Section 2.2 in a way that, for the nominal ship speed, for each sea state, given by a significant wave height *Hs* and wave spectrum presented in Section 2.1.3, and for each heading angle β, probabilities of not satisfying limit state functions given in Section 2.3 are calculated. Probability distribution functions for pitch, vertical acceleration at FP, slamming, propeller emergence for a heading angle of 180°, and a roll angle for beam seas (β = 90°) are presented in Figure 4. Horizontal lines denote exceedance probabilities of 5%, 50%, and 95%, where it may be noticed that they correspond to different *Hs*, depending on the seakeeping criterion.

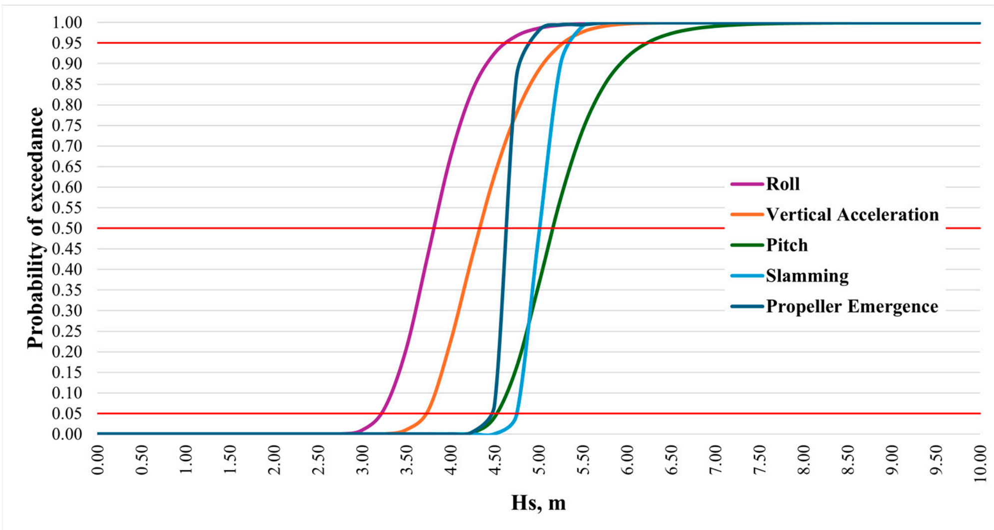

Figure 4. Cumulative distributions (Horizontal lines denote exceedance probabilities of 5%, 50%, and 95%).

The results are then presented in the form of probabilistic operability diagrams. Probability plots for each of the five criteria evaluated are presented in Figure 5 for three exceedance probabilities: 5%, 50%, and 95%. Radial coordinates indicate the sea state according to the Douglas scale, while the angular coordinate is a heading angle between the ship and waves, where 180° denotes head seas. For the clarity of presentation, sea states are presented in the Douglas scale, given in Table 4.

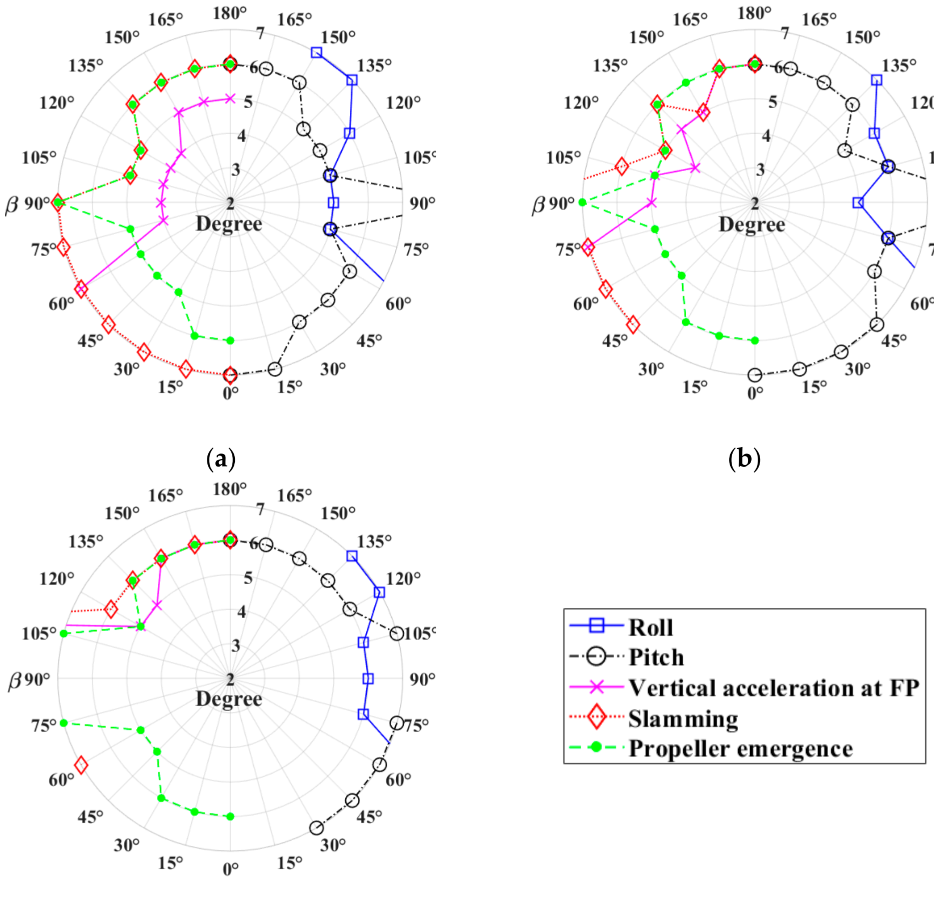

(**a**) (**b**) (**c**)

Figure 5. Polar plots for probabilities of exceeding limit states of: (**a**) 5%; (**b**) 50%; (**c**) 95%.

Table 4. Douglas scale of sea states.

Degree	Wave Height (m)	Description
0	0	Calm (glassy)
1	0–0.1	Calm (rippled)
2	0.1–0.5	Smooth (wavelets)
3	0.5–1.25	Slight
4	1.25–2.5	Moderate
5	2.5–4	Rough
6	4–6	Very rough
7	6–9	High
8	9–14	Very high
9	>14	Phenomenal

Obviously, the severity of the sea state for which each criterion is exceeded is increasing with an increased probability level. Thus, for sea states in the first diagram, there is only a 5% chance of exceeding each criterion. If the ship owner or ship master is averse to taking the risk, he will consider that diagram. On the other hand, if he is willing to take the risk, then a third diagram can be used, as the operability values would almost certainly be exceeded on the sea states indicated on the diagram.

4. Discussion

4.1. Application in Ship Design

The probabilistic approach to the operability diagrams may be used in ship design as the decision-making tool when acquiring a new ship for a specific service. For that purpose, the Operability Index (OI) is proposed, representing the ratio, expressed as a percentage, between the number of sea states (for all available peak periods) with significant wave heights that do not exceed the limiting significant wave height (n_{ss}, β) over the total number of sea states (N) in a certain wave scatter diagram. The OI reads [1]:

$$\text{OI }(\%) = \frac{\sum_{H_{1/3},T_P} n_{ss,\beta}\left(H_s < H_s^{lim}\right)}{N}\cdot 100, \tag{25}$$

In the present study, the Probabilistic Operability Index (POI (%)) is proposed as:

$$\text{POI}(\%) = \sum_{H_{1/3},T_P} f_{H_{1/3},T_p} P\left(H_s < H_s^{lim}\right)\cdot 100, \tag{26}$$

where f_{H_s,T_P} is the relative frequency of the occurrence of the sea state, described by H_s and Tp, given as

$$f_{H_s,T_P} = \frac{n_{H_s,T_p}}{N}, \tag{27}$$

where n_{H_s,T_P} is the number of sea states with H_S and Tp. $P\left(H_s < H_s^{lim}\right)$ is the probability that the seakeeping limiting value is not exceeded at sea states defined by H_S and Tp, calculated by the approach outlined in Section 2. Expressions (25)–(27) require a wave scatter diagram relevant to the ship's operational area to determine the number of sea states defined by H_S and Tp. Additionally, it should be clarified that the application of these expressions assumes a constant ship speed. Consequently, different operability indices are calculated for varying ship speeds.

The process is illustrated by calculating the POI (%) and OI (%) for the histogram of significant wave heights (Figure 3) for the shipping route in the Adriatic Sea (Figure 2). Thus, POI = 98.7% and OI = 98.9% for a speed of 17 kn are obtained.

The POI, as defined by Equation (26), is well-suited for application in risk-based decision making. To incorporate this into decision making, the cost of the non-fulfillment of ship operations should be included by estimating the total risk associated with a given sailing route. However, estimating the cost of non-fulfillment is challenging, as it is company-specific and lacks publicly available references.

A rough estimate can be made by considering the primary cost categories associated with delays, namely:

- The operational costs of delay, including increased fuel consumption due to rerouting, which can be approximately USD 3000–USD 5000 per additional hour of voyage time. A similar cost may apply for crew overtime;
- Port and logistics costs related to late arrivals, rescheduling, and supply chain disruptions, estimated at USD 5000–USD 25,000;
- Passenger compensation, including partial refunds, food, and accommodation expenses, which can exceed USD 25,000.

According to a response generated by ChatGPT (GPT-4-turbo, OpenAI, April 2024; retrieved 31 March 2025), for a 3 to 6 h delay—a realistic scenario previously observed on the Ancona–Split route—the estimated cost could be anywhere from USD 10,000 to USD 100,000+, depending on fuel adjustments, port penalties, and passenger compensation. Longer delays (overnight cancellations) could push costs beyond USD 250,000. For a lifetime risk assessment, this value should be scaled based on the total number of voyages.

4.2. Application in DSS for Ship Operation

The probabilistic approach can be used in ship operation for tactical DSS. When a ship encounters heavy weather, a probabilistic operability plot could be a useful tool to help the ship master evaluating the consequences of potential maneuvers, i.e., changing the course and/or reducing the ship speed. This is illustrated in Figure 6, where the effect of maneuvering in heavy weather is presented. On the right-hand side of the polar plot, results are presented for a nominal ship speed of 17 kn, while results on the left-hand side refer to the reduced ship speed of 5 knots. Although differences in this example are not very large, the shipmaster could evaluate what would be the consequences of the potential speed or course changes.

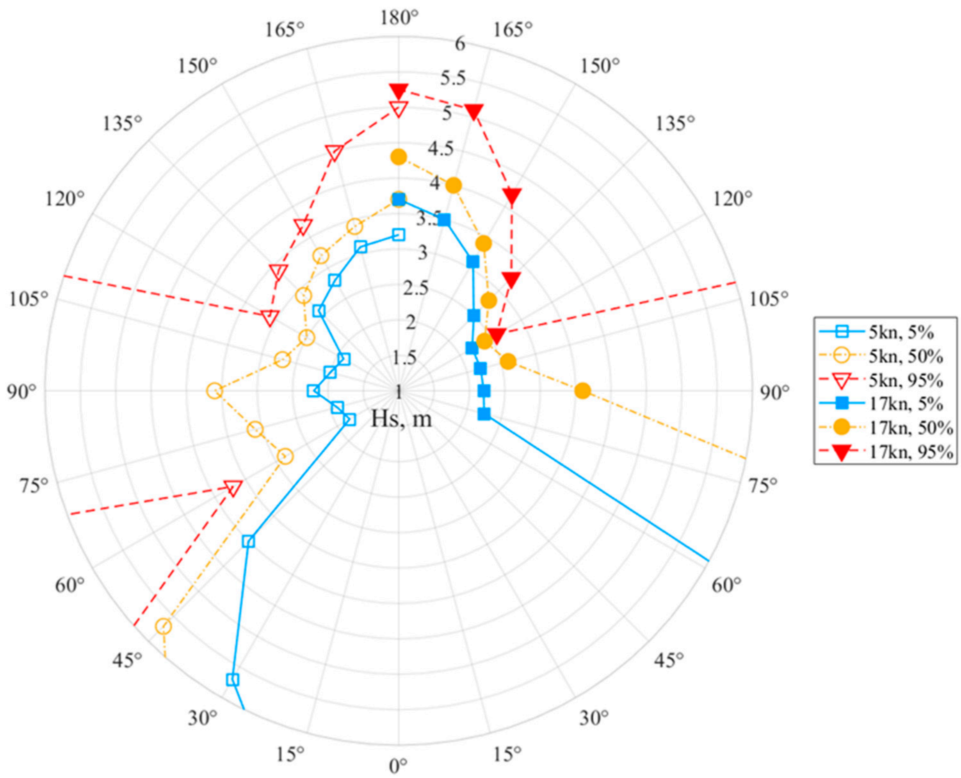

Figure 6. Polar plots representing the effect of ship speed on probabilities of exceeding limit states (Left: Ship speed 5 knots; Right: Ship speed 17 knots.)

If the costs related to the delay specified in Section 4.1 are considered, then it may be stated that for the 5% exceeding probability, the risk involved, obtained by multiplying the costs of delay with 0.05, is rather small and hardly altering the sailing route would be justified. This is not the case for the 95% exceeding probability, where risk reduction by modifying the sailing parameters would be cost-efficient and a different combination can be considered.

4.3. Correlation with the Experience on the Shipping Route

The ship analyzed in the present study is similar to the actual ship sailing on the route from Ancona to Split and vice versa. Although the ship is not the same, it is of interest to analyze publicly available heavy weather examples that occurred on the route concerned. There are rare examples of the inconveniences that big waves generated by 'jugo' wind caused to the passenger ships, like the one analyzed herein. 'Jugo' is a southeast wind causing the highest waves in the Adriatic Sea [41].

The marine accident that happened on 1 November 2012, just after midnight, was described in [42]. Seventy vehicles were damaged in a ferry on the voyage from Ancona to Split because of the large roll amplitudes. During a severe storm, vehicles began to slide and collide with other vehicles and sides of the ferry. The maximum significant wave height along the route on the night of the accident was 5.31 m, as may be seen from the Mediterranean Sea Wave Reanalysis database [43]. This significant wave height corresponds to Sea State 6 according to the Douglas scale (Table 4). The significant wave height at the time of the accident is shown in Figure 7.

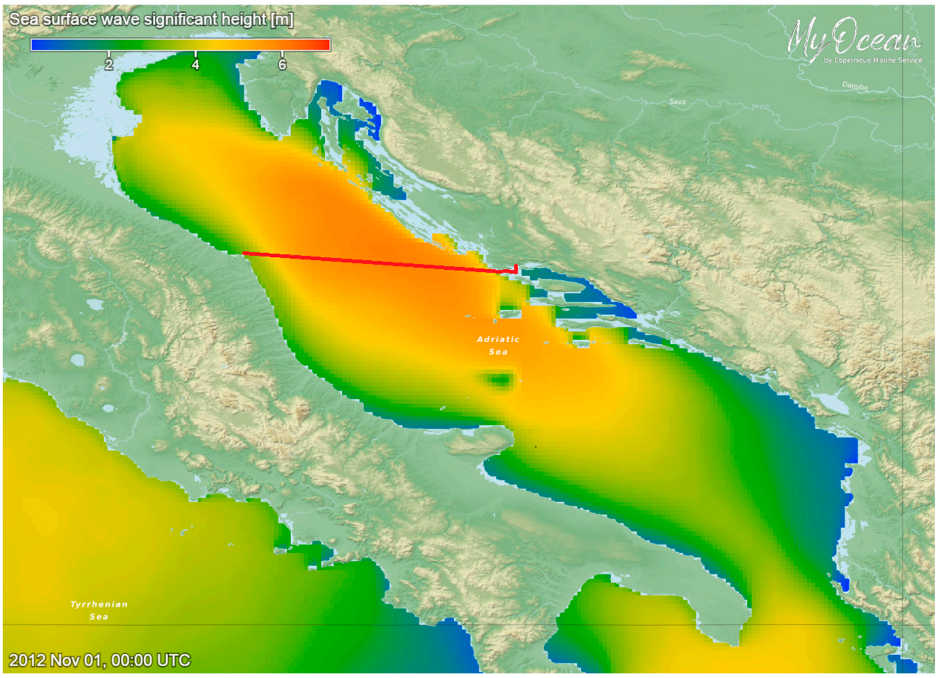

Figure 7. Significant wave height in the Adriatic Sea on 1 November 2012 (generated using E.U. Copernicus Marine Service Information [44]).

Another accidental event was recorded recently, on 23 December, when a delay of 6 h occurred because of the heavy weather. The reconstruction of sea states in the time of the delay can be carried out using Mediterranean Sea Waves Analysis and Forecast [45]. The sea states along the route are shown in Figure 8. The maximum significant wave height along the route was only about 3.13 m. The significant wave height corresponds to Sea State 5 according to the Douglas scale.

It is interesting to mention that the maximum recorded significant wave height along the route in the Mediterranean Sea Wave Reanalysis database, since January 1985, was 6.12 m, which occurred on 1 February 1986. The severity of sea states along the route from 1 January 1985 to 31 May 2013 is presented in Figure 9. One may notice that rough Sea State 5 (2.5 m < H_S < 4 m), according to the Douglas scale, is not rare along the shipping route. Very rough seas, corresponding to 6 on the Douglas scale, with a significant wave height above 4 m occur on average once per year.

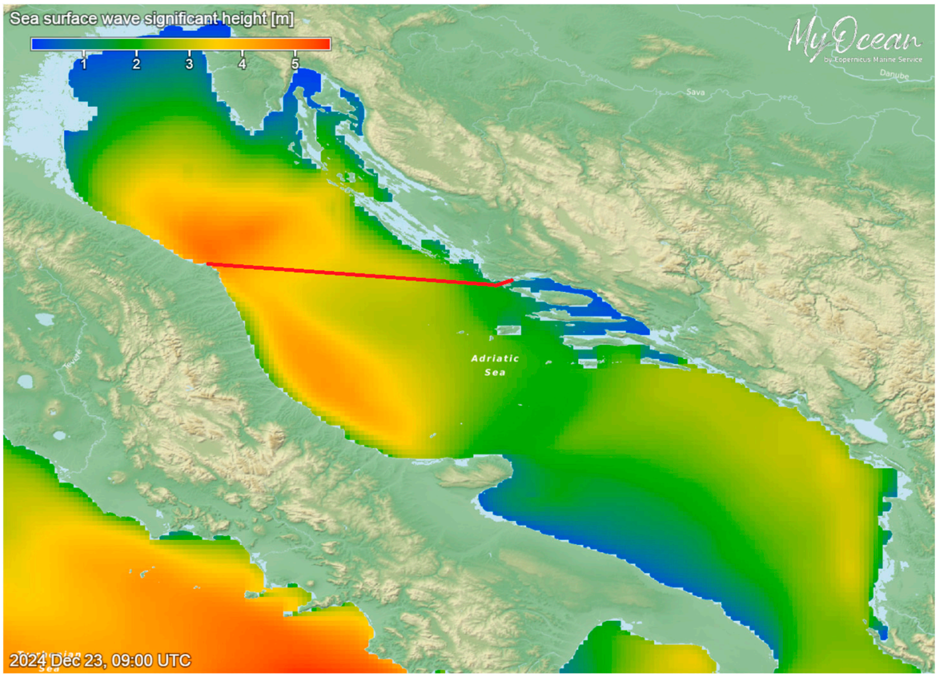

Figure 8. Significant wave height in the Adriatic Sea on 24 December 2024 (generated using E.U. Copernicus Marine Service Information [46]).

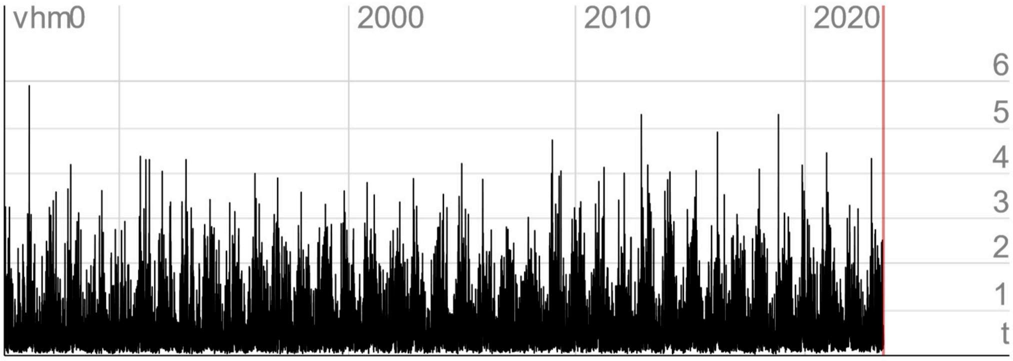

Figure 9. Significant wave height along the route Ancona–Split from January 1985 to May 2023 (generated using E.U. Copernicus Marine Service Information).

The examples presented from the sailing route concerned may be compared to the operability diagrams in Figure 5, where special attention should be paid to the heading angles of 45° and 135°. One may see that diagrams with a 5% exceeding probability are rather pessimistic, as even Sea State 4 is considered critical regarding the criterion of vertical acceleration at FP. However, for the 50% and 95% exceeding probabilities, the operability diagrams look credible, as the ship operability in Sea States 5 and 6 is questionable. For Sea State 5, the most critical criteria are the vertical acceleration at FP and propeller emergence, while for Sea State 6, most of the criteria are unsatisfactory.

4.4. Limitations of the Model

This study focuses on a single ship model, specifically a passenger ferry operating on a key and frequent route in the Adriatic Sea. This route is significant due to its high frequency of use and delays attract public attention, as discussed in Section 4.3. Another reason for selecting this route is that the environmental conditions along the route are well-defined [24]. For shipping routes in general, considerable uncertainty in environmental descriptions should be included in the limit state equations discussed in Section 2.3.

One simplification applied in this study is the use of a single-parameter JONSWAP-type wave spectrum for the Adriatic Sea [30]. Although this formulation provides a reasonable approximation for many fully developed wind-generated sea states in the Adriatic, the variation of peak wave periods (Tp) with significant wave heights (H_S) should be considered. Particularly, if other wave environments, such as the North Sea or open oceans, are considered, the operability plots should be extended for different combinations of H_S and Tp, as well as for other wave spectral models.

Although this study can be extended to other ship types, the careful consideration of ship-specific uncertainties in the ship response, heavy weather maneuvering, seakeeping criteria, and limiting values should be conducted. These additional considerations limit the generalizability of this study's conclusions to other vessel types.

This study does not consider wind effects, although strong winds, including cross-winds or headwinds, can influence ship maneuverability. It is important to note that maritime disasters have occurred due to wind effects in addition to the wave action. In the Adriatic, however, the strongest winds and highest waves do not occur simultaneously [24]. Extreme wind speeds are recorded during the northeastern 'bura' wind, which blows across the shorter axis of the Adriatic basin and generally lasts for a short duration. Despite being the strongest wind, the 'bura' does not generate the highest waves because of the limited fetch. In contrast, the southeastern **'jugo' winds** blow with a lower intensity but are more persistent and have a longer fetch, generating the highest waves in the Adriatic [24].

As a result, the 'bura' wind creates maneuverability challenges and can lead to dangerous situations for ships in ports and confined waters, while shipping safety in open seas is more affected by high waves generated by the 'jugo'. An example of the 'bura' wind's impact on maneuvering a cruise ship in the protected Bay of Kotor in the Adriatic can be found in [47]. In contrast, ferry accidents in the open Adriatic Sea, as discussed in Section 4.3, are generally attributed to waves, as reported by witnesses.

It is important to clarify that only delay-related costs are considered in the present study (Sections 4.1 and 4.2), while other potential costs caused by heavy weather, such as damage to cargo, equipment, or ship structures, are omitted. This approach is justified for the Adriatic Sea, which is the mildest sea basin in the Mediterranean [24]. As a result, ship structural damage is rare due to the extremely low probability of severe environmental conditions in the Adriatic. Ship structures are generally designed to withstand more extreme conditions.

However, the inclusion of other costs in the risk assessment is straightforward, as described in Section 2.5. Using risk as a performance indicator to account for structural consequences induced by different limit states to evaluate optimal ship routing is presented in [36].

5. Conclusions

This study contributes by formulating and solving limit state functions for various ship operability criteria, incorporating epistemic uncertainties in seakeeping responses and uncertainties in operability limiting values. The reliability analysis was conducted using Comrel software, employing the second-order reliability method.

The results of this study are presented in probabilistic operability diagrams, i.e., polar plots providing significant wave heights and heading angles for which seakeeping criteria will be exceeded with certain probabilities. Probabilistic operability diagrams are more informative than "deterministic" diagrams, and this approach could be further extended for use in risk-based decision making, providing that consequences of exceeding seakeeping criteria are defined.

The probabilistic approach can be used in ship design as the decision-making tool when acquiring a new ship for a specific service. For that purpose, a novel probabilistic operability index is defined, representing an extension of the commonly used operability index. Furthermore, the approach can be used as a part of an advanced, risk-based tactical decision support system, assisting ship masters in making real-time decisions on heavy weather maneuvering.

It was also shown how the proposed system can be validated using numerical wave databases, in this case, Mediterranean Sea Wave Reanalysis and Mediterranean Sea Waves Analysis and Forecast, both part of the Copernicus Marine Service.

Recommendations for Future Development

This study is limited to a passenger ferry operating on a route in the Adriatic Sea. However, the analysis can be extended to other ship types, such as container ships and tankers, which operate in significantly more severe oceanic conditions. The influence of strong winds, including crosswinds and headwinds, on the ship maneuverability should also be considered. Additionally, incorporating a wave–structure interaction could be crucial for certain vessel types, such as large container ships.

To ensure the reliability of the model, validation using ships operating in extreme conditions is necessary. Furthermore, integrating artificial intelligence methods could enhance the model's predictive accuracy.

Author Contributions: Conceptualization, J.P.; methodology, J.P. and T.P.; software, T.P.; validation, J.P.; formal analysis, T.P.; investigation, T.P.; resources, J.P.; data curation, T.P.; writing—original draft preparation, T.P.; writing—review and editing, J.P. and T.P; visualization, T.P.; supervision, J.P.; project administration, T.P.; funding acquisition, J.P. All authors have read and agreed to the published version of the manuscript.

Funding: This work was supported by the Croatian Science Foundation under the project HRZZ-IP-2022-10-2821.

Institutional Review Board Statement: Not applicable.

Informed Consent Statement: Not applicable.

Data Availability Statement: The original contributions presented in this study are included in the article. Further inquiries can be directed to the corresponding authors.

Acknowledgments: The costs of voyage delays are estimated by ChatGPT. This study has been conducted using E.U. Copernicus Marine Service Information; https://doi.org/10.25423/cmcc/medsea_multiyear_wav_006_012 (accessed on 3 March 2025); and https://doi.org/10.25423/cmcc/medsea_analysisforecast_wav_006_017_medwam4 (accessed on 4 March 2025).

Conflicts of Interest: The authors declare no conflicts of interest.

References

1. Fonseca, N.; Guedes Soares, C. Sensitivity of the expected ships availability to different seakeeping criteria. In Proceedings of the OMAE'02 21st International Conference on Offshore Mechanics and Artic Engineering, Oslo, Norway, 23–28 June 2002; Volume 4, pp. 595–603. [CrossRef]
2. Gil Rosa, J.; Wang, S.; Guedes Soares, C. Improvement of ship hulls for comfort in passenger vessels. In *Maritime Technology and Engineering 5 Volume 2*, 1st ed.; Guedes Soares, C., Ed.; CRC Press: London, UK, 2021. [CrossRef]
3. Scamardella, A.; Piscopo, V. Passenger ship seakeeping optimization by the Overall Motion Sickness Incidence. *Ocean Eng.* **2014**, *76*, 86–97. [CrossRef]
4. Gutsch, M.; Steen, S.; Sprenger, F. Operability robustness index as seakeeping performance criterion for offshore vessels. *Ocean Eng.* **2020**, *217*, 107931. [CrossRef]
5. Saröz, K.; Saröz, E. Habitability Assessment of Passenger Vessels Based on ISO Criteria. *Mar. Technol.* **2005**, *42*, 43–51. [CrossRef]

6. Carchen, A.; Gaggero, T.; Besio, G.; Mazzino, A.; Villa, D. A method for the probabilistic assessment of the on-board comfort on a passenger vessel route. *Ocean Eng.* **2021**, *225*, 108702. [CrossRef]
7. Bitner-Gregersen, E.M.; Skjong, R. Concept for a risk-based Navigation Decision Assistant. *Mar. Struct.* **2009**, *22*, 275–286. [CrossRef]
8. Ghaemi, H.; Olszewski, H. Total ship operability-review, concept and criteria. *Pol. Marit. Res.* **2017**, *24*, 74–81. [CrossRef]
9. Dong, Y.; Frangopol, D.M.; Sabatino, S. A decision support system for mission-based ship routing considering multiple performance criteria. *Reliab. Eng. Syst. Saf.* **2016**, *150*, 190–201. [CrossRef]
10. Nielsen, U.D.; Iseki, T. Prediction of first-order vessel responses with applications to Decision Support Systems. In Proceedings of the SNAME 5th World Maritime Technology Conference, Providence, RI, USA, 4–6 November 2015. [CrossRef]
11. Li, L.; Haver, S.; Berlin, N. Assessment of operational limits: Effects of uncertainties in sea state description. *Mar. Struct.* **2021**, *77*, 102975. [CrossRef]
12. Pennino, S.; Gaglione, S.; Innac, A.; Piscopo, V.; Scamardella, A. Development of a New Ship Adaptive Weather Routing Model Based on Seakeeping Analysis and Optimization. *J. Mar. Sci. Eng.* **2020**, *8*, 270. [CrossRef]
13. Vettor, R.; Guedes Soares, C. Rough weather avoidance effect on the wave climate experienced by oceangoing vessels. *Appl. Ocean Res.* **2016**, *59*, 606–615. [CrossRef]
14. Tezdogan, T.; Incecik, A.; Turan, O. Operability assessment of high speed passenger ships based on human comfort criteria. *Ocean Eng.* **2014**, *89*, 32–52. [CrossRef]
15. Sariöz, K.; Narli, E. Effect of criteria on seakeeping performance assessment. *Ocean Eng.* **2005**, *32*, 1161–1173. [CrossRef]
16. Bitner-Gregersen, E.M.; Waseda, T.; Parunov, J.; Yim, S.; Hirdaris, S.; Ma, N.; Guedes Soares, C. Uncertainties in long-term wave modelling. *Mar. Struct.* **2022**, *84*, 103217. [CrossRef]
17. Parunov, J.; Guedes Soares, C.; Hirdaris, S.; Wang, X. Uncertainties in modelling the low-frequency wave-induced global loads in ships. *Mar. Struct.* **2022**, *86*, 103307. [CrossRef]
18. Spanos, D.; Papanikolaou, A.; Papatzanakis, G. Risk-Based Onboard Guidance to the Master for Avoiding Dangerous Seaways. In Proceedings of the 6th OSAKA Colloquium on Seakeeping and Stability of Ships, Osaka, Japan, 26–28 March 2008.
19. Papanikolaou, A.; Mohammed, E.A.; Hirdaris, S. Stochastic uncertainty modelling for ship design loads and operational guidance. *Ocean Eng.* **2014**, *86*, 47–57. [CrossRef]
20. Nielsen, U.D.; Friis-Hansen, P.; Jensen, J.J. A step towards risk-based decision support for ships—Evaluation of limit states using parallel system analysis. *Mar. Struct.* **2009**, *22*, 209–224. [CrossRef]
21. Mannarini, G.; Carelli, L.; Orović, J.; Martinkus, C.P.; Coppini, G. Towards Least-CO_2 Ferry Routes in the Adriatic Sea. *J. Mar. Sci. Eng.* **2021**, *9*, 115. [CrossRef]
22. Jensen, J.J.; Mansour, A.E.; Olsen, A.S. Estimation of ship motions using closed-form expressions. *Ocean Eng.* **2003**, *31*, 61–85. [CrossRef]
23. Petranović, T.; Mikulić, A.; Gledić, I.; Parunov, J. Comparative analysis of closed-form expressions and other commonly used seakeeping methods. *Ocean Eng.* **2023**, *281*, 114977. [CrossRef]
24. Katalinić, M.; Parunov, J. Comprehensive wind and wave statistics and extreme values for design and analysis of marine structures in the Adriatic Sea. *J. Mar. Sci. Eng.* **2021**, *9*, 522. [CrossRef]
25. Jensen, J.J.; Mansour, A.E. Estimation of ship long-term wave-induced bending moment using closed-form expressions. *Int. J. Marit. Eng.* **2002**, 41–55.
26. Jensen, J.J.; Pedersen, P.T.; Shi, B.; Wang, S.; Petricic, M.; Mansour, A.E. Wave induced extreme hull girder loads on containerships. *Trans. SNAME* **2008**, *116*, 128–151.
27. Nielsen, U.D.; Mounet, R.E.G.; Brodtkorb, A.H. Tuning of transfer functions for analysis of wave-ship interactions. *Mar. Struct.* **2021**, *79*, 103029. [CrossRef]
28. Hansen, S.V.; Pedersen, E. On an advanced shipboard information and decision-making system for safe and efficient passage planning. *TransNav Int. J. Mar. Navig. Saf. Sea Transp.* **2008**, *2*, 69–73.
29. Tabain, T. Standard wind wave spectrum for the Adriatic Sea revisited (1977–1997). *Brodogradnja* **1997**, *45*, 303–313.
30. Katalinić, M.; Ćorak, M.; Parunov, J. Optimized wave spectrum definition for the Adriatic Sea. *Naše More* **2020**, *67*, 19–23. [CrossRef]
31. Guedes Soares, C. Effect of transfer function uncertainty on short-term ship responses. *Ocean Eng.* **1991**, *18*, 329–362. [CrossRef]
32. Zu, M.; Garme, K.; Rosén, A. Seakeeping criteria revisited. *Ocean Eng.* **2024**, *297*, 116785. [CrossRef]
33. Lloyd, A.R.J.M. *Seakeeping: Ship Behavior in Rough Weather*; A.R.J.M. Lloyd: Andover, UK, 1998.
34. Ćorak, M.; Vujičić, S.; Petranović, T.; Parunov, J. Critical overview of the operability limiting criteria of passenger ships in the Adriatic Sea. In *Trends in Maritime Technology and Engineering*, 1st ed.; Guedes Soares, C., Santos, T.A., Eds.; CRC Press: London, UK, 2022; Volume 1. [CrossRef]
35. *STRUREL*, version 2021; Structural Reliability Analysis Programs—COMREL, SYSREL, COSTREL User Manual; RCP Consult GmbH: Munchen, Germany, 2021.

36. Decò, A.; Frangopol, D.M. Risk-informed optimal routing of ships considering different damage scenarios and operational conditions. *Reliab. Eng. Syst. Saf.* **2013**, *119*, 126–140. [CrossRef]
37. Goerlandt, F.; Montewka, J. Maritime transportation risk analysis: Review and analysis in light of some foundational issues. *Reliab. Eng. Syst. Saf.* **2015**, *138*, 115–134. [CrossRef]
38. Li, X.; Zhang, X.; Yuan, Y. Dynamic Multi-Attribute Decision-Making Method for Risk-Based Ship Design. *Appl. Sci.* **2024**, *14*, 5387. [CrossRef]
39. Hsu, W.-K.K.; Chen, J.-W.; Huynh, N.T.; Lin, Y.-Y. Risk Assessment of Navigation Safety for Ferries. *J. Mar. Sci. Eng.* **2022**, *10*, 700. [CrossRef]
40. Guedes Soares, C.; Teixeira, A.P. Risk assessment in maritime transportation. *Reliab. Eng. Syst. Saf.* **2001**, *74*, 299–309. [CrossRef]
41. Mikulić, A.; Parunov, J. A wave directionality and a within-year wave climate variability effects on the long-term extreme significant wave heights prediction in the Adriatic Sea. *J. Mar. Sci. Eng.* **2023**, *11*, 42. [CrossRef]
42. Mudronja, L.; Katalinić, M.; Vidan, P.; Parunov, J. Route planning based on ship roll in numerically modelled heavy seas. In Proceedings of the XXII Symposium Theory and Practice of Naval Architectures (SORTA 2016), Trogir, Croatia, 6–8 October 2016.
43. Korres, G.; Ravdas, M.; Zacharioudaki, A.; Denaxa, D.; Sotiropoulou, M. Mediterranean Sea Waves Reanalysis (CMEMS Med-Waves, MedWAM3 system) (Version 1) [Data set]. Copernicus Monitoring Environment Marine Service (CMEMS) 2021. Available online: https://doi.org/10.25423/CMCC/MEDSEA_MULTIYEAR_WAV_006_012_MEDWAM3I (accessed on 3 March 2025).
44. E.U. Copernicus Marine Service Information. Available online: https://data.marine.copernicus.eu/-/hjndsmdng7 (accessed on 3 March 2025).
45. Korres, G.; Oikonomou, C.; Denaxa, D.; Sotiropoulou, M. Mediterranean Sea Waves Analysis and Forecast (Copernicus Marine Service MED-Waves, MEDWAM4 System) (Version 1) [Data Set]. Copernicus Marine Service (CMS) 2023. Available online: https://doi.org/10.25423/CMCC/MEDSEA_ANALYSISFORECAST_WAV_006_017_MEDWAM4 (accessed on 4 March 2025).
46. E.U. Copernicus Marine Service Information. Available online: https://data.marine.copernicus.eu/-/7oz0pusqco (accessed on 4 March 2025).
47. CrewCenter. Available online: http://crew-center.com/video-cruise-ship-battles-fierce-storm-bay-kotor (accessed on 1 April 2025).

Disclaimer/Publisher's Note: The statements, opinions and data contained in all publications are solely those of the individual author(s) and contributor(s) and not of MDPI and/or the editor(s). MDPI and/or the editor(s) disclaim responsibility for any injury to people or property resulting from any ideas, methods, instructions or products referred to in the content.

Article 3

Article published by MDPI in Journal of Marine Science and Engineering on 14 September 2021.
DOI: 10.3390/jmse9091002

Journal of
Marine Science and Engineering

MDPI

Article

Method for Prediction of Extreme Wave Loads Based on Ship Operability Analysis Using Hindcast Wave Database

Tamara Petranović [1], Antonio Mikulić [1], Marko Katalinić [2], Maro Ćorak [3] and Joško Parunov [1,*]

[1] Faculty of Mechanical Engineering and Naval Architecture, University of Zagreb, 10000 Zagreb, Croatia; tamara.petranovic@fsb.hr (T.P.); antonio.mikulic@fsb.hr (A.M.)
[2] Faculty of Maritime Studies, University of Split, 21000 Split, Croatia; marko.katalinic@pfst.hr
[3] Maritime Department, University of Dubrovnik, 20000 Dubrovnik, Croatia; mcorak@unidu.hr
* Correspondence: josko.parunov@fsb.hr

Abstract: The method for the prediction of extreme vertical wave bending moments on a passenger ship based on the hindcast database along the shipping route is presented. Operability analysis is performed to identify sea states when the ship is not able to normally operate and which are likely to be avoided. Closed-form expressions are used for the calculation of transfer functions of ship motions and loads. Multiple operability criteria are used and compared to the corresponding limiting values. The most probable extreme wave bending moments for the short-term sea states at discrete locations along the shipping route are calculated, and annual maximum extreme values are determined. Gumbel probability distribution is then fitted to the annual extreme values, and wave bending moments corresponding to a return period of 20 years are determined for discrete locations. The system reliability approach is used to calculate combined extreme vertical wave bending moment along the shipping route. The method is employed on the example of a passenger ship sailing across the Adriatic Sea (Split, Croatia, to Ancona, Italy). The contribution of the study is the method for the extreme values of wave loads using the hindcast wave database and accounting for ship operational restrictions.

Keywords: seakeeping operability criteria; operability analysis; wave bending moment; transfer functions; hindcast wave database

check for updates

Citation: Petranović, T.; Mikulić, A.; Katalinić, M.; Ćorak, M.; Parunov, J. Method for Prediction of Extreme Wave Loads Based on Ship Operability Analysis Using Hindcast Wave Database. *J. Mar. Sci. Eng.* **2021**, *9*, 1002. https://doi.org/10.3390/jmse9091002

Academic Editor: Decheng Wan

Received: 29 August 2021
Accepted: 10 September 2021
Published: 14 September 2021

Publisher's Note: MDPI stays neutral with regard to jurisdictional claims in published maps and institutional affiliations.

Copyright: © 2021 by the authors. Licensee MDPI, Basel, Switzerland. This article is an open access article distributed under the terms and conditions of the Creative Commons Attribution (CC BY) license (https://creativecommons.org/licenses/by/4.0/).

1. Introduction

The extreme wave loads on ships are usually determined by weighting short-term sea state responses by their probabilities of occurrences. When linear seakeeping computations are performed, the transfer functions of ship responses are combined with the wave spectra to define short-term responses. The sea state statistics contained in the wave scatter diagram are then used to compute the long-term distribution from which design value can be derived. Extreme value adopted as the design value of global wave load is usually calculated from the long-term distribution for exceeding probability of 10^{-8}. The procedure recommended by the International Association of Classification Societies (IACS) for the computation of long-term global wave loads on ships is given in [1].

The recommended procedure assumes that the wave heading angles are uniformly distributed in all sea states. The possibility that the shipmaster changes heading angle in extreme sea conditions is not considered [2]. Such maneuvers are normally taken to reduce excessive ship responses in heavy weather, most often the ship rolling motion [3]. Consequently, the probability of beam seas is reduced, which is ignored in common computational procedure, but could affect the extreme wave loads [1]. The effect of the heavy weather avoidance is also neglected, although shipmasters in practice tend to avoid the most severe sea states, e.g., by changing ship course or by waiting for favorable weather forecast [4]. The avoidance of heavy weather is partially considered by accepting the wave atlas Global Wave Statistics (GWS) as the source of the wave data [5]. Namely, data in the GWS are collected by the observations from merchant ships that sail along standard trading routes, excluding thus implicitly the most severe weather conditions [3]. Another difficulty represents the fact that weather routing is not the same for all ship types. For example, container ships experience frequent weather routing while oil tankers and bulk carriers rarely change their planned course [6]. Wave statistics in the GWS are subjected to the uncertainties of visual wave observations and wave directionality, as equal probability of waves from all directions is assumed [3].

Alternative methods for the computation of extreme wave loads on ships are considered nowadays to account rationally for mentioned environmental and operational uncertainties. Thus, IACS recently redefined the vertical hull girder loads for container ships using the direct calculation approach [7]. The routing factor has been introduced to reduce the design loads, which were found larger compared to the rule formulation. The improvement of the wave data accuracy is considered by using hindcast numerical wave databases [8,9]. An example of the application of the hindcast database for vessel response prediction and fatigue damage estimation is presented in [10]. To efficiently employ the wave hindcast database for the computation of wave loads on ships, it is essential to account appropriately for weather routing effects. One possible approach is to compare the hindcast database to the visual observations [11].

Although hindcast databases have already been used in ship seakeeping and structural analysis (e.g., [8–10]), incorporation of the operability analysis in the calculation of the extreme wave loads on ships is still missing. That aspect is crucial to obtain realistic estimates of extreme wave loads. In the present study, a method is proposed to calculate extreme wave loads that a ship encounters along a specific route using the hindcast database and accounting for operational restrictions. A case study of a passenger ship sailing from Croatian port Split to Italian port Ancona and vice versa in the Adriatic Sea is presented. All sea states along the shipping route contained in the hindcast wave database for the period from January 1997 to January 2020 are considered in four available locations along the route. The most probable short-term extreme vertical wave bending moments are determined for each sea state that the ship could encounter. The probability distribution of annual extreme values is then determined for each location. System probability is determined by combining extreme wave bending moments along the route, and bending moments for large return periods are calculated. The effect of heavy weather avoidance is accounted for by ship operability analysis, considering different operability criteria. Wave loads are calculated for three cases:

1. Without any operational restrictions, i.e., for all sea states that ship could potentially encounter along the route;
2. Full operational restrictions, i.e., the case when sea states not satisfying any of the operational criteria are avoided;
3. Partial operability restrictions, i.e., the case when speed is considerably reduced for sea states not satisfying any of the operational criteria.

The focus of the present study is on the probabilistic method for the computation of extreme wave loads. Therefore, a simplified but efficient approach for the calculation of wave-induced responses is used, employing closed-form expressions formulated by Jensen et al. [12]. Seakeeping limiting values for operational criteria are taken specifically for the passenger ship [13].

The paper is organized as follows: The ship and shipping route used in the analysis are described in Section 2. Operability analysis is described in Section 3. The method for the prediction of extreme wave bending moments is given in Section 4, while the results of the analysis are provided in Section 5. Discussion of the results is given in Section 6, and conclusions of the study are provided at the end of the paper. In Appendix A, histograms of annual maximum vertical wave bending moments without and with operational restrictions are given, and in Appendix B, histograms of annual maximum vertical wave bending moments for a case with reduced speed are presented.

2. Ship and Shipping Route

2.1. Ship Particulars

The passenger ship (Figure 1) used for the seakeeping operability analysis is similar to the ferry currently used for coastal and international lines in the Adriatic Sea. The main particulars of the ship that correspond to the features of the vessel within the "larger ferry category" are provided in Table 1.

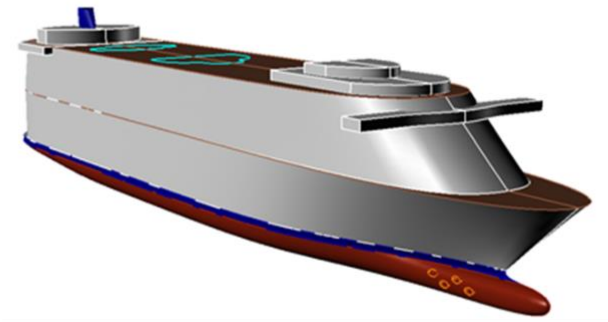

Figure 1. 3D model of the ship used in the study (Adopted from [14]).

Table 1. Main particulars of the ship (Adopted from [14]).

Particular	Value	Measuring Unit	Description
L_{OA}	114	m	Length overall
L_{PP}	103.2	m	Length between perpendiculars
B	18.7	m	Width
T	5	m	Draft
Δ	6565	t	Displacement
C_B	0.617	-	Block coefficient
GM	1.94	m	Metacentric height
v_{max}	17	kn	Maximum speed

2.2. Shiping Route

The passenger ship used in the study is intended to sail between the Croatian port Split and Italian port Ancona across the Adriatic Sea. The heading from Split to Ancona is 275° in nautical coordinates, and that from Ancona to Split is 95° (0° is toward the north). Operability criteria and loads of the ship are determined in four points near the shipping route, with geographical coordinates given in Table 2. The sailing route of the passenger ship, together with four considered points, is shown in Figure 2.

Table 2. Locations of points in the Adriatic Sea (Adopted from [15]).

Point in the Adriatic Sea	Latitude (°)	Longitude (°)
Point 1	43.5	15.5
Point 2	43.5	15
Point 3	43.5	14.5
Point 4	43.5	14

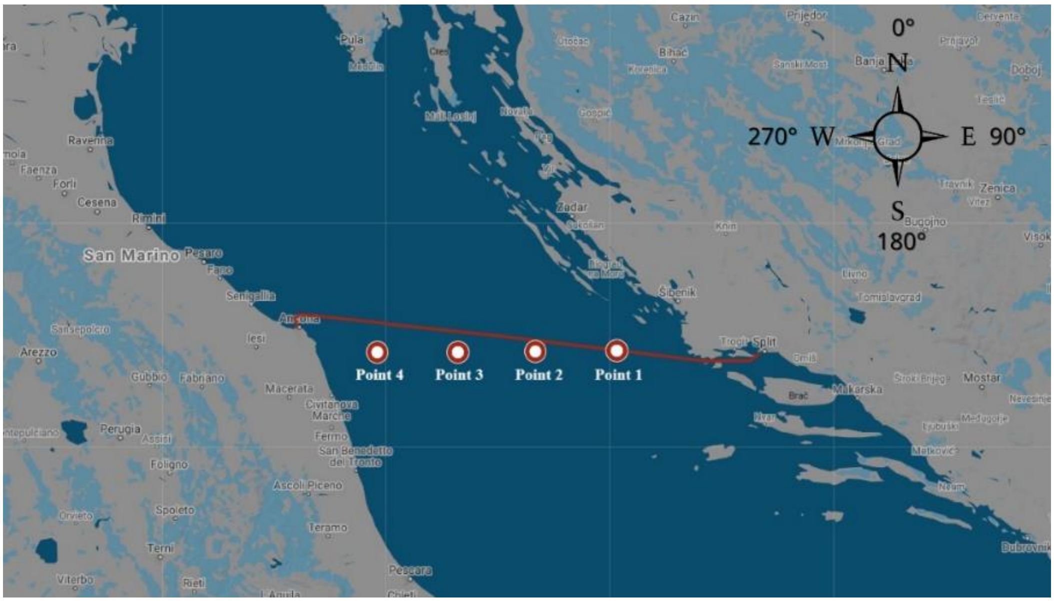

Figure 2. Points near the Split–Ancona route (Adopted from [15]).

3. Operability Analysis

3.1. Transfer Functions for Motions

Wave-induced ship motions are estimated by using closed-form, semi-analytical expressions [12]. The procedure requires only the main ship dimensions as input data: ship length, width, draft, block coefficient, and speed. Closed-form equations for the motion in the vertical plane are derived according to the linear strip theory by neglecting the coupling terms between heave and pitch and assuming a constant sectional added mass, equal to the displaced water. Semi-analytical expressions for transfer functions of heave and pitch are available in [12].

The transfer function of roll is defined in [12] as:

$$\Phi_\varphi = \frac{|M|}{\sqrt{\left[-\overline{\omega}^2 (T_N/2\pi)^2 + 1\right]^2 C_{44}^2 + \overline{\omega}^2 B_{44}^2}} \tag{1}$$

where $\overline{\omega}$ is the encounter frequency, $|M|$ is the amplitude of the roll excitation moment, B_{44} is the hydrodynamic roll damping, C_{44} is the restoring moment coefficient, and T_N is the natural roll period. The viscous roll damping needs to be included in the calculation, and in the present study, 20% of critical damping is used.

3.2. Wave Data

WorldWaves hindcast wave database, containing numerical wave simulation results, calibrated by satellite data over 39 evenly scattered points in the Adriatic Sea for a 23-year period (Figure 3) is employed. Historical information about sea states in four locations near the sailing route is used for this study (location numbers 10, 12, 15, and 18 in Figure 3). Each point contains 12 physical parameters measured every 6 h from January 1997 to January 2020, which makes a total of 33,600 recorded logs. For the purposes of this study, the significant wave height, the peak wave period, the mean wave directions, and time and date records are used [16].

Table 3 shows the maximum recorded significant wave heights in four considered points together with the dates of recordings. It is interesting to notice that maximum significant wave height at three locations is recorded on the same date, indicating a high spatial correlation among extreme sea states on this route.

Figure 3. Thirty-nine evenly distributed locations in the Adriatic Sea (Adopted from [14]).

Table 3. Maximum significant wave heights in 4 locations near the sailing route.

Point in the Adriatic Sea (Figure 2)	Max. H_S (m)	Date
1	5.89	29 October 2018
2	6.18	29 October 2018
3	5.98	29 October 2018
4	5.65	11 November 2013

3.3. JONSWAP Wave Spectrum

The Joint North Sea Wave Project (JONSWAP) wave spectrum, which is the adjustment of the Pierson–Moskowitz spectrum for the existence of a limited fetch and wind persistence, is employed in this study for the semi-enclosed basin of the Adriatic Sea. Adequacy of the JONSWAP wave spectrum formulation for the Adriatic Sea is shown in [16].

The JONSWAP wave spectrum used in the present study is defined by Det Norske Veritas [17]:

$$S_J(\omega) = A_\gamma S_{PM}(\omega)\gamma^{exp\left(-0.5\left(\frac{\omega-\omega_p}{\sigma\omega_p}\right)^2\right)}, \quad (2)$$

where γ is a non-dimensional peak shape parameter, $A_\gamma = 1 - 0.287\ln(\gamma)$ is a normalizing factor, $S_{PM}(\omega)$ is the Pierson–Moskowitz spectrum, $\omega_p = 2\pi/T_p$ is the angular spectral peak frequency, T_p is the peak wave period, and σ is the spectral width parameter.

The non-dimensional peak shape parameter reads:

$$\begin{gathered} -\gamma = 5\ for\ \frac{T_p}{\sqrt{H_s}} \leq 3.6; \\ \gamma = exp\left(5.75 - 1.15\frac{T_p}{\sqrt{H_s}}\right)\ for\ 3.6 < \frac{T_p}{\sqrt{H_s}} < 5; \\ \gamma = 1\ for\ 5 \leq \frac{T_p}{\sqrt{H_s}}. \end{gathered} \quad (3)$$

3.4. Operability Criteria and Limits

Seakeeping operability criteria considered in this paper are the root mean square (RMS) of roll, the RMS of pitch, the RMS of the vertical acceleration at the forward perpendicular (FP), the probability of slamming, the probability of green water, the probability of propeller emergence, and the weighted average motion sickness incidence (WAMSI). The operability analysis is performed to estimate the percentage of time during which the ship may not be able to sail on the given route and with a given speed. Limiting values of selected operability criteria are shown in Table 4. Limiting values employed are universal for all ship types, except limiting values of the roll and the vertical acceleration at FP, which are specific for passenger ships [13].

Table 4. Operability criteria limiting values.

Operability Criterion	Limiting Value
RMS of roll	2.5°
RMS of pitch	1.5°
RMS of vertical acceleration at FP	0.05 g
Probability of slamming	0.03
Probability of green water	0.05
Probability of propeller emergence	0.25
WAMSI	20% in 4 h

Expressions for calculating operability criteria using response spectra and corresponding spectral moments are provided, e.g., in [18].

The passenger comfort criterion used in the present study is the WAMSI, given by:

$$\text{WAMSI} = \frac{\int \text{MSI}\, W\, dx}{\int W\, dx} \tag{4}$$

where MSI is the motion sickness incidence and W is the weighting function. Integrals in Equation (4) are determined along the length of the passenger deck. The weighting function represents the distribution of the people on the passenger deck, taken equal to 1 in the present study, which means that equally weighted subjects are evenly distributed along the passenger deck. The MSI is defined as the percentage of subjects who experienced nausea within a certain amount of time calculated according to the expressions provided in [19]:

$$\text{MSI} = 100\left[0.5 + erf\left(\frac{log_{10}\left(\frac{0.798\sqrt{m_{0_v}}}{g}\right) - \mu_{MSI}}{0.4}\right)\right], \tag{5}$$

where:

$$\mu_{\text{MSI}} = -0.819 + 2.32\left(log_{10}\left(\sqrt{\frac{m_{0_v}}{m_{2_u}}}\right)\right)^2, \tag{6}$$

where m_{0_v} and m_{2_u} are the zeroth moment of the response spectrum of vertical acceleration and the second moment of the response spectrum of vertical motion.

Recently, Overall Motion Sickness Incidence (OMSI) has been introduced as a measure of passenger comfort, defined as the mean MSI over the length and breadth of the passenger deck [20], which is not considered in the present study.

4. Method for the Prediction of Extreme Wave Loads

The transfer function of vertical wave-induced bending moment (VWBM) at midship is calculated according to the closed-form expression [12]:

$$\Phi_M = \kappa\frac{1-kT}{(k_e L_{pp})^2}\left[1-\cos\left(\frac{k_e L_{pp}}{2}\right) - \frac{k_e L_{pp}}{4}\sin\left(\frac{k_e L_{pp}}{2}\right)\right]\cdot F_V(F_n)\cdot F_C(C_B)\cdot\sqrt[3]{|\cos\beta|}\cdot\rho g B_0 L_{pp}^2 \tag{7}$$

where k_e represents the effective wave number, β is the heading angle, κ is the Smith correction factor, $F_V(F_n)$ is the speed correction factor, $F_C(C_B)$ is the correction factor for the block coefficient, $\rho = 1025\ \text{kg/m}^3$ is the sea density, and B_0 is the measured maximum ship breadth at the waterline. Details on how to calculate terms appearing in Equation (7) are given in [12].

The most probable extreme value (MPEV) of VWBM in the short-term sea state depends on the sea state duration T_d = 21,600 s , which corresponds to wave data recording at 6-hour intervals:

$$\mathrm{MPEV(VWBM)} = \sqrt{m_{0_M} \cdot 2ln\left(\frac{T_d}{T_z}\right)}. \tag{8}$$

T_z is the average zero-crossing period of the response, and it is defined as:

$$T_z = 2\pi\sqrt{\frac{m_{0_M}}{m_{2_M}}} \tag{9}$$

where m_{0_M} and m_{2_M} are the zeroth and second moments of the response spectrum of VWBM [21].

For a period of the availability of wave data (January 1997 to January 2020), annual maximum VWBMs are extracted for all sea states in four locations along the route. Histograms are fitted with Gumbel distribution, which is commonly used as the extreme value distribution function. Parameters of Gumbel distribution are estimated using the method of moments [22,23].

The probability of exceedance of the long-term extreme VWBM can be written as:

$$Q = \frac{1}{RP} \tag{10}$$

and the probability of non-exceedance is:

$$F = 1 - Q. \tag{11}$$

where RP is the return period in years [23].

To determine the resulting extreme value distribution along the shipping route, extreme value distributions at individual locations are to be statistically combined. A certain level of VWBM is exceeded along the whole route if exceeded in any of the locations along the route. This can be modeled by considering individual locations as members in a series probabilistic system. First-order upper and lower bounds on the extreme value distribution along the route can be set by considering members of the series system as statistically independent or fully correlated, respectively. The concept was initially proposed by Mansour and Preston considering wave zones in GWS along the route [24]. If one looks at the data given in Table 3, it appears that extreme values at different locations along the route occur at the same time, so the correlation of sea states between locations could be quite large.

If sea states along the location are assumed statistically independent, the system probability of non-exceedance of the extreme vertical bending moment along the sailing route $P_{ne,SI}$ reads:

$$P_{ne,SI} = \prod_{i=1}^{n}(P_{ne_i})^{k_i}, \tag{12}$$

while the system probability of non-exceedance of extreme vertical bending moment for fully correlated sea states along the route $P_{ne,FC}$ is [25]:

$$P_{ne,FC} = \min_i (P_{ne_i})^{k_i}. \tag{13}$$

k_i appearing in Equations (12) and (13) represents the fraction of time that the ship spends in each of n wave locations. If the time spent in port is neglected, then $\sum_{i=1}^{n} k_i = 1$. It is assumed in this study that the ship spends an equal amount of time at each of four locations; i.e., n = 4 and k_i = 0.25. If probability distributions are different for two opposite traveling directions at the same location, then n = 8 and k_i = 0.125.

Combined probability distributions along the route, given by Equations (12) and (13), can be calculated numerically. Combined probability distributions are plotted on the VWBM $-$ P_{ne} diagram, and VWBMs for a 20-year return period are obtained.

5. Results

5.1. Operability Plot

The polar plot in Figure 4 represents the limit values of calculated operability criteria for different wave heading angles and significant wave heights. Only a maximum ship speed of 17 knots is considered in the operability analysis. Values in the polar plot are estimated for the modal spectral frequency ω_m, which is in the Adriatic Sea given as [17]:

$$\omega_m = 0.52 + \frac{1.4}{0.7 + H_s}. \tag{14}$$

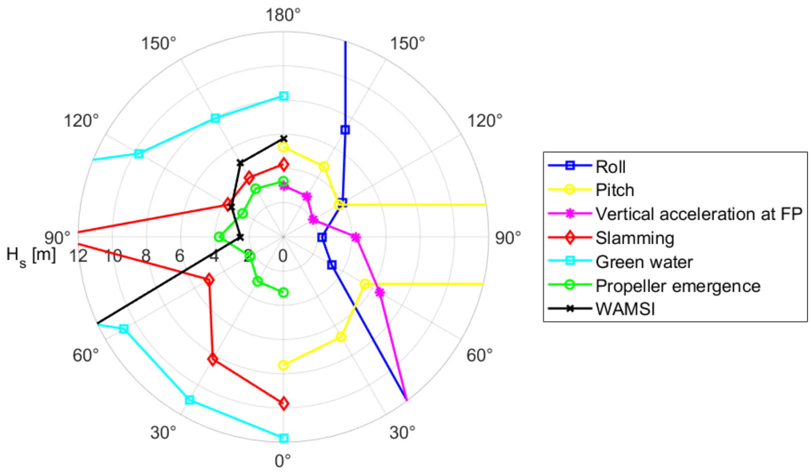

Figure 4. Polar plot (head sea is 180°) (Adopted from [15]).

When the ship sails from Ancona to Split, during the most frequent south-eastern wind, waves encounter the ship at 220°, which is equal to 140° due to symmetry. From Figure 4, one may notice that the limiting vertical acceleration at the FP is exceeded firstly at the significant wave height $H_s = 2.75\ m$. When the ship sails from Split to Ancona, waves encounter the ship at 40°, and it can be seen from Figure 4 that the limit value of the propeller emergence is exceeded firstly at significant wave height $H_s = 2.75\ m$.

The frequencies of exceedance of operability criteria limits for all sea states contained in the hindcasted wave database are presented in Table 5. Frequencies of exceedance for each criterion are obtained by dividing the number of exceedances by the total number of sea states. The total frequency of exceedance when at least one criterion is not satisfied is given in the last column of Table 5. Values outside parentheses in Table 5 refer to westward voyages from Split to Ancona, and values in parentheses are valid for the opposite direction. It can be seen the route from Ancona to Split has an appreciably larger frequency of exceeding operability criteria than the direction from Split to Ancona.

5.2. Probability Distributions of Extreme VWBM at Individual Locations

Short-term yearly extreme VWBMs are calculated in four points along the sailing route for all sea states and only for sea states satisfying operability criteria. The fitting of the Gumbel distribution to the histogram of VWBM is presented in Figures A1–A3 in Appendix A. It may be noticed that the Gumbel distribution in some of the cases does not follow VWBM histograms, so other distribution functions may also be considered for that purpose. However, as the Gumbel distribution is often used for modeling annual extreme values of waves and wave-induced responses (e.g., [18]) it is adopted in the present study as well.

Table 5. Frequencies (in %) of exceeding operability criteria limits for wave data at points 1, 2, 3, and 4 (Figure 2) for the route Split to Ancona (values for the opposite route in parentheses) (Adopted from [15]).

Point	Operability Criteria							
	Roll	Pitch	Vertical Acc. at FP	Slamming	Green Water	Propeller Emergence	WAMSI	Total
1	0.40 (0.17)	0 (0.04)	0.11 (2.12)	0 (0.11)	0 (0)	1.89 (1.14)	0.01 (0.14)	2.06 (2.62)
2	0.36 (0.16)	0 (0.07)	0.11 (2.76)	0 (0.17)	0 (0)	2.13 (1.34)	0.01 (0.15)	2.25 (3.24)
3	0.38 (0.22)	0 (0.07)	0.11 (2.89)	0 (0.18)	0 (0)	2.02 (1.38)	0.02 (0.18)	2.15 (3.40)
4	0.55 (0.36)	0 (0.08)	0.09 (3.44)	0.003 (0.23)	0 (0)	1.82 (1.56)	0.02 (0.23)	1.97 (4.03)

According to the Equation (7), VWBMs are the same in both sailing directions. Consequently, there are no differences in extreme values when operability criteria are not considered. However, the extreme VWBMs calculated only for those sea states satisfying operability criteria are different for two sailing directions due to differences in meeting the operability criteria.

For a 20-year return period, $F = 0.95$ is determined using Equations (10) and (11). The most probable long-term extreme value of VWBM is then obtained from the corresponding Gumbel probability distribution and presented in Table 6. It may be seen that in sea states meeting seakeeping operability criteria, extreme VWBMs are quite similar in different points along the route. Expectedly, extreme wave moments are considerably larger in sea states when operability criteria were not considered than moments when the operability criteria were considered.

Table 6. The most probable long-term extreme values of vertical wave bending moments for a 20-year return period at individual locations along the route (MNm).

Point (Figure 2)	Long-Term Extreme VWBM for 20-Year Return Period (MNm)		
	All Sea States	Sea States Satisfying Operability Criteria	
		Split–Ancona 275°	Ancona–Split 95°
1	124	76	68
2	139	76	73
3	152	78	73
4	150	77	68

5.3. System Probabilities

System probabilities of extreme VWBM for all sea states and for only those sea states satisfying operability criteria are shown in Figure 5. The curves obtained in Figure 5 are determined numerically by the procedure described in Section 4.

For the long return period of 20 years, bounds of extreme VWBM can be determined from diagrams in Figure 5. These values are presented in Table 7, where the left column represents values determined from fully correlated system probabilities and the right column represents statistically independent system probabilities.

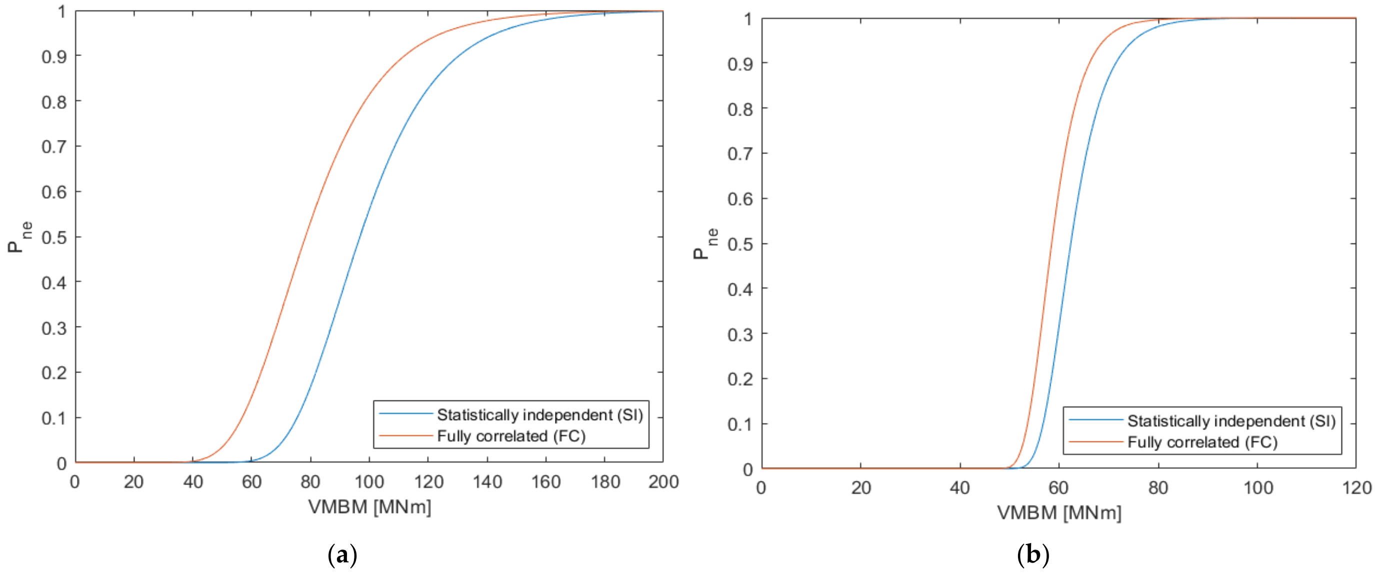

Figure 5. System probabilities of non-exceedance of extreme VWBM calculated for (**a**) all sea states and (**b**) sea states satisfying operability criteria.

Table 7. Bounds of extreme vertical bending moments.

	VWBM (MNm) Determined from $P_{ne,FC}$	VWBM (MNm) Determined from $P_{ne,SI}$
All sea states	125	143
Sea states satisfying operability criteria	69	75

It may be seen from Table 7 that the effect of possible operational restrictions is huge, as the extreme VWBMs are halved if operational restrictions are imposed. The effect of the assumption of the statistical independence is to increase VWBM by about 10% compared to the assumption of full correlation between different locations along the route. The assumption of full correlation seems to be more realistic, according to Table 3. Namely, extreme sea states and consequently extreme wave bending moments at different locations are likely to be achieved during the same voyage.

5.4. The Effect of the Speed Reduction in Severe Sea States

It is unlikely that navigation will be completely suspended during heavy seas. If waves increase during the voyage, and the possibility of exceeding the limits of operability criteria appears, the captain will either reduce the speed or change the direction of navigation.

Extreme VWBMs in Sections 5.2 and 5.3 are calculated for a case where the ship is sailing with a constant speed of 17 knots. To investigate the effect of speed reduction, only for those sea states where the operability criteria limits are exceeded, speed is reduced to 5 knots. Histograms of annual maximum VWBM calculated for courses 275° and 95° are shown in Figures A4 and A5 in Appendix B, together with the Gumbel distribution fitted. The most probable long-term extreme VWBMs for a return period of 20 years at each location are shown in Table 8. Figure 6 presents system probabilities of non-exceedance of the extreme VWBM, and Table 9 presents the bounds of the most probable long-term extreme VWBM for this case.

Table 8. The most probable long-term extreme values of vertical wave bending moments for a 20-year return period calculated for a speed of 17 knots on sea states satisfying operability criteria and a speed of 5 knots on sea states not satisfying operability criteria.

Point (Figure 2)	Long-Term Extreme VWBM for 20-Year Return Period (MNm)	
	Split–Ancona 275°	Ancona–Split 95°
1	104	103
2	116	117
3	126	126
4	124	125

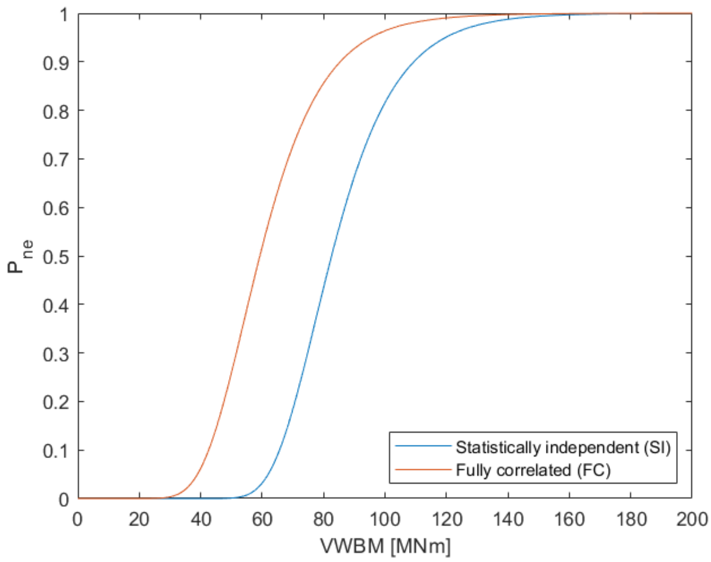

Figure 6. System probabilities of non-exceedance of extreme VWBM for reduced speed.

Table 9. Bounds of extreme vertical bending moments calculated for speed of 5 knots on sea states not satisfying operability criteria.

VWBM (MNm) Determined from $P_{ne,FC}$	VWBM (MNm) Determined from $P_{ne,SI}$
95	120

6. Discussion

The most probable extreme VWBM for the return period of 20 years along the shipping route is summarized in Figure 7. Results are shown for statistically independent and fully correlated extreme values along the shipping route and using different assumptions about the consequences of the operability analysis.

The first, albeit unrealistic option is to use full ship speed in all sea states recorded along the traveling route (in Figure 7a). If all sea states not satisfying operability criteria are avoided, the most probable extreme wave loads are reduced by a factor of 2 (in Figure 7b). If these sea states are not avoided, but ship speed is reduced to the minimum cruising speed, then extreme VWBM decreases by about 20% compared to the full speed (in Figure 7c). The effect of the correlation between short-term sea states along the route is to reduce extremes obtained by assuming statistical independence by 8–21%.

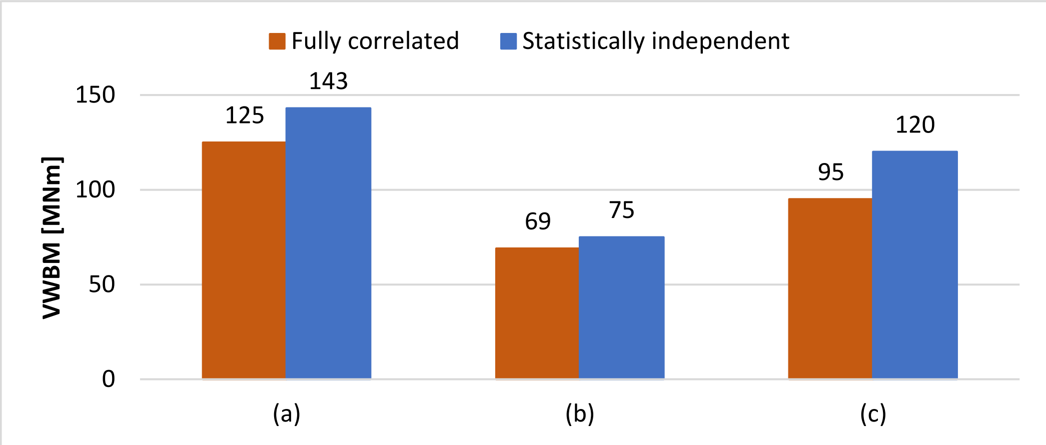

Figure 7. Comparison of extreme VWBMs determined from fully correlated and statistically independent system probabilities for (**a**) all sea states, (**b**) only sea states satisfying operability criteria with speed of 17 knots, and (**c**) a case when ship speed is reduced to 5 knots on sea states not satisfying operability criteria.

The results presented in Figure 7 are compared to the commonly used long-term procedure for the calculation of the extreme wave loads [1]. A combined wave scatter diagram is obtained for four considered locations. All heading angles in the interval 0–2π are assumed to be equally probable and the JONSWAP wave spectrum is used. Constant ship speed of 17 and 5 knots is used in two separate analyses. VWBM corresponding to 10^{-8} probability level is extracted from the long-term distribution and considered as the extreme value for the return period of 20 years. Software developed in [26] is used for a long-term analysis. The most probable extreme VWBM of 145 and 123 MNm is obtained for ship speed of 17 and 5 knots, respectively. These values are almost identical to the corresponding results presented in Figure 7 for the statistically independent case.

Validation of the method for the prediction of extreme wave loads could ideally be done by comparison with full-scale measurements. Such long-term measurement campaigns are, however, rare and difficult to organize [27]. An alternative approach would be to compare the results of the operability analysis with the practice of shipmasters of actual ships in service. This can be done by organizing an interview with shipmasters having experience with similar ships and in a similar wave environment to the one analyzed in the present study. An example of such an interview regarding analysis of a large container ship is presented in [28].

The rare examples of passenger ship accidents in the Adriatic Sea caused by large waves are a possible source of validation of the operability analysis. One such accident happened in November 2012, at 3 a.m., to the ferry sailing from Ancona to Split. Seventy vehicles collided with other vehicles and sides of the ferry, which caused great damage. The accident happened because the roll amplitudes were too large [28]. Significant wave height at the time of the accident was just above 5 m, while wave heading angle was about 140°. Comparing these values with the operability plot in Figure 4, one may conclude that ship was sailing at the operability limit for roll motion while limiting values for bow acceleration and pitch motion were largely exceeded. It is interesting to notice that the shipmaster had to change the course to following waves to avoid large rolling amplitudes [28].

The present analysis is performed for a ship sailing in the Adriatic Sea, as a specific sea environment. Similar analysis can be performed for other ship types and other shipping routes. When other ship types are analyzed, differences are expected in the first place regarding operability criteria limiting values, as the values adopted in the present study are valid for the passenger ships. Regarding different wave environments, the North Atlantic, which is considered as the design wave environment for ocean-going ships sailing without limitation, is of particular interest. Such analysis for the sailing route in the North Atlantic could be performed using, e.g., the ERA5 wave database [25].

It is to be mentioned that the Gumbel distribution is not always a perfect fit to the histogram of annual extreme VWBM, as may be seen in the appendices. Therefore, other distribution functions may also be considered for that purpose. The goodness-of-fit analysis is to be performed to find out the appropriate probability distribution.

To perform the extreme value analysis, it is necessary to have wave information for a period of at least 20 years [29], which is satisfied in the present study. For the analysis based on the long-term distribution, a minimum length of 20% of the desired return period is advised [30]. A convergence study to determine the sensitivity of predicted extreme values on the length of the wave data set is nevertheless recommended.

It should be noted that only linear wave loads are considered in this study. The most important effect of nonlinearity is the difference between sagging and hogging VWBM. The effect is particularly important for fine-form ships with low block coefficients, where sagging and hogging bending moments are larger and smaller than linear values, respectively. Simplified corrections for nonlinear VWBM that can be implemented in the present procedure to extend linear computation are presented in [31,32].

7. Conclusions

The method for calculating long-term extreme values of wave loads on a ship along a defined traveling route is described. The method is based on the hindcast wave database at discrete locations along the shipping route and ship operability analysis. Multiple operability criteria are considered, while transfer functions of wave-induced motions and loads are determined using closed-form expressions developed by Jensen et al. [12]. As the hindcast databases provide sea states in regular time intervals, the most probable extreme values of wave loads are determined for short-term sea states with a duration equal to the time resolution of the database (6 h). Annual maximum values of wave-induced loads are then determined for each location along the route, and Gumbel distribution is fitted. Gumbel distributions are then statistically combined along the route considering sea states at individual locations as independent or fully correlated members of a serial probabilistic system. The procedure enables a determination of the most probable values of wave loads for long return periods that may be used in ship structural design. The present method and the commonly used long-term distribution method result in almost the same long-term extreme values if the assumption of statistical independence among sea states at different locations is adopted. Furthermore, the presented method enables consideration of correlation among wave zones and quantification of the sensitivity of wave loads regarding operational criteria when direct calculation methods are used in ship structural design.

The following conclusions in terms of numerical results are obtained in the study:

- Operational criteria are not satisfied in 2–4% of sea states in four locations along the shipping route.
- If sea states where operability criteria are not satisfied are completely avoided, long-term extreme vertical wave bending moment is reduced by a factor of 2.
- If ship speed is reduced to the minimum cruising speed in sea states where operability criteria are not satisfied, instead of avoiding those sea states, long-term extreme vertical wave bending moment is reduced by about 20%.
- If the assumption of full statistical correlation among sea states along the shipping route is adopted, long-term extreme vertical wave bending moment is reduced by 8–21%. It should be mentioned that wave data in the database indicate that assumption of correlation is justified for this specific, relatively short shipping route.

Author Contributions: Conceptualization, J.P. and T.P.; methodology, J.P. and T.P.; software, A.M. and T.P.; validation, J.P., T.P. and M.Ć.; formal analysis, J.P. and T.P.; investigation, J.P. and T.P.; resources, J.P and M.K.; data curation, M.K.; writing—original draft preparation, T.P.; writing—review and editing, J.P.; visualization, J.P.; supervision, J.P.; project administration, J.P.; funding acquisition, J.P. All authors have read and agreed to the published version of the manuscript.

Funding: This work has been fully supported by Croatian Science Foundation under the project IP-2019-04-2085.

Institutional Review Board Statement: Not applicable.

Acknowledgments: This work has been fully supported by Croatian Science Foundation under the project MODUS (IP-2019-04-2085). The WorldWaves data used in the study are provided by Fugro OCEANOR AS.

Conflicts of Interest: The authors declare no conflict of interest. The funders had no role in the design of the study; in the collection, analyses, or interpretation of data; in the writing of the manuscript; or in the decision to publish the results.

Appendix A. Annual Maximum Vertical Wave Bending Moments

Appendix A.1. All Sea States

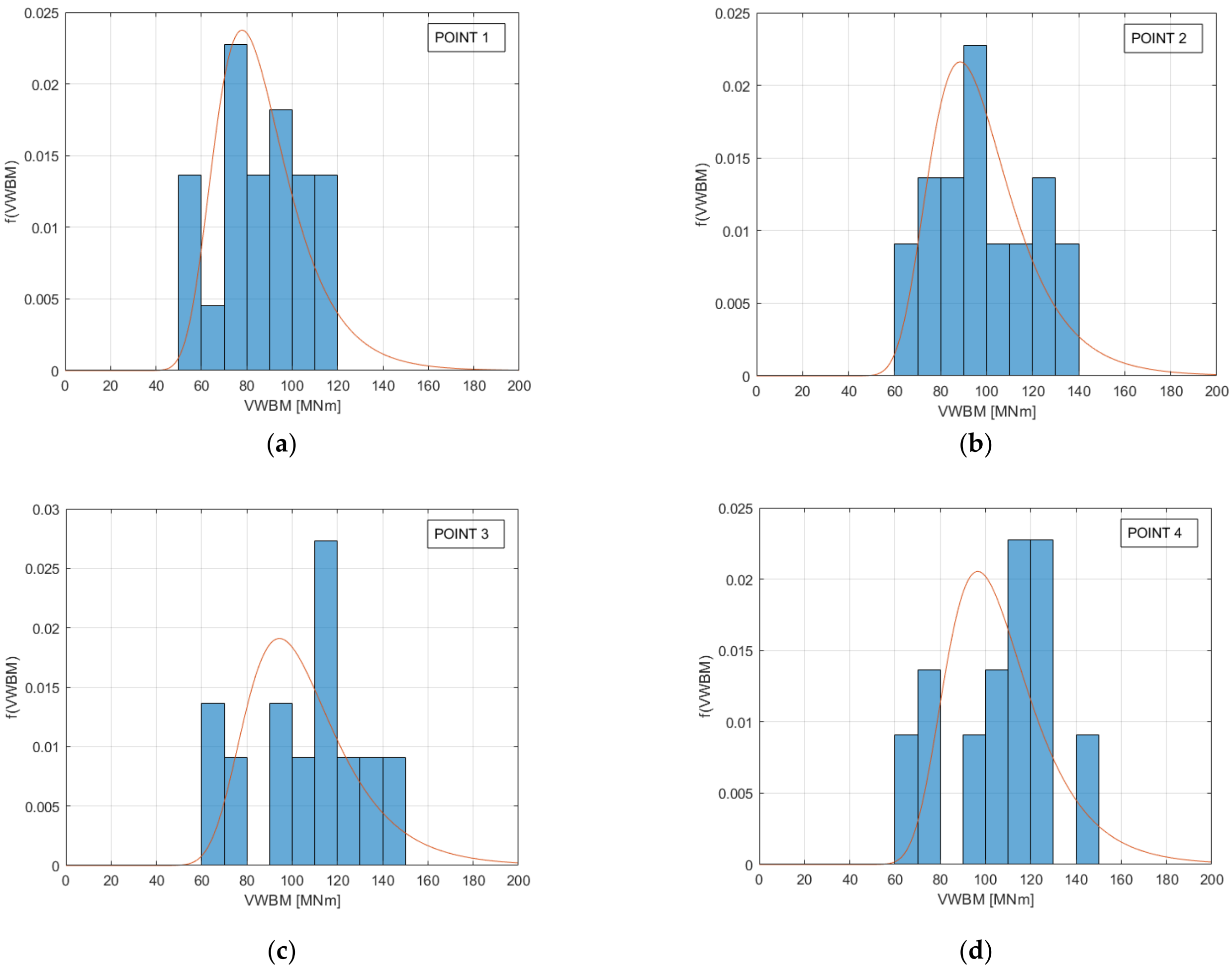

Figure A1. Annual maximum vertical wave bending moments calculated for all sea states: (**a**) at point 1; (**b**) at point 2; (**c**) at point 3; (**d**) at point 4.

Appendix A.2. Sea States Satisfying Operability Criteria on the Sailing Route from Split to Ancona

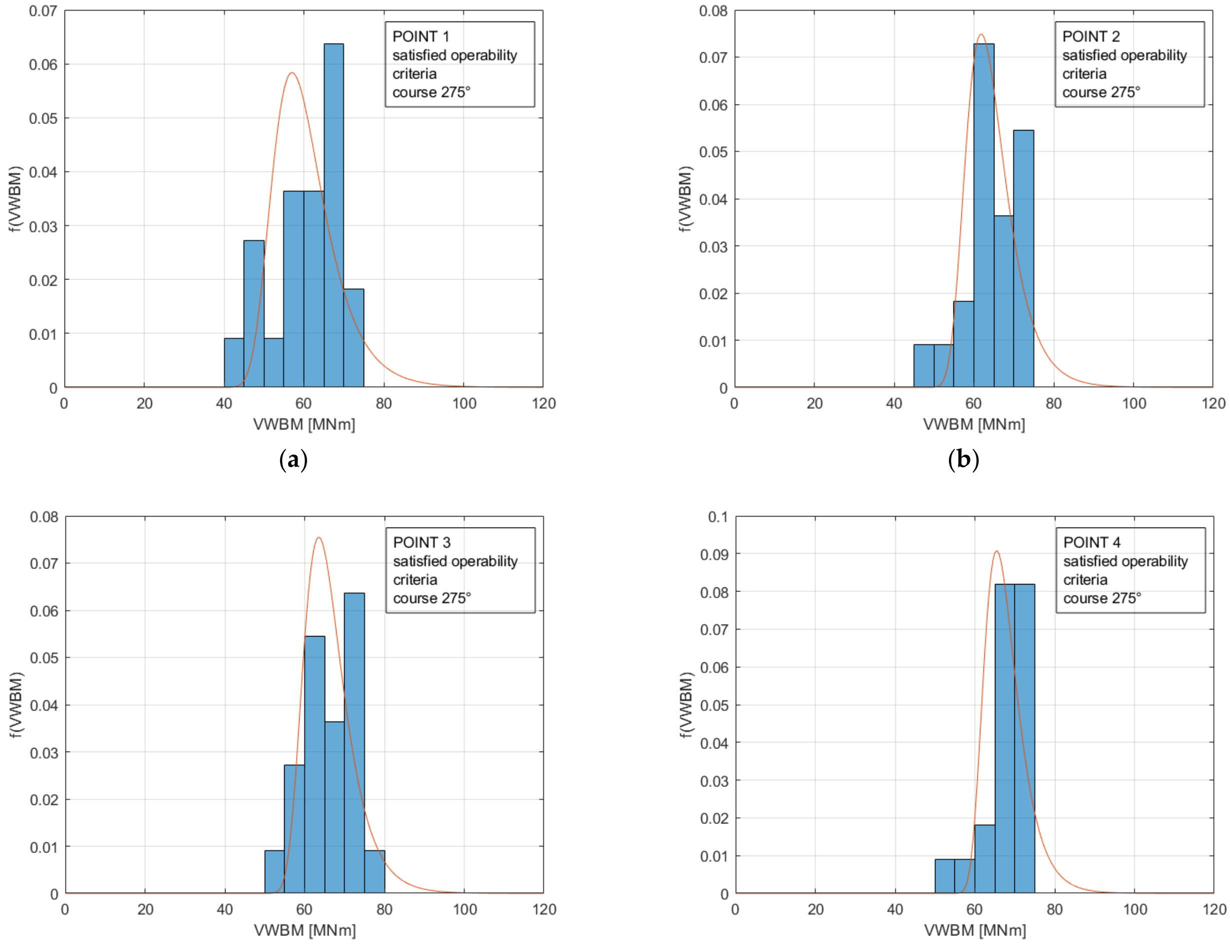

(**a**) (**b**) (**c**) (**d**)

Figure A2. Annual maximum vertical wave bending moments calculated for the ship sailing from Split to Ancona for sea states satisfying operability criteria: (**a**) at point 1; (**b**) at point 2; (**c**) at point 3; (**d**) at point 4.

Appendix A.3. Sea States Satisfying Operability Criteria on the Sailing Route from Ancona to Split

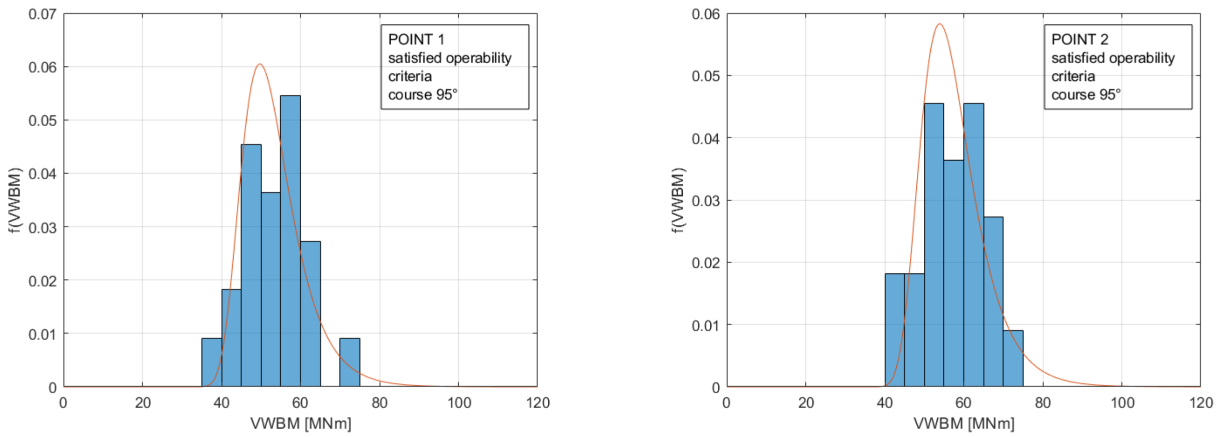

(**a**) (**b**)

Figure A3. *Cont.*

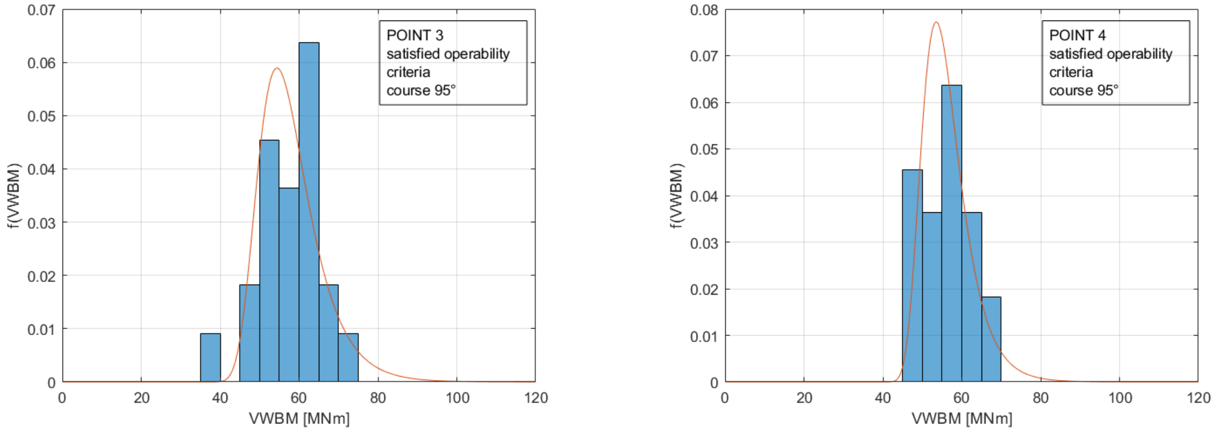

(c) (d)

Figure A3. Annual maximum vertical wave bending moments calculated for the ship sailing from Ancona to Split for sea states satisfying operability criteria: (**a**) at point 1; (**b**) at point 2; (**c**) at point 3; (**d**) at point 4.

Appendix B. Annual Maximum Vertical Wave Bending Moments for a Case of Reduced Speed on Sea States That Do Not Meet Operability Criteria

Appendix B.1. Voyage from Split to Ancona

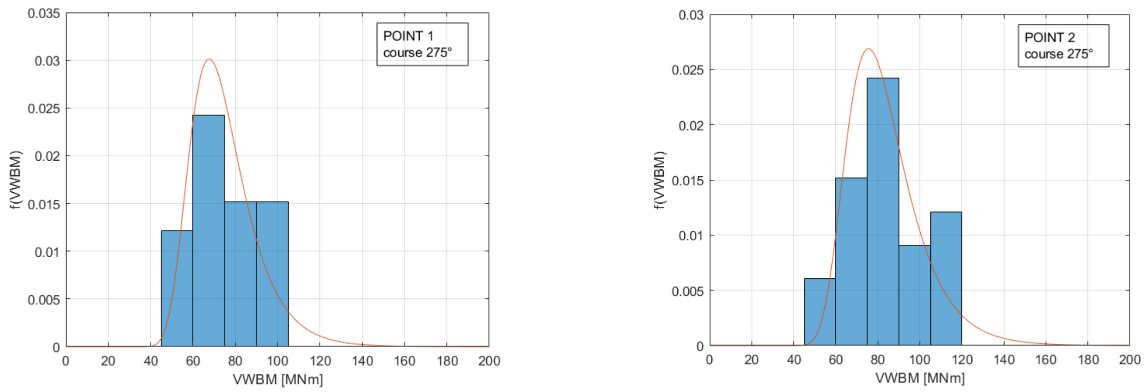

(a) (b)

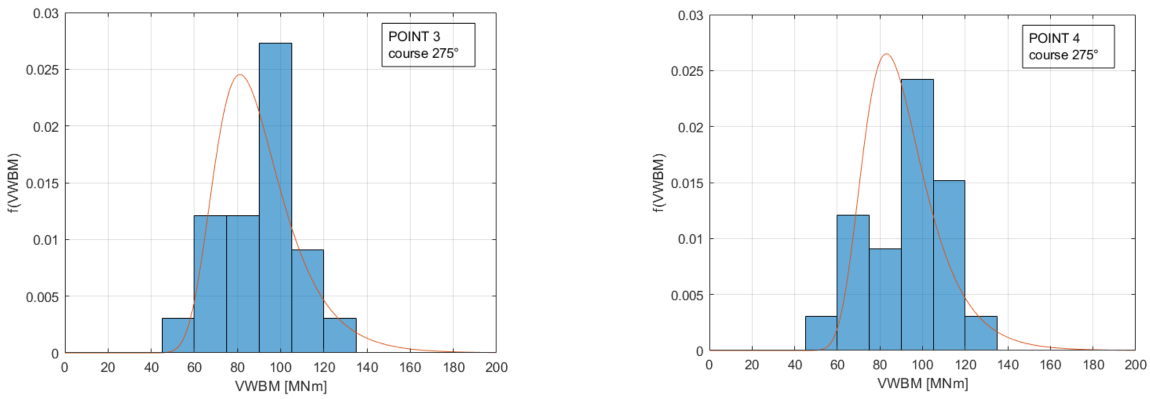

(c) (d)

Figure A4. Annual maximum VWBM calculated for a speed of 17 knots on sea states satisfying operability criteria and a speed of 5 knots on sea states not satisfying operability criteria: (**a**) at point 1; (**b**) at point 2; (**c**) at point 3; (**d**) at point 4 on course 275°.

Appendix B.2. Voyage from Ancona to Split

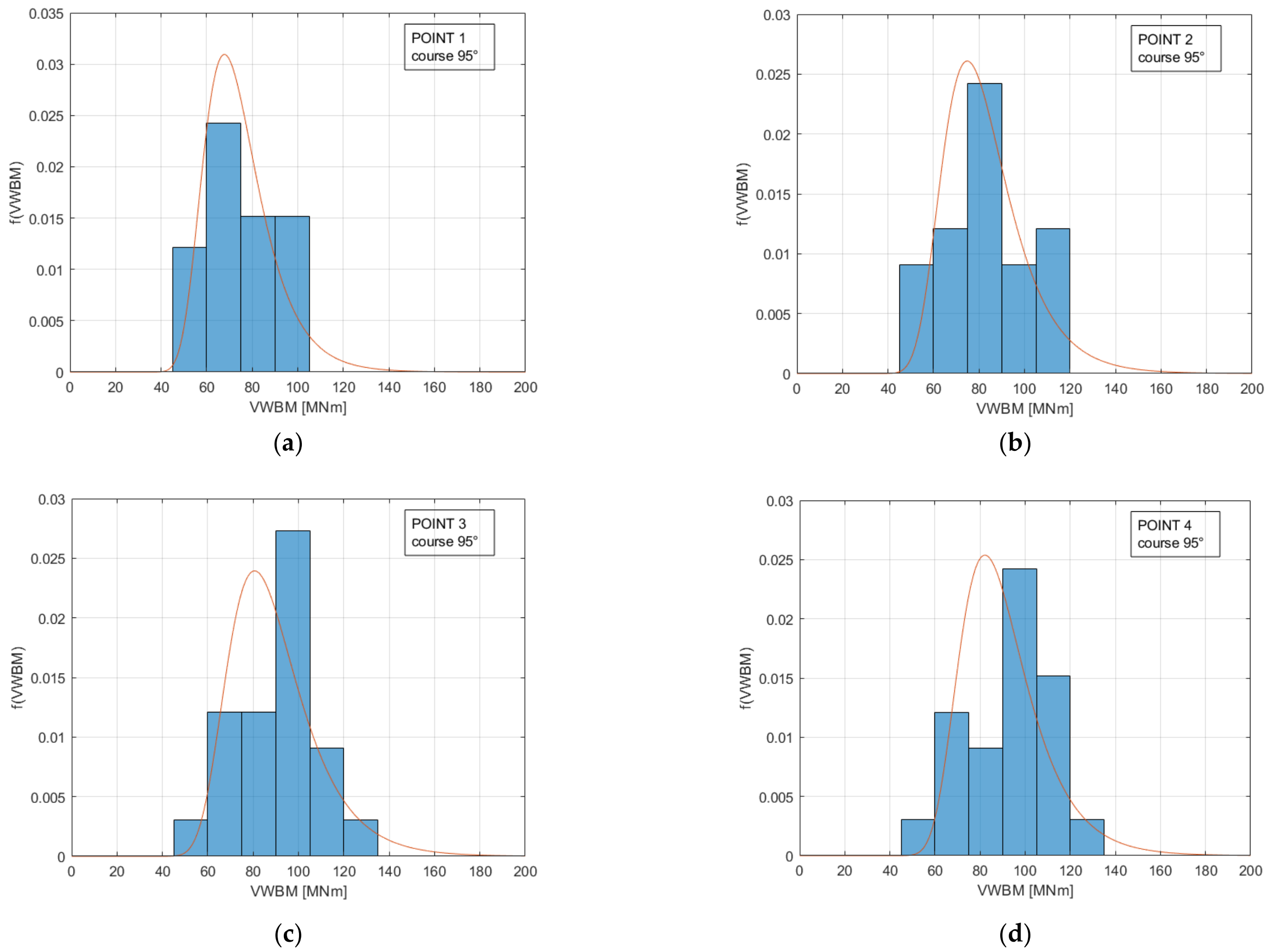

Figure A5. Annual maximum VWBM calculated for a speed of 17 knots on sea states satisfying operability criteria and a speed of 5 knots on sea states not satisfying operability criteria: (**a**) at point 1; (**b**) at point 2; (**c**) at point 3; (**d**) at point 4 on course 95°.

References

1. IACS Rec. *No. 34. Standard Wave Data*; IACS: London, UK, 2001.
2. Moan, T.; Shu, Z.; Drummen, I.; Amlashi, H. Comparative reliability analysis of ships—Considering different ship types and the effect of ship operations on loads. *Trans. Soc. Nav. Archit. Mar. Eng.* **2007**, *114*, 16–54.
3. Guedes Soares, C. On the Definition of Rule Requirements for Wave Induced Vertical Bending Moments. *Mar. Struct.* **1996**, *9*, 409–425. [CrossRef]
4. Prpić-Oršić, J.; Parunov, J.; Šikić, I. Operation of ULCS—Real Life. *Int. J. Nav. Archit. Ocean. Eng.* **2014**, *6*, 1014–1023. [CrossRef]
5. Hogben, N.; Dacunha, N.M.C.; Oliver, G.F. *Global Wave Statistics*; Feltham: British Maritime Technology Ltd.: London, UK, 1986.
6. Bitner-Gregersen, E.M.; Dong, S.; Fu, T.; Ma, N.; Maisondieu, C.; Miyake, R.; Rychlik, I. Sea state conditions for marine structures' analysis and model tests. *Ocean. Eng.* **2016**, *119*, 309–322. [CrossRef]
7. Derbanne, Q.; Shiguntov, V.; Storhaug, G.; Xie, G.; Zheng, G. Rule formulation of vertical hull girder wave loads based on direct computation. In Proceedings of the PRADS 2016, Copenhagen, Denmark, 4–8 September 2016.
8. de Hauteclocque, G.; Johnson, M.; Zhu, T.; Austefjord, H.; Bitner-Gregersen, E. Assesment of global wave datasets for long term response of ships. In Proceedings of the ASME 2020 39th International Conference on Ocean, Offshore and Arctic Engineering OMAE 2020, Fort Lauderdale, FL, USA, 28 June–3 July 2020.
9. Perrault, D.E. Probability of Sea Condition for Ship Strength, Stability, and Motion Studies. *J. Ship Res.* **2021**, *65*, 1–14. [CrossRef]
10. Schirmann, M.L.; Collette, M.D.; Gose, J.W. Significance of wave data source selection for vessel response prediction and fatigue damage estimation. *Ocean. Eng.* **2020**, *216*, 107610. [CrossRef]
11. Vettor, R.; Guedes Soares, C. Assessment of the Storm Avoidance Effect on the Wave Climate along the Main North Atlantic Routes. *J. Navig.* **2016**, *69*, 127–144. [CrossRef]

12. Jensen, J.J.; Mansour, A.E.; Olsen, A.S. Estimation of ship motions using closed-form expressions. *Ocean. Eng.* **2004**, *31*, 61–85. [CrossRef]
13. Ghaemi, M.H.; Olszewski, H. Total ship operability -review, concept and criteria. *Pol. Marit. Res.* **2017**, *24*, 74–81. [CrossRef]
14. Katalinić, M.; Parunov, J.; Mikulić, A. Toward operability analysis of a passenger ship in the Adriatic Sea based on the JONSWAP-Adriatic wave spectrum. In Proceedings of the XXIV Symposium Theory and Practice of Naval Architectures (SORTA 2020), Malinska, Croatia, 15–17 October 2020.
15. Petranović, T.; Katalinić, M.; Mikulić, A.; Parunov, J. Operability study of passenger ship in the Adriatic Sea using hindcast database. In Proceedings of the 8th International Conference on Marine Structures (MARSTRUCT 2021), Trondheim, Norway, 7–9 June 2021.
16. Katalinić, M.; Parunov, J. Comprehensive Wind and Wave Statistics and Extreme Values for Design and Analysis of Marine Structures in the Adriatic Sea. *J. Mar. Sci. Eng.* **2021**, *9*, 522. [CrossRef]
17. Katalinić, M.; Ćorak, M.; Parunov, J. Optimized Wave Spectrum Definition for the Adriatic Sea. *Naše More* **2020**, *67*, 19–23. [CrossRef]
18. DNV GL. *Recommended Practice DNVGL RP C-205: Environmental Conditions and Environmental Loads*; Edition August 2017; Det Norske Veritas Germanischer Lloyd: Oslo, Norway, 2017.
19. Lloyd, A.R.J.M. *Seakeeping: Ship Behaviour in Rough Water*; Gosport: Hampshire, UK, 1998.
20. Scamardella, A.; Piscopo, V. Passenger ship seakeeping optimization by the Overall Motion Sickness Incidence. *Ocean. Eng.* **2014**, *76*, 86–97. [CrossRef]
21. DNV GL. *Class Guideline DNVGL CG 0130: Wave Loads*; Det Norske Veritas Germanischer Lloyd: Oslo, Norway, 2018.
22. Mansour, A.; Liu, D. *The Principles of Naval Architecture Series: Strength of Ships And Ocean Structures*; The Society of Naval Architects and Marine Engineers: Jersey City, NJ, USA, 2008; pp. 4–56.
23. Katalinić, M.; Parunov, J. Uncertainties of Estimating Extreme Significant Wave Height for Engineering Applications Depending on the Approach and Fitting Technique—Adriatic Sea Case Study. *J. Mar. Sci. Eng.* **2020**, *8*, 259. [CrossRef]
24. Mansour, A.E.; Preston, D.B. Return periods and encounter probabilities. *Appl. Ocean. Res.* **1995**, *17*, 127–136. [CrossRef]
25. Mikulić, A.; Katalinić, M.; Ćorak, M.; Parunov, J. The effect of spatial correlation of sea states on extreme wave loads of ships. *Ships Offshore Struct.* **2021**, *16* (Suppl. S1), 22–32. [CrossRef]
26. Ćorak, M.; Parunov, J.; Guedes Soares, C. Long-term prediction of combined wave and whipping bending moments of container ships. *Ships Offshore Struct.* **2015**, *10*, 4–19. [CrossRef]
27. Jiao, J.; Ren, H.; Guedes Soares, C. A review of large-scale model at-sea measurements for ship hydrodynamics and structural loads. *Ocean. Eng.* **2021**, *227*, 108863. [CrossRef]
28. Mudronja, L.; Katalinić, M.; Vidan, P.; Parunov, J. Route planning based on ship roll in numerically modelled heavy seas. In Proceedings of the XXII Symposium Theory and Practice of Naval Architectures (SORTA 2016), Trogir, Croatia, 6–8 October 2016.
29. World Meteorological Organization. *Guide to Wave Analysis and Forecasting*; Secretariat of the World Meteorological Organization: Geneva, Switzerland, 1998.
30. Lavidas, G.; Venugopal, V. Wave energy resource evaluation and characterisation for the Libyan Sea. *Int. J. Mar. Energy* **2017**, *18*, 1–14. [CrossRef]
31. Mansour, A.E.; Wasson, J.-P. Charts for Estimating Nonlinear Hogging and Sagging Bending Moments. *J. Ship Res.* **1995**, *39*, 240–249. [CrossRef]
32. Mansour, A.E.; Jensen, J.J. Slightly Nonlinear Extreme Loads and Load Combinations. *J. Ship Res.* **1995**, *39*, 139–149. [CrossRef]